

UCSF

UC San Francisco Electronic Theses and Dissertations

Title

The Role of the Inactive X-Chromosome in Longevity and Neurodegeneration

Permalink

<https://escholarship.org/uc/item/7fd1h258>

Author

Davis, Emily J

Publication Date

2020

Peer reviewed|Thesis/dissertation

The Role of the Inactive X-Chromosome in Longevity and Neurodegeneration

by
Emily Davis

DISSERTATION

Submitted in partial satisfaction of the requirements for degree of
DOCTOR OF PHILOSOPHY

in

Biomedical Sciences

in the

GRADUATE DIVISION

of the

UNIVERSITY OF CALIFORNIA, SAN FRANCISCO

Approved:

DocuSigned by:

Saul Villeda

Saul Villeda

711626DA5837464...

Chair

DocuSigned by:

Dena Dubal

Dena Dubal

DF40821EE4774FD...

DocuSigned by:

Barbara Panning

Barbara Panning

B18F20197C95417...

Committee Members

Acknowledgments

First, I must thank my advisor, Dena Dubal, for her unwavering support, positivity, and mentorship throughout my time in graduate school. You helped me see what I'm capable of. Second, I am grateful for my amazing thesis committee, my chair Saul Villeda, and Barbara Panning. Your scientific insights and advice were generously given and greatly appreciated. It has been my pleasure and honor to be mentored by such brilliant, kind, and inspiring scientists. Thank you to my collaborators at UCSF and beyond for their contributions to this work.

I would like to thank the members of the Dubal lab, both past and present; without your friendship and support this work would not have been possible. Thank you to Elena Miñones-Moyano for mentoring me both in and out of lab and teaching me cell culture. Thank you to Julio Leon for your humor, encouragement, and expertise. Thank you to Samira Abdulai-Saiku, Shweta Gupta, and Cana Park for your input and mentorship. Thank you to Chen Chen for your hard work. Thank you to Arturo Moreno for being a true friend and confidant. And finally, a huge thank you to lab manager Dan Wang – you will always be my 'lab mom' and I will always remember you for your kindness and strength.

I would like to thank UCSF and the BMS program for being such a supportive community. To Demian Sainz, I can't thank you enough for your support as program coordinator and always being there to listen and help. Thank you to the 2015 BMS cohort for the camaraderie and normalizing the struggles of graduate school.

Finally, I would like to thank my family and friends for their love and support. Thank you to my parents for always believing in me. Thank you to Sam, the best little brother I could ever ask for and the voice of reason. Thank you to my roommates, both past and present, for providing food and emotional support in large quantities. Last but not least, thank you to Chris Neal for being my email editor, my biggest supporter, and my best friend, throughout grad school and, hopefully, for many years beyond.

Contributions

Chapter 2 is a reprint of the previously published work:

Davis, E. J., Lobach, I., & Dubal, D.B. (2018). “Female XX sex chromosomes increase survival and extend lifespan in aging mice.” *Aging Cell* 18:e12871. <https://doi.org/10.1111/accel.12871>

AUTHOR CONTRIBUTIONS

E.J.D., I.L., and D.B.D. carried out experimental studies and analyses and wrote the manuscript.

All authors discussed results and commented on the manuscript.

Chapter 3 is a reprint of the previously published work:

Davis, E. J., Broestl, L., Abdulai-Saiku, S., Worden, K., Bonham, L. W., Miñones-Moyano, E., Moreno, A.J., Wang, D., Chang, K., Williams, G., Garay, B.I., Lobach, I., Devidze, N., Kim, D., Anderson-Bergman, C., Yu, G., White, C.C., Harris, J.A., Miller, B.L., Bennett, D.A., Arnold, A.P., De Jager, P.L., Palop, J.J., Panning, B., Yokoyama, J.S., Mucke, L., Dubal, D. B. (2020). “A second X chromosome contributes to resilience in a mouse model of Alzheimer’s disease”. *Science Translational Medicine*, 12(558), eaaz5677.

<https://doi.org/10.1126/scitranslmed.aaz5677>

AUTHOR CONTRIBUTIONS

Conceptualization and design of studies were by E.J.D (Kdm6a mouse experiments), L.B. (sex difference and FCG mouse experiments), K.W. (FCG mouse experiments), S.A.S. (lentiviral and cell culture experiments), L.W.B. (human data), J.S.Y. (human data), D.B.D. (mouse and human experiments). Data acquisition, analysis, interpretation, or some combination were performed by E.J.D. (Kdm6a mouse data acquisition, analysis, and all data interpretation), L.B. (sex-bias, FCG, and XY* mouse model data acquisition, analysis, and interpretation), S.A.S. (Kdm6a lentiviral cell culture and mouse data acquisition, analysis, and interpretation), K.W. (FCG mouse data acquisition, analysis, and interpretation), L.W.B. (human expression data and genetic data

acquisition, analysis, interpretation), E.M. (cell culture data acquisition, analysis, interpretation), A.J.M. (immunohistochemistry, A β ELISA data acquisition, analysis, and interpretation), D.W. (A β ELISA data acquisition and analysis; XY* behavior, Kdm6a mouse PCR, Kdm6a mouse behavior data acquisition and interpretation), K.C. (human mortality meta-analysis data acquisition, analysis and interpretation), G.W. (RNA FISH data acquisition, analysis and interpretation), B.I.G. (human mortality meta-analysis data acquisition, analysis, and interpretation), I.L. (mouse mortality and behavior biostatistics and interpretation), N.D. (sex bias mouse behavior data acquisition, analysis, interpretation), D.K. (immunohistochemistry and sex bias mouse behavior data acquisition, analysis, interpretation), C.A. (biostatistics of human mortality meta-analysis and mouse behavior studies), G.Y. (A β ELISA data acquisition and analysis), C.C.W. (human data interpretation), J.A.H. (lentiviral data interpretation and analysis), B.L.M. (human data interpretation), D.A.B. (human data interpretation), A.P.A. (FCG and XY* mouse model interpretation), P.L.D. (human data interpretation), J.J.P. (hAPP mouse survival data acquisition and interpretation, mouse behavior data interpretation), B.P. (FISH acquisition and analysis, Kdm6a mouse data interpretation), J.S.Y. (human brain expression and human genetic data acquisition, analysis, interpretation), L.M. (sex-bias, FCG, and XY* mouse data interpretation), D.B.D. (mouse and human data acquisition, analysis, and interpretation). E.J.D., L.B., and D.B.D. wrote the original draft. All authors reviewed and contributed to the final draft.

The Role of the Inactive X-Chromosome in Longevity and Neurodegeneration

Emily J. Davis

Abstract

Biologic sex matters in aging and neurodegeneration. A female advantage in lifespan is seen in humans and throughout the animal kingdom, and men and women suffer differing vulnerabilities to age-related neurodegenerative disorders, including Alzheimer's disease (AD). More women suffer from AD, largely due to their longevity, as AD risk is highest in advanced age. In contrast, men with the disease die faster in populations worldwide and show greater cognitive deficits. We show the contribution of sex chromosome complement to these observations, in particular, the importance of the X chromosome. Using genetically modified mice we demonstrate (Chapter 2) that having XX sex chromosome complement increases survival during aging in male and female mice. We also show that XX sex chromosome complement in combination with ovaries extends lifespan. We go on to show (Chapter 3) that having two X chromosomes decreased mortality and conferred resilience to AD-related vulnerability in mice expressing the human amyloid precursor protein (hAPP). We then investigated how a second X chromosome can confer resilience against AD-related deficits. While XY and XX organisms express only one active X due to X chromosome inactivation (XCI), a few factors escape XCI and therefore are higher in females compared to males. One of these genes, *Kdm6a*, escapes in both mice and humans and is a histone demethylase linked to cognitive functions. We thus determined whether higher levels of *Kdm6a* – as found in the XX brain – could counter AD-related vulnerability in the XY brain. We first confirmed that the presence of a second X chromosome increased levels of *Kdm6a* in mouse hippocampus; it did so independent of gonadal phenotype or the presence of a Y chromosome.

We then used lentiviral vectors in mice to modulate *Kdm6a* expression *in vivo* and *in vitro*. Overexpression of *Kdm6a* in the hippocampus of XY hAPP mice to higher levels observed in XX hAPP mice attenuated spatial learning and memory deficits in the Morris water maze. Similarly, overexpression of *Kdm6a* in XY primary neurons decreased A β toxicity *in vitro*. Furthermore, knockdown of *Kdm6a* in XX neurons to levels observed in XY neurons worsened A β toxicity *in vitro*. Finally, in humans, genetic variation in *KDM6A* was linked to higher brain expression and associated with less cognitive decline in aging and preclinical AD, suggesting relevance to human brain health. Our findings highlight the importance of sex chromosomes in aging and disease, as well as reveal a role for the baseline XCI escapee *Kdm6a* in countering AD-related deficits.

Table of Contents

Chapter 1 – Introduction	1
Summary	1
Sex as a Biological Variable	1
Four Core Genotypes and XY* Mouse Models.....	3
Sex Chromosome Dosage Compensation and Related Mechanisms.....	5
X Chromosome Inactivation Escapee Genes	7
Aims of This Study	9
 Chapter 2 – Female XX sex chromosomes increase survival and extend lifespan in aging mice	 10
Summary	10
Introduction	10
Results.....	11
Discussion.....	12
Materials and Methods	13
Figures	16
Tables.....	19
 Chapter 3 – A second X chromosome contributes to resilience in a mouse model of Alzheimer’s disease	 22
Summary	22
Introduction	23
Results.....	24
Discussion.....	33
Materials and Methods	39
Figures.....	56

Tables	87
Chapter 4 – Conclusion and Future Directions.....	91
Summary	91
Four Core Genotypes Lifespan	91
Further Characterization of Kdm6a Expression and Role in Neurodegeneration	93
Underlying Mechanisms of Protective Effects of Kdm6a Overexpression	95
Xi Reactivation in Aging and Neurodegeneration	97
References	100

List of Figures

Figure 2.1. XX sex chromosomes contribute to female longevity	16
Figure 2.2. XX sex chromosomes extended lifespan in combination with ovaries and independently increased survival during aging	18
Figure 3.1. A meta-analysis of hazard ratios for male and female mortality in AD populations worldwide.....	56
Figure 3.2. Male sex increases mortality, cognitive deficits, and synaptic protein abnormalities in hAPP mice.....	57
Figure 3.3. Male and female hAPP mouse mortality on a mixed genetic background	59
Figure 3.4. Human and mouse gonadal hormones in aging	60
Figure 3.5. Swim speeds and visible platform performance of mice in a water maze test.....	61
Figure 3.6. Male sex and cognitive deficits under several conditions	63
Figure 3.7. Male sex worsens cognition in another transgenic hAPP line.....	65
Figure 3.8. A β and related proteins in XX-and XY-hAPP mice crossed with FCG and XY* models.....	66
Figure 3.9. Western blot image of hAPP, t-Tau, p-Tau, and loading controls.....	67
Figure 3.10. 3D6 immunostaining specificity for A β plaques	68
Figure 3.11. A β plaque area in very old female hAPP mice	69
Figure 3.12. hAPP mRNA expression with and without gonadectomy	70
Figure 3.13. Sex chromosomes mediate increased male vulnerability to mortality and cognitive impairments in hAPP mice	71
Figure 3.14. Independent, replicate water maze cohort of FCG mice crossed with hAPP mice	73
Figure 3.15. Sex chromosomes and fear memory impairment in male hAPP mice.....	74

Figure 3.16. A second X chromosome confers resilience against AD-related cognitive impairments in XY (male) and XO (female) hAPP mice.....	75
Figure 3.17. A second X chromosome elevates <i>Kdm6a</i> expression independent of gonads or the Y chromosome in mice	77
Figure 3.18. <i>KDM6A</i> genetic variation associates with cognitive resilience in humans	79
Figure 3.19. KDM6A variant, other clinical exam scores, and assessment of women only.....	80
Figure 3.20. <i>Kdm6a</i> knockdown in XX mouse neurons worsens, whereas <i>Kdm6a</i> overexpression in XY neurons attenuates A β toxicity in vitro	82
Figure 3.21. Cell death induced by A β toxicity and assessed by LDH release assay	84
Figure 3.22. <i>Kdm6a</i> overexpression in hippocampus attenuates male vulnerability to cognitive impairments in XY-hAPP mice	85
Figure 3.23. <i>Kdm6a</i> overexpression and other behavioral tasks in male XY-hAPP mice ..	86
Figure 4.1. Diagram of female <i>Xist</i> ^{Δ/+} C57Bl/6J (<i>M. musculus</i>) crossed with wildtype male from CAST/EiJ (<i>M. castaneus</i>) and the resultant skewed offspring	99

List of Tables

Table 2.1. Stratified proportional hazard model shows XX(O) had significantly decreased mortality compared to the each of the other FCG experimental groups	20
Table 2.2. Cox proportional hazard model shows significant main effect of sex chromosome complement	20
Table 2.3. Stratified proportional hazard model of sex chromosome effect within gonadal sex group.....	20
Table 2.4. Stratified proportional hazard model of gonadal sex effect within sex chromosome group.....	20
Table 2.5. Stratified proportional hazard model following grid search method (Lerman 1980) in mice with ovaries.....	21
Table 2.6. Stratified proportional hazard model following grid search method (Lerman 1980) in mice with testes.....	21
Table 3.1. <i>KDM6A</i> in AD and Control Brain Tissues.....	87
Table 3.2. GSE 15222 Cohort Characteristics	87
Table 3.3. Mayo and Mount Sinai Brain Bank Sample Characteristics.....	88
Table 3.4. ADNI Cohort characteristics	89
Table 3.5. Longitudinal and Subgroup Analyses in the ADNI Cohort	90

List of Abbreviations

AD = Alzheimer's disease

A β = β -amyloid

CNS = central nervous system

CSF = cerebrospinal fluid

FCG = four core genotypes

FISH = fluorescent in situ hybridization

hAPP = human amyloid precursor protein

iPSC = induced pluripotent stem cells

KD = knock-down

Kdm6a = lysine demethylase 6a

MCI = mild cognitive impairment

NIH = National Institute of Health

OE = overexpression

PAR = pseudoautosomal region

SD = standard deviation

Sry = sex-determining region of the Y chromosome

UTY = ubiquitously transcribed tetratricopeptide repeat containing, Y-Linked

XCI = X-chromosome inactivation

Xa = active X chromosome

Xi = inactive X chromosome

Chapter 1 – Introduction

SUMMARY

This chapter provides a broad overview of the importance of sex in understanding aging and neurodegeneration, and basic coverage of chromosome biology. Two key mouse models used throughout this thesis are discussed. A brief overview of the aims of this thesis is given.

Sex as a Biological Variable

In 2016, the NIH began requiring sex as a biological variable of any invertebrate animal and human studies in research design, analysis, and reporting (Arnegard, Whitten et al. 2020). Any studies that intend to focus on one sex must provide strong justification for doing so. In prior decades, biomedical research often excluded female animals and participants, drawing conclusions from male-only studies. The rationale was that male and female animals have similar enough biology and that males had less variability because of a lack of an estrous cycle (Beery and Zucker 2011). Over-reliance on male animals obscured our understanding of the role of sex on health outcomes, disease susceptibility, response to treatment, and the underlying biology and mechanisms of disease. It is becoming recognized that fundamental biological mechanisms are sex-dependent and our understanding of these sex differences may lead to novel therapies and approaches for the benefit of all.

One fundamental biological phenomenon is aging. Females (XX) live longer than males (XY) in both normal aging (United Nations 2015, Colchero, Rau et al. 2016) and during times of famine and epidemics (Zarulli, Barthold Jones et al. 2018). Aging is also the primary risk factor for cognitive decline and neurodegenerative disease. The sex difference in longevity is also observed in models of neurodegenerative disease (Lapane, Gambassi et al. 2001, Sejvar, Holman et al. 2005, Forsaa, Larsen et al. 2010) and men show greater cognitive decline with aging (Cerhan, Folsom et al. 1998, Casaletto, Elahi et al. 2019). While at first glance one might

assume these differences are due to differences in hormonal signaling, there is mounting evidence for the importance of sex chromosome complement. For example, birds have the ZW sex determination system, meaning males are the sex with homomorphic sex chromosome complement (ZZ) while females are heteromorphic (ZW). A paper by Pipoly et al. supports the idea that the sex with homomorphic sex chromosome complement is longer-lived (females in the case of mammals and males in the case of birds) as adult sex ratios are biased towards the sex with homomorphic sex chromosome complement (Pipoly, Bokony et al. 2015). More attention and exploration of the role of sex chromosomes is warranted for understanding sex differences in aging and aging-related neurodegeneration diseases.

I would be remiss to discuss the importance of sex as a biological variable without mentioning the distinction between the terms 'sex' and 'gender'. Sex, as used throughout this thesis, is defined as the biological status of 'male' or 'female' determined by reproductive organs and other functions as determined by sex chromosomes. Sex can be applied to humans as well as animals. Gender, in contrast, is a person's self-representation as female or male, or how social institutions respond to a person based on the individual's gender presentation. It is based on socially constructed roles, attitudes, feelings, behaviors, attributes, and activities most often assigned to and considered appropriate for men and women. Sex differences are due to biological factors at the genetic, molecular, cellular, anatomical, and physiological levels that interact with one another while gender differences are caused by environmental factors related to the aforementioned societal and cultural roles and expectations of an individual. Therefore, 'gender' is a term best used for describing human beings and is not well informed by work done with animals. With this in mind, the work of this thesis focuses on sex and sex differences most often as it relates to preclinical models and research, with an emphasis on work done in mice.

To understand sex differences in aging and neurodegeneration and identify the key factors involved, a robust experimental framework is required. Arthur Arnold has been a key figure in the development of such a framework and it is his framework that is used throughout this thesis.

Briefly, sex differences are classified into three distinct categories: (1) activational effects of gonadal hormones, (2) organizational effects of gonadal hormones, or (3) sex chromosome effects. Activational effects of gonadal hormones are reversible transient effects of gonadal hormone production whereas organizational effects of gonads are permanent, differentiating effects due to gonadal hormone production during development. To determine if a gonadal effect is due to the activational versus organizational effects, gonadectomy can be used. If gonadectomy abolishes a phenotype then that phenotype is likely due to the activational effects of gonads. Phenotypes that are not abolished by gonadectomy must be either sex chromosome-complement dependent in nature or a result of the organizational effects of hormones during development. To determine if an effect is due to organizational effects of hormones or sex chromosome complement, masculinization of females by exposure to androgens in early development and feminization of males through deprivation of testosterone or androgen receptors during early development can be used. If these manipulations don't resolve the sex difference, then the remaining category to consider is sex chromosome complement. This conceptual research strategy for discovering factors that causes sex differences has been coined the A-O-S approach by Arnold (activational then organizational then sex chromosome). Below is a description of two key mouse models used for studying sex differences.

Four Core Genotypes and XY* Mouse Models

Several mouse models that manipulate sex chromosome complement and gonadal hormones exist to help uncover and distinguish the underlying causes of sex differences. These models can be used in conjunction with mouse models of neurodegeneration as well as for lifespan curves of normal aging. For the purposes of this introduction and thesis, I will discuss two models used in our lab and research, the Four Core Genotypes (FCG) and XY* models.

The FCG model allows the separation of sex chromosome complement from gonadal phenotype and hormone expression. The Sry gene that leads to the development of testes and

male behavior and presentation has been deleted from the Y chromosome. In its place there is an autosomal Sry expression. By decoupling Y-chromosome inheritance from testes development four genotypes are created: XX mice with ovaries, XY mice with testes, and XX mice with testes and XY mice with ovaries. It should be noted that gonadal hormones in FCG mice show comparable levels in mice with ovaries (XX vs. XY) and in those with testes (XX vs. XY) throughout the lifespan. This is supported by FCG studies of hormone levels in perinatal (Itoh, Mackie et al. 2015), neonatal (Wagner, Xu et al. 2004), adult (Gatewood, Wills et al. 2006, Corre, Friedel et al. 2016), and aged mice (McCullough, Mirza et al. 2016). The FCG model can be used to determine if a phenotype is due to sex chromosome complement or gonadal. An effect due to sex chromosome complement would show a main effect in XX versus XY regardless of gonads (XX(O) and XX(T) versus XY(O) and XY(T)). An effect due to gonads would show a main effect in ovaries versus testes regardless of sex chromosome complement (XX(O) and XY(O) versus XX(T) and XY(T)).

The other mouse model used in the context of this thesis is the XY* model (Eicher, Hale et al. 1991). This model takes advantage of a pseudoautosomal region (PAR) in male mice that recombines abnormally with the X chromosome during meiosis to derive mice with varying sex chromosome dosage. The resultant offspring have four possible genotypes that are equivalent to: XX, XY, XO, and XXY. The XY* model can be used to determine if a phenotype is due to the presence/absence of a second X chromosome or the presence/absence of a Y chromosome. If an effect were due to the presence/absence of a second X chromosome then the main effect would be between XX and XXY versus XO and XY. An effect due to the presence/absence of a Y chromosome would show a main effect between XX and XO versus XXY and XY. It should be noted that the XY* model is an imperfect model for human chromosomal disorders Turner syndrome (XO females) and Klinefelter syndrome (XXY males). This is because in the XXY mice produced, the second X chromosome is fused to the Y chromosome by its disrupted PAR. Similarly, XO mice may have one X chromosome plus the PAR by itself.

Sex Chromosome Dosage Compensation and Related Mechanisms

A crucial aspect in analyzing sex differences is understanding the process of sex determination and dosage compensation. Dosage compensation occurs in order to balance gene expression between members of different sexes in a species. There are four main mechanisms seen in eukaryotic organisms, which I will briefly describe. In *Caenorhabditis elegans* (worms), sex is determined by an XO sex determination system with XX worms developing as hermaphrodites and XO worms developing as male. Dosage compensation is achieved through decreased transcription of both X chromosomes in hermaphrodites by half (Meyer 2000). Meanwhile, in *Drosophila melanogaster*, sex is determined by X chromosomes to autosomes ratio. The Y chromosome encoding genes necessary for sperm production but does not itself confer 'maleness' (Rideout, Narsaiya et al. 2015). Dosage compensation is achieved by males having a two-fold increase in X-chromosome transcription (Lucchesi and Kuroda 2015). Birds and some snakes have a ZW sex determination system with ZZ animals being male and ZW being female; in this system the Z is equivalent to the X chromosome in that is larger with more genes. Rather than a global dosage compensation mechanism, birds have a gene-selective dosage compensation mechanism (McQueen, McBride et al. 2001, Hirst, Major et al. 2018). Finally, in placental animals, one X is predominantly transcribed (active X, or X_a) while the other X is heavily silenced (inactive X, or X_i) through a process known as X chromosome inactivation (XCI). XCI is an important mechanism for maintaining dosage compensation of X-linked gene expression between the sexes. There are several mechanisms related to dosage compensation that could explain sex differences, a few of which are described below.

Females inherit an X chromosome from each parent, a maternal X and a paternal X, that possess distinct epigenetic marks from the parent of origin. These marks influence expression and thereby could underlie differential cellular responses to neuronal stress and aging. On average, an XX brain will have 50% of cells expressing the maternal X and the other 50% of cells

expressing the paternal X. Whereas in XY males, 100% of cells have maternal X-linked genomic imprinting. It should be noted that in inbred mouse strains the only difference between maternal and paternal X chromosomes are these epigenetic imprints whereas outbred strains and humans also have genetically divergent X chromosomes. In a mouse model of Turner syndrome, it has been shown that parent of origin X chromosome influences cognitive function with maternally inherited X chromosome mice having impaired reversal learning compared to paternally inherited X chromosome mice (Davies, Isles et al. 2005). In humans, Turner syndrome patients with paternal X had better verbal skills and higher executive functioning compared to those with a maternal X (Skuse, James et al. 1997). This cellular heterogeneity of X-linked genomic imprinting in females may explain, for example, why females often lower occurrence and less severe phenotypes of various X-linked genetic disorders from color blindness(Deeb 2005) to autism (Skuse 2000).

Another mechanism at play is the potential roles of long non-coding RNA, *Xist*. *Xist* is expressed from the Xi and initiates XCI by coating the soon-to-be Xi and recruiting silencing machinery such as the polycomb-group proteins. Whichever X is coated by *Xist* becomes the inactive X while the other X remains active. Deletion of *Xist* on one X chromosome early in development prevents XCI in that X, but conditional deletion of *Xist* after XCI has occurred does not result in Xi reactivation (Csankovszki, Panning et al. 1999). It's possible that *Xist* is involved with mechanisms outside of XCI. One such mechanism identified recently is through the sequestering of micro RNA (miRNA), also known as miRNA sponging (Marshall, Stewart et al. 2019) and has been shown to impact age-related disorders (Chen, Li et al. 2020, Cheng, Luo et al. 2020, Li, Hou et al. 2020, Lin, Xu et al. 2020).

A separate but related mechanism is reactivation of the inactive X. Here, genes initially undergo XCI and are not expressed from Xi. Then, during cellular reprogramming (Payer 2016) and potentially during aging or in response to stress, the repressive marks on Xi are removed and previously inactivated Xi-encoded genes are expressed. There is evidence to suggest that Xi can

be reactivated in cancer cells (Kokalj-Vokac, Saint-Ruf et al. 1991, Ganesan, Silver et al. 2002) and reactivation may occur during normal aging (Wareham, Lyon et al. 1987, Bennett-Baker, Wilkowski et al. 2003, Schoeftner, Blanco et al. 2009). It remains to be determined if reactivation can occur in the brain and what role Xi reactivation may be in aging and neurodegeneration.

There is also emerging evidence that supports biallelic expression of a limited number of X-linked genes. In mammals, XCI is initiated and completed during early embryonic development and is believed to be maintained throughout the lifetime of somatic cells. While it is widely assumed the inactive X is completely silenced, there are a small number of genes which have been shown to escape inactivation (Balaton and Brown 2016). Since they do not undergo dosage compensation these genes are always expressed at a higher level in 2X mammals. It's worth noting that mechanisms mentioned in this section are not mutually exclusive and likely act synergistically. The role of specific XCI escapee genes is discussed further in the following section.

X Chromosome Inactivation Escapee Genes

While it is commonly assumed that the Xi of 2X genotypes is invariably silenced, some genes are transcribed from both the Xi and the Xa. While escapee genes are transcribed from the Xi, this transcription is not to the full capacity that is seen on the Xa chromosome. An escapee gene is often defined as a gene that is expressed at least 10% of the expression of the Xa (Carrel and Willard 2005). The exact number and identity of these escapees varies based on cell type, tissue type, and the model used, but approximately 3-7% of all expressed X-linked genes escape XCI in mice (Berletch, Ma et al. 2015); that range increases to 12-20% in humans (Balaton, Cotton et al. 2015, Tukiainen, Villani et al. 2017). Even if escape is a fraction of expression compared to that seen on the active X, could still have profound effects; it is also unknown how much these differences in RNA expression are seen at the protein level. Identification of XCI escapee genes was first established in 2005 using hybrid human-rodent cell lines (Carrel and Willard 2005). Since

then, several recent studies have highlighted the importance of escapee genes in disease outcomes and sex differences. It has been posited that XCI escapee genes may be protected for XX versus XY in the case of cancer (Dunford, Weinstock et al. 2017). There are also examples where XCI escapee genes are linked to increased autoimmune disorders in XX individuals (Souyris, Cenac et al. 2018, Itoh, Golden et al. 2019).

XCI escapees may play significant roles in brain aging. Several of the most robust escapees, *Kdm6a*, *Kdm5c*, *Ddx3x*, and *Eif2s3x* are seen in both human and mouse and escape in the brain. KDM6A and KDM5C are both histone demethylases. As an H3K27me3 demethylase, KDM6A has been previously shown to play a significant role in embryonic development (Agger, Cloos et al. 2007, Shpargel, Sengoku et al. 2012, Welstead, Creighton et al. 2012). To highlight its importance in the brain, it should be noted that mutations in *KDM6A* are associated with Kabuki syndrome, a developmental disorder with intellectual disability as a common symptom (Miyake, Koshimizu et al. 2013, Miyake, Mizuno et al. 2013). KDM5C has been shown to act as a transcriptional repressor acting through the REST complex (Tahiliani, Mei et al. 2007) and mutations are associated with X-linked mental retardation (Jensen, Amende et al. 2005). DDX3X is an important DEAD-box RNA helicase that regulates the WNT signaling pathway and whose loss of function is associated with intellectual disability (Snijders Blok, Madsen et al. 2015). Less is known about EIF2S3X, a subunit of the eukaryotic initiation factor 2, important for the initiation of translation. It should be noted that all the aforementioned escapees have known Y-homologs, genes located on the Y chromosome with shared structure. However, their Y-homologs are often differentially expressed (Xu, Deng et al. 2008) and have a different or unknown function (Wang, Lee et al. 2012, Yamauchi, Riel et al. 2014, Faralli, Wang et al. 2016).

Aims of This Study

The purpose of this thesis is to highlight the importance of sex chromosome biology, particularly the X chromosome, in understanding sex differences in both aging and

neurodegeneration. Chapter 2 discusses the importance the second X chromosome in lifespan of the FCG model, as well as an interaction between ovaries and XX sex chromosome complement in longevity. Chapter 3 covers the use of the hAPP mouse model of AD and A β toxicity neuronal cell culture assay to identify the second X chromosome as the reason for improved resilience in XX mice and cells; it further demonstrates the protective/rescuing effect of an X-linked gene, Kdm6a, which is normally expressed higher in 2X compared to 1X animals and humans. The final chapter outlines future directions of the aforementioned work as well as ways to explore the possibility of Xi reactivation with aging and aging-related stress.

Chapter 2 – Female XX sex chromosomes increase survival and extend lifespan in aging mice

SUMMARY

Female longevity is observed in humans and much of the animal kingdom, but its causes remain elusive. Using a genetic manipulation that generates XX and XY mice, each with either ovaries or testes, we show that the female XX sex chromosome complement increases survival during aging in male and female mice. In combination with ovaries, it also extends lifespan. Understanding causes of sex-based differences in aging could lead to new pathways to counter age-induced decline in both sexes.

INTRODUCTION

Women live longer than men around the world, regardless of culture or socioeconomic status (United Nations 2015, Zarulli, Barthold Jones et al. 2018). Female longevity is also observed in the animal kingdom (Clutton-Brock and Isvaran 2007, Barrett and Richardson 2011, Bronikowski, Altmann et al. 2011) due to causes that may be extrinsic, intrinsic, or both. Extrinsic causes of sex difference in invertebrates can signal antagonistic survival strategies; female pheromones reduce male lifespan in *Drosophila* (Gendron, Kuo et al. 2014) and male secretions shorten hermaphrodite lifespan in *C. elegans* (Maures, Booth et al. 2014). Intrinsic effects – operating within the organism – underlie longer life in organisms following removal of reproductive cells or organs in *C. elegans* hermaphrodites (Berman and Kenyon 2006), male and female dogs (Hoffman, Creevy et al. 2013), and possibly men as suggested by a study of eunuchs (Min, Lee et al. 2012). Nonetheless, causes of intrinsic sex difference in lifespan remain largely unknown. The pervasive nature of female longevity in humans, even in early death during severe epidemics and famine (Zarulli, Barthold Jones et al. 2018), suggests a role for innate biology in the survival

gap between the sexes. Here, we sought to identify intrinsic causes of female longevity in mammalian lifespan.

RESULTS

The genetic manipulation of SRY generates XX and XY mice, each with either ovaries (O) or testes (T): XX(O), XX(T), XY(O), XY(T) (**Figure 2.1a**). Gonadal hormone levels in FCG mice with the same gonads are comparable, regardless of their sex chromosomes (Gatewood, Wills et al. 2006, McCullough, Mirza et al. 2016). In FCG model mice, a sex difference with a main effect that statistically differs by genotype (XX vs. XY) is sex chromosome-mediated; one that differs by phenotype (ovaries vs. testes) is gonadal-sex mediated (**Figure 2.1b**). Examples of age-relevant FCG mouse studies show that XX improves blood pressure regulation (Pessoa, Slump et al. 2015) and attenuates experimental brain injuries (Du, Itoh et al. 2014, McCullough, Mirza et al. 2016).

To explore sex-based differences in lifespan, we generated and aged over 200 mice from the FCG model on a congenic C57BL/6J background and investigated aging-dependent mortality from midlife to old age (12–30mos) (**Figure 2.1c**). We first examined whether mortality in ‘typical’ females (XX,O) and males (XY,T) recapitulates the pattern of female longevity. Indeed, aging females (XX,O) lived longer than aging males (XY,T) (**Figure 2.1d; Table 2.1**).

We next measured main effects of sex chromosomes and gonads on survival in aging. XX mice with ovaries or testes lived longer than XY mice of either gonadal phenotype, indicating a main effect of sex chromosomes on lifespan (**Figure 2.1e; Table 2.2**). Mice with ovaries (XX & XY) tended to live longer than those with testes (XX & XY), suggesting a gonadal influence on lifespan (**Figure 2.1f; Table 2.2**). Collectively, these data indicate that the XX genotype increases survival in aging – and suggest a protective effect of ovaries.

To further understand benefits of femaleness on survival in aging, we directly compared the four groups of mice. In mice with ovaries, XX increased lifespan compared to XY (**Figure**

2.2a; Table 2.3). In mice with testes, mortality tended to be higher overall and did not differ between XX and XY genotypes (**Figure 2.2b; Table 2.3**). Ovaries increased lifespan in XX, but not XY mice (**Figure 2.2c,d; Table 2.4**). This suggests that female gonadal hormones, through organizational (long-term) or activational (short-term) effects, increase lifespan in the presence of a second X chromosome.

Since the XX genotype showed a main effect on overall survival, we next tested whether it increases resilience against death anytime during aging. We used the grid search method (Lerman 1980) to determine the point in time when XX and XY lifespan curves change in relation to each other in mice with matching gonads. We then measured statistical differences between the two curves before and after that point to assess whether XX increases survival at any time in aging. In mice with ovaries, XX increased survival after 21 months (**Figure 2.2e; Table 2.5**). In mice with testes, XX also increased survival, but the benefit was earlier, prior to 23 months, and did not alter maximal lifespan (**Figure 2.2f; Table 2.6**). Thus, independent of maximal lifespan, the XX genotype increased survival during aging in both male and female mice, albeit at different times.

DISCUSSION

It is important to note that lifespan and its interventions in mice are influenced by strain, substrain, environment, diet, and factors yet unidentified (Austad and Fischer 2016). Thus, the presence, extent, and direction of sex bias in lifespan can vary across mouse colonies, even among C57BL6 substrains. Future studies examining mixed genetic backgrounds across geographic sites will be valuable. Nonetheless, our data are clear and indicate that female sex derived from the XX sex chromosome complement, combined with ovarian gonad exposure, extended lifespan; furthermore, the XX genotype itself increased survival in aging male and female mice.

Whether the presence of a second X chromosome or the lack of a Y, dictates genetic causes of this intrinsic, female-advantage remains to be determined. Further, how hormone signaling induces ovarian-mediated survival in the presence of a second X chromosome deserves study. Major pathways underlying an XX–ovarian interaction could include IGF1 signaling (Brooks and Garratt 2017), telomeres (Barrett and Richardson 2011), or mitochondrial functions (Gaignard, Savouroux et al. 2015).

Evolutionary pressure may lie upon increased survival and longer lifespan in females to ensure additional care and better fitness for generations of genetic offspring. Alternatively, more male death could benefit the next generation by reducing competition for resources and mates. The identification and modulation of intrinsic, XX-derived mechanisms of female-advantage could open new pathways to modify and increase healthy aging in both sexes.

MATERIALS AND METHODS

Transgenic Mice

Mice for survival curve studies were on a congenic C57BL/6J background and kept on a 12-h light/dark cycle with *ad libitum* access to food and water. Mice were fed standard rodent chow (LabDiet PicoLab Rodent Diet 20 #5053). The standard housing group was five mice per cage based on gonadal sex. Cage bedding was changed once per week. Mice were genotyped using primers to detect the presence of the:

Y chromosome:

SSTY1 Forward primer: CTGGAGCTCTACAGTGATGA

SSTY1 Reverse primer: CAGTTACCAATCAACACATCAC

SRY gene:

SRY Forward primer: AGCCCTACAGCCACATGATA

SRY Reverse primer: GTCTTGCCTGTATGTGATGG

Autosomal control gene

MYO Forward primer: TTACGTCCATCGTGGACAGCAT

MYO Reverse primer: TGGGCTGGGTGTTAGTCTTAT

All animal studies were approved by the Institutional Animal Care and Use Committee of the University of California, San Francisco and conducted in compliance with NIH guidelines.

Inclusion/Exclusion criteria for survival curves

All mice included in this study were bred from the Fore Core Genotypes model (Lovell-Badge and Robertson 1990, Mahadevaiah, Odorisio et al. 1998, Arnold 2004). Mice used for breeding (XY,T) and mice that went missing (random genotypes) were excluded from the analyses. Survival was assessed following weaning at approximately 21 days up until the age indicated. Some mice were euthanized to adhere to the stringent criteria developed by UCSF LARC veterinarians to prevent suffering. Deaths were censored if they occurred for reasons unrelated to natural aging, including: fight wounds, prolapsed anus, eyes bulging, paraphimosis, and dehydration. Ages are represented by months and each month is defined as 30 days.

Statistics

Cox proportional hazards models were applied to estimate main effects of sex chromosome complement and gonads. Specific pairwise comparisons within sex chromosome complement and gonadal type were made using a proportional hazard model with stratification of genotype and phenotype. Prior to using Cox proportional hazard models, potential deviations from the proportional hazard assumption were examined in a model with time-varying coefficients; there was not sufficient evidence to support a time-varying effect of the variables.

A grid search method (Lerman 1980) was used to test if there is a difference in the survival pattern between XX vs. XY in mice with ovaries and in mice with testes. The method estimates a point in time at which the relative survival pattern between two curves changes. The change point

is the time when survival between two curves is different before that time and no longer different after that time; or vice versa. We then examined differences in the survival patterns before and after the determined time point with Cox proportional hazard models. Since we previously found that XX increases survival as a main effect, the hypothesis following the grid search method was formulated as one-sided to determine when in the lifespan XX increases survival compared to XY in mice with ovaries or testes.

FIGURES

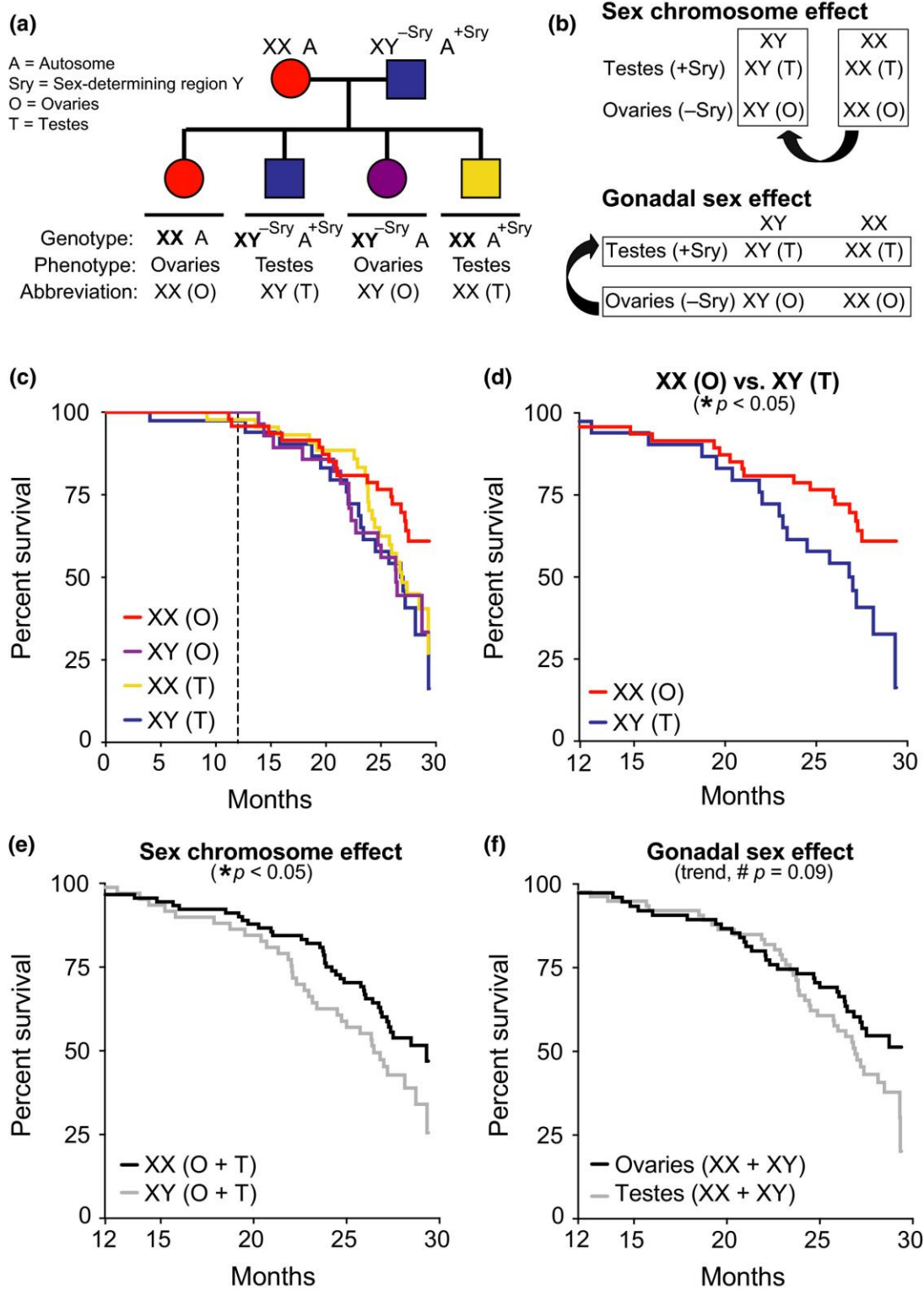


Figure 2.1. XX sex chromosomes contribute to female longevity. (a) Diagram of FCG model. XX females were crossed with XY males with the *Sry* on an autosome instead of the Y

chromosome. **(b)** Strategy to identify causes of sexual dimorphism using the FCG model by testing main effect of sex chromosomes (top) and main effect of gonads (bottom). **(c–f)** Kaplan–Meier curves of FCG aging cohort ($n = 261$ mice): XX(O) $n = 64$, XY(T) $n = 48$, XX(T) $n = 94$, and XY(O) $n = 55$. **(c)** In all groups, survival was tracked until 30 months and statistical analyses were performed with left censoring prior to 12 months as indicated by dotted vertical line. **(d)** Stratified pairwise hazard model comparisons show that XX(O) mice exhibit less mortality than XY(T) mice (XX(O), HR = 0.45, CI = 0.23–0.88, * $p = 0.02$). Cox proportional hazard model analysis shows **(e)** main effect of sex chromosome complement (XX, HR = 0.60, CI = 0.37–0.96, * $p = 0.03$) and **(f)** trend in gonadal effect (ovaries, HR = 0.66, CI = 0.41–1.06, # $p = 0.09$). HR = hazard ratio and CI = confidence interval; HR < 1 is decreased mortality risk (statistical details in **Tables 2.1** and **2.2**)

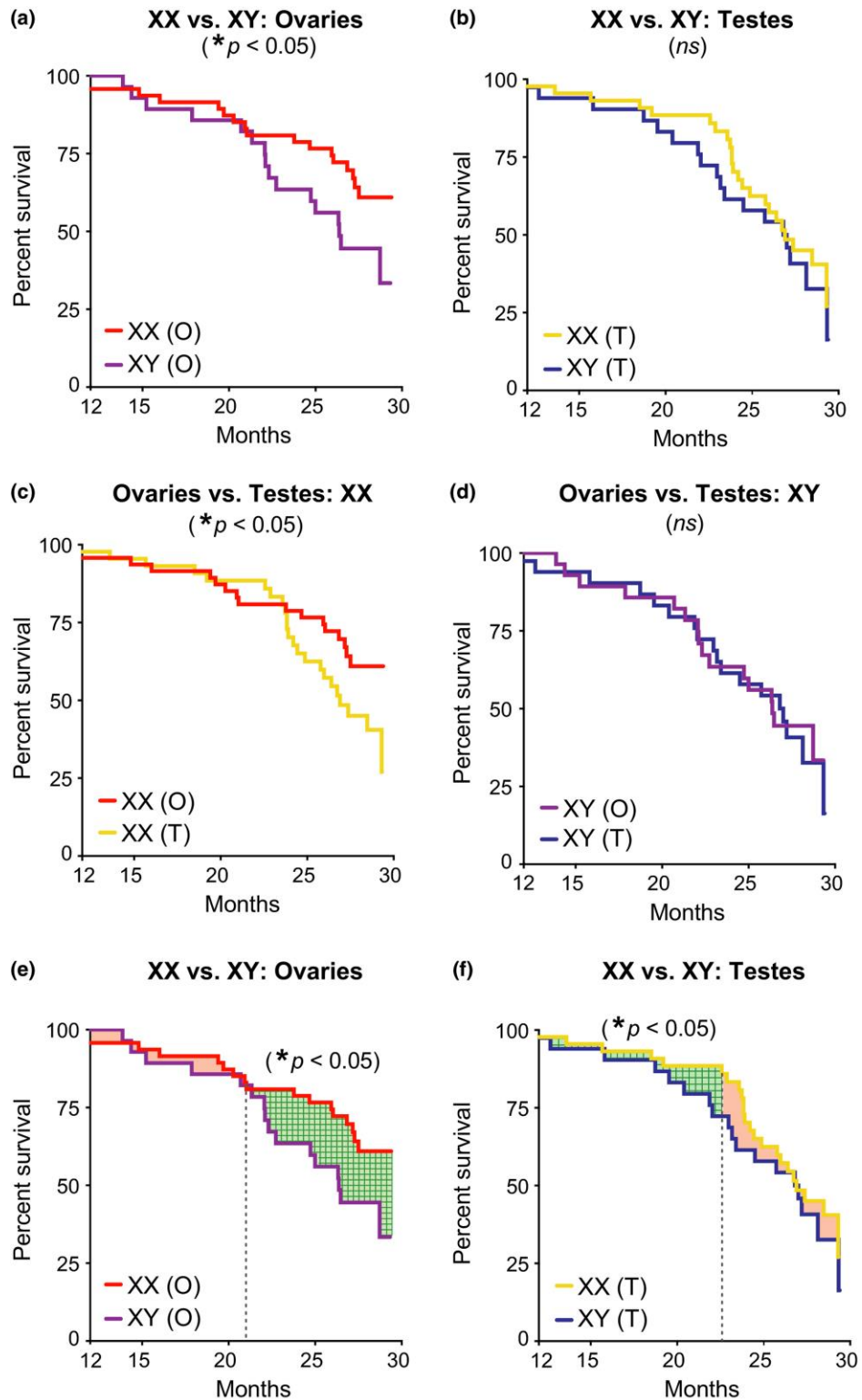


Figure 2.2. XX sex chromosomes extended lifespan in combination with ovaries and independently increased survival during aging. (a–f) Kaplan–Meier curves of FCG aging cohort ($n = 261$ mice): XX(O) $n = 64$, XY(T) $n = 48$, XX(T) $n = 94$, and XY(O) $n = 55$. (a) In mice with ovaries, XX decreased mortality compared to XY (XX, HR = 0.46, CI = 0.23–0.94, $*p = 0.03$).

(b) In mice with testes, mortality tended to be higher overall and did not differ between XX and XY genotypes (XX, HR = 0.81, CI = 0.43–1.50, $p = 0.53$). (c) In XX mice, ovaries decreased mortality compared to testes (ovaries, HR = 0.51, CI = 0.26–0.99, $*p = 0.05$). (d) In XY mice, mortality was lower overall and did not differ between those with testes or ovaries (ovaries, HR = 0.96, CI = 0.48–1.90, $p = 0.90$). (e, f) XX increased survival during aging in mice with ovaries and testes, as determined by a grid search method that statistically identifies the point in time that curves change in relation to each other (indicated by dotted vertical line); differences in lifespan before and after that time point are shaded (significant differences = green grid pattern; no difference = shaded red). (e) In mice with ovaries, the relationship between XX and XY lifespan curves changed at 21 months with no difference before then (XX, HR = 0.52, SE = 0.64, $p = 0.31$) and significant difference afterward (XX, HR = 0.37, SE = 0.45, $*p = 0.01$). (f) In mice with testes, the relationship between XX and XY lifespan curves changed at 23 months with a significant difference before then (XX, HR = 0.36, SE = 0.60, $*p < 0.05$) and no difference afterward (HR = -0.78, SE = 0.33, $p = 0.23$). HR = hazard ratio, CI = confidence interval, and SE = standard error; HR < 1 is decreased mortality risk (statistical details in **Tables 2.3–2.6**)

TABLES

Table 2.1. Stratified proportional hazard model shows XX(O) had significantly decreased mortality compared to the each of the other FCG experimental groups. HR=Hazard Ratio estimate, risk of death, CI=Confidence Interval. References are XX and ovaries. Table summarizes results in **Fig. 2.1c,d**

	HR	95% CI	P value	Significance
XX(O) vs. XY(T)	0.45	0.23-0.88	0.020	*
XX(O) vs. XX(T)	0.51	0.26-0.99	0.046	*
XX(O) vs. XY(O)	0.46	0.23-0.94	0.033	*

Table 2.2. Cox proportional hazard model shows significant main effect of sex chromosome complement. XX decreases mortality and ovaries tend to decrease mortality. HR=Hazard Ratio estimate, risk of death, CI=Confidence Interval. References are XX and ovaries. Table summarizes results in **Fig. 2.1e,f**.

	HR	SE	z	95% CI	P value	Significance
Main Effect: XY vs. XX	0.60	0.14	-2.15	0.37-0.96	0.032	*
Main Effect: Testes vs. Ovaries	0.66	0.16	-1.72	0.41-1.06	0.086	#

Table 2.3. Stratified proportional hazard model of sex chromosome effect within gonadal sex group. XX sex chromosome complement decreased overall mortality in mice with ovaries but not in those with testes. HR=Hazard Ratio estimate, risk of death. CI=Confidence Interval. Reference is XX genotype. Table summarizes results in **Fig. 2.2a,b**.

	HR	95% CI	P value	Significance
XY vs. XX: Mice with Ovaries	0.46	0.23-0.94	0.033	*
XY vs. XX: Mice with Testes	0.81	0.43-1.5	0.53	n.s.

Table 2.4. Stratified proportional hazard model of gonadal sex effect within sex chromosome group. Ovaries decrease mortality in XX but not in XY mice. HR=Hazard Ratio estimate, risk of death. CI=Confidence Interval. Reference is Ovaries. Table summarizes results given in **Fig. 2.2c,d**.

	HR	95% CI	P value	Significance
Testes vs. Ovaries: Mice with XX Genotype	0.51	0.26-0.99	0.046	*
Testes vs. Ovaries: Mice with XY Genotype	0.96	0.48-1.9	0.900	n.s.

Table 2.5. Stratified proportional hazard model following grid search method (Lerman 1980) in mice with ovaries. XX decreases death during aging, compared to XY, after 21 months of age. HR=Hazard Ratio estimate, risk of death. SE=Standard Error. Reference is XX genotype. Table summarizes results in **Fig. 2.2e**.

Time interval	HR	SE	P-value	Significance
12mo-21mo	0.52	0.64	0.31	n.s.
21mo-30mo	0.37	0.45	0.013	*

Table 2.6. Stratified proportional hazard model following grid search method (Lerman 1980) in mice with testes. XX decreases early death during aging, compared to XY, before 23 months of age. HR=Hazard Ratio estimate, risk of death. SE=Standard Error. Reference is XX genotype. Table summarizes results in **Fig. 2.2f**.

Time interval	HR	SE	P-value	Significance
12mo-23mo	0.36	0.60	0.045	*
23mo-30mo	0.78	0.33	0.23	n.s.

Chapter 3 – A second X chromosome contributes to resilience in a mouse model of Alzheimer’s disease

SUMMARY

A major sex difference in Alzheimer’s disease (AD) is that men with the disease die earlier than women and show more cognitive deficits. Here, we show that the X chromosome affects AD-related vulnerability in mice expressing the human amyloid precursor protein (hAPP). XY-hAPP mice genetically modified to develop testicles or ovaries showed worse mortality and deficits than did XX-hAPP mice with either gonad, indicating a potential sex chromosome effect. To dissect whether the absence of a second X chromosome or the presence of a Y chromosome conferred a disadvantage on male mice, we varied sex chromosome dosage. With or without a Y chromosome, hAPP mice with one X chromosome showed worse mortality and deficits than did those with two X chromosomes. Thus, adding a second X chromosome conferred resilience to XY males and XO females. In addition, the Y chromosome, its sex-determining region Y gene (*Sry*), or testicular development modified mortality in hAPP mice with one X chromosome such that XY males with testicles survived longer than did XY or XO females with ovaries. Furthermore, a second X chromosome conferred resilience, in part, through the candidate gene *Kdm6a*, that does not undergo inactivation. In humans, genetic variation in *KDM6A* was linked to higher brain expression and associated with less cognitive decline in aging and preclinical AD, suggesting its relevance to human brain health. Our study suggests a potential role for sex chromosomes in modulating disease vulnerability related to AD.

INTRODUCTION

The expansion of translational neuroscience to investigate sex differences and their mechanistic underpinnings is of major consequence to human health (McCarthy, Woolley et al.

2017). Understanding what makes one sex more vulnerable (or resilient) to aging and disease unravels new pathways to target with treatments that could benefit both sexes.

Alzheimer's disease (AD) is the most common neurodegenerative condition and a global health threat. In the absence of effective medical treatments, more than 50 million men and women worldwide will suffer from this devastating condition by 2050 (Wimo and Prince 2015). The burdens of the disease combined with failed clinical trials (Elmaleh, Farlow et al. 2019) warrant a deeper understanding of the heterogeneous nature of AD, with the goal of developing better therapies.

Being male or female, defined here as harboring a different sex chromosome complement (XY versus XX), is an understudied biologic variable that contributes heterogeneity to AD. Sex differences in AD reveal differing vulnerabilities in men and women (Mielke, Vemuri et al. 2014, Dubal 2020). Many more women suffer from AD, largely due to their longevity (Hebert, Scherr et al. 2001) as they live to advanced ages, when AD risk and incidence is highest. In contrast, men with the disease die earlier in populations worldwide, indicating a male disadvantage with early-onset (Heyman, Wilkinson et al. 1987, Claus, van Gool et al. 1998, Ueki, Shinjo et al. 2001) and late-onset (Stern, Tang et al. 1997, Lapane, Gambassi et al. 2001) subtypes of AD. Furthermore, in aging and preclinical AD before the age of 85 years, men show worse cognition (Buckley, Mormino et al. 2018), more cognitive decline (Cerhan, Folsom et al. 1998, Jack, Wiste et al. 2015, Casaletto, Elahi et al. 2019), and increased measures of neurodegeneration (Jack, Thorneau et al. 2016), despite similar deposition of amyloid and tau (Jack, Wiste et al. 2015, Jack, Wiste et al. 2017), the pathological hallmarks of AD. This could underlie higher prevalence (Jack, Thorneau et al. 2019) and earlier onset of mild cognitive impairment (MCI) in men compared to women in some populations (Petersen, Roberts et al. 2010, Roberts, Geda et al. 2012). Here, we assess sex-biased mortality in AD by meta-analysis, investigate whether sex chromosomes affect vulnerability in a mouse model of AD, and test whether an X chromosome gene influences cognition in the mouse model or associates with cognition in a human population.

RESULTS

Male sex increases mortality in AD and in hAPP mice

We conducted a meta-analysis of data collected on mortality in human populations worldwide. Only longitudinal studies that defined the time variable as age of disease onset or duration of disease after onset were included; cross-sectional studies were excluded. Our meta-analysis showed that male sex significantly increased risk for death in AD by 62% compared to female sex (male hazard ratio (HR) 1.63, CI 1.45 to 1.84, $P < 0.0001$; **Figure 3.1**). We then examined mortality in 3,161 transgenic mice that expressed mutated forms of the human amyloid precursor protein (hAPP) (line J20) (Mucke, Masliah et al. 2000) and exhibited premature death, cognitive impairments, and pathological markers of the disease. Male hAPP mice died significantly earlier than did female hAPP mice on two background strains, C57BL6/J ($P < 0.001$, **Figure 3.2A**) and a mixed F1 generation of C57BL6/J crossed with FVB/N ($P < 0.05$, **Figure 3.3**).

Men and women undergo depletion of circulating gonadal hormones with aging (Morley, Kaiser et al. 1997, Ferrini and Barrett-Connor 1998, Veldhuis 2008), but mice do not (Nelson, Latham et al. 1975, Nelson, Felicio et al. 1992) (**Figure 3.4**). Because AD is a disease of aging, we simulated human reproductive aging in male and female non-transgenic and hAPP mice by gonadectomy to deplete circulating hormones (**Figure 3.2B**) and assessed survival in gonadectomized male and female hAPP mice. Male hAPP mice still died significantly faster than did female mice ($P < 0.05$, **Figure 3.2C**). We explored whether hAPP mice showed a sex difference in cognitive functions independent of gonadal hormones. To reduce confounders, equalize hormones between sexes, and model reproductive aging of humans, we gonadectomized all non-transgenic and hAPP mice.

Male sex increases cognitive and molecular deficits in hAPP mice

We tested spatial learning and memory of gonadectomized mice in the Morris water maze and found that hAPP mice were impaired ($P < 0.05$, **Figure 3.2D**). However, male hAPP mice traveled significantly longer distances to find the hidden platform than did females, indicating poorer learning capacity ($P < 0.05$, **Figure 3.2D**). In a probe trial, male hAPP mice lacked memory retention, in contrast to all other groups (**Figure 3.2E**). All mice located the target platform equally well when visible (**Figure 3.2D**) and male and female mice within each group swam at equal speeds, although hAPP mice overall swam marginally slower ($P < 0.001$, **Figure 3.5A**).

In passive avoidance testing, which measures hippocampus- and amygdala-dependent fear memory, male hAPP mice, but not females, quickly reentered the dark chamber where they received a shock during training ($P < 0.05$, **Figure 3.2F**). Male hAPP mice, but not females, lost the fear memory ($P < 0.05$, **Figure 3.2G and H**). Male vulnerability to deficits was significant with gonadectomy at young, middle or old life stages ($P < 0.05$ to $P < 0.001$, **Figure 3.6**), across a range of cognitive and behavioral tasks ($P < 0.05$ to $P < 0.001$, **Figure 3.6**), and in an independent transgenic line of hAPP mice, hAPP-J9, which show milder deficits (Mucke, Masliah et al. 2000, Chin, Palop et al. 2005, Roberson, Halabisky et al. 2011) ($P < 0.05$, **Figure 3.7**).

Male hAPP mice showed significantly decreased expression of the neuronal activity-related protein calbindin ($P < 0.05$, **Figure 3.2I**) in the hippocampus. Male and female hAPP mice did not differ in soluble β -amyloid ($A\beta$) (**Figure 3.2J**) or protein expression of hAPP, total tau, and phospho-tau in the hippocampus (**Figures 3.8A to D and 3.9**) when cognitive and behavioral deficits had emerged (3 to 4 months). They also did not differ in amyloid plaque deposition (**Figure 3.2K and L; Figure 3.10**) during middle age (14.5 to 15 months); however, females tended to show more plaques at a very old age (24 to 27 months) (**Figure 3.11**) as previously observed (Callahan, Lipinski et al. 2001), despite decreased behavioral deficits compared to males.

We examined hAPP mRNA expression in the presence and absence of gonads and found that hAPP mRNA expression was equivalent across the experimental groups (**Figure 3.12**).

Therefore, any unintentional gonadal hormone influences at the promoter of hAPP-J20 mice were not observed, a critical measure when directly comparing sexes in transgenic disease models.

Sex chromosomes mediate increased male vulnerability in hAPP mice

To dissect the etiology of male disadvantage related to AD after gonadectomy, we examined Four Core Genotypes (FCG) (Mahadevaiah, Odorisio et al. 1998, Arnold and Chen 2009) mice. In normal mice and humans, the *Sry* gene on the Y chromosome encodes a protein that initiates development of testes followed by perinatal masculinization of the body and brain (McCarthy and Arnold 2011). In the FCG mouse model, *Sry* is transposed onto an autosome from the Y chromosome. This genetic manipulation enables generation of XX and XY mice, each with either female ovarian (F, –*Sry*) or male testicular (M, +*Sry*) development: XX(F) ovaries, XX(M) testes, XY(F) ovaries, XY(M) testes. A sex difference that varies by gonads is gonadal sex-mediated; one that varies by chromosome complement is sex chromosome-mediated (**Figure 3.13A**).

We crossed FCG mice with hAPP mice to produce eight genotypes that included the four sex genotypes with or without hAPP (**Figure 3.13B**). After sexual differentiation and reproductive maturity, we gonadectomized mice and assessed survival, cognition, and biochemical markers (**Figure 3.13C**). XY-hAPP mice sexually differentiated as either male (M, testicular phenotype, +*Sry*) or female (F, ovarian phenotype, –*Sry*) died faster than did XX-hAPP mice of either gonadal phenotype (**Figure 3.13D to F**). In addition to the main effect of sex chromosomes, sex chromosomes interacted with gonadal phenotype in XY-hAPP mice. That is, XY-hAPP males (+*Sry*) survived longer than XY-hAPP females (–*Sry*) ($P < 0.05$, **Figure 3.13G**), an effect not observed in XX-hAPP mice.

To determine whether sex chromosomes mediate male vulnerability to A β -related cognitive deficits, we tested mice in the Morris water maze. In finding the hidden platform, male or female XY-hAPP mice showed significantly worse learning than did male or female XX-hAPP

mice ($P < 0.01$, **Figure 3.13H and I; Figure 3.14A**). In contrast, all non-transgenic mice without hAPP learned similarly (**Figure 3.13H and I; Figure 3.14A**). In a probe trial, XY-hAPP mice lacked memory retention (**Figure 3.13J and K; Figure 3.14B**) whereas all XX (non-transgenic and hAPP) mice remembered, regardless of being male or female ($P < 0.05$, **Figure 3.13J; Figure 3.14B**). All mice swam at equal speeds and located a visible target platform equally (**Figure 3.14B and C**). In passive avoidance testing, male or female XY-hAPP mice showed significantly worse fear memory than did male or female XX-hAPP and non-transgenic mice ($P < 0.001$ and $P < 0.01$ respectively, **Figure 3.15**). As in non-FCG hAPP mice, male or female XX and XY mice did not differ in the amount of soluble $A\beta$ in the hippocampus brain (**Figure 3.8E**) at the age of cognitive and behavioral testing.

A second X chromosome confers resilience to AD-related vulnerability in XY (male) and XO (female) hAPP mice

To further dissect causes of the sex chromosomal effects, we determined whether the presence of a Y or the lack of a second X chromosome conferred male disadvantage in hAPP mice. We investigated the XY* model (Eicher, Hale et al. 1991, Arnold 2009) of sex chromosomal biology in mice with and without hAPP. The Y* chromosome in XY* males contains an altered pseudoautosomal region that recombines abnormally with the X chromosome during meiosis. Progeny of XY* males crossed with XX females include four sex genotypes roughly equivalent to the following: XX and XO mice with ovaries, and XY and XXY mice with testes. A sexual dimorphism that varies by the presence or absence of a Y is Y-chromosome-mediated; one that varies by the presence of one versus two X's, is X chromosome-mediated (**Figure 3.16A**).

We crossed XY* males with hAPP females to produce eight genotypes of mice exhibiting varying dosages of X- and Y-chromosomes, with or without hAPP (**Figure 3.16B**). We gonadectomized mice and then assessed survival, cognition, and biochemistry (**Figure 3.16C**). Mice with one X chromosome (XY-hAPP and XO-hAPP) died significantly faster than did those

with two X chromosomes (XX-hAPP and XXY-hAPP) ($P < 0.01$, **Figure 3.16D to F**). Therefore, the addition of an X chromosome to XY-hAPP mice prevented male vulnerability, extending survival to that observed in XX-hAPP females. In addition to the main effect of X dose ($P < 0.01$, **Figure 3.16E**), but not of Y (**Figure 3.16F**), the Y interacted with the X, that is, XY-hAPP mice survived longer than XO-hAPP mice ($P < 0.01$, **Figure 3.16G**).

We then tested whether the addition of an X to XY-hAPP mice reduced male vulnerability to cognitive deficits in the passive avoidance task (**Figure 3.16H to J**). Both male and female hAPP mice with one X chromosome (XY-hAPP and XO-hAPP) showed significant forgetting of fear memory ($P < 0.05$, **Figure 3.16H to J**) whereas those with two X chromosomes (XX-hAPP and XXY-hAPP) did not forget (**Figure 3.16H to J**). In contrast, all mice without hAPP had comparable and robust fear memory. As in FCG-hAPP mice, XY*-hAPP mice with 1X or 2X chromosomes did not differ in amount of soluble A β in the hippocampus (**Figure 3.8F**). Thus, although hAPP mice with 1X or 2X chromosomes had comparable amounts of A β , hAPP mice with 2X's were less impaired.

A second X chromosome elevates *Kdm6a* expression independent of gonadal phenotype or the Y chromosome

We sought to understand how a second X chromosome could confer resilience, because XY and XX mice express only one active X due to X chromosome inactivation in females. Whereas X chromosome inactivation silences one X chromosome in mammalian XX cells, a small subset of X-linked genes escape X chromosome inactivation and show transcription from both alleles leading to higher expression in females (Carrel and Willard 2005, Berletch, Yang et al. 2010, Yang, Babak et al. 2010, Tukiainen, Villani et al. 2017). Of those, we focused on lysine-specific demethylase 6a (*Kdm6a*, also known as *Utx*), an H3K27-demethylase that consistently escapes X chromosome inactivation in both mice and humans (Greenfield, Carrel et al. 1998,

Berletch, Ma et al. 2015). Loss of function mutations in *KDM6A* cause cognitive deficits in humans (Lederer, Grisart et al. 2012, Miyake, Koshimizu et al. 2013, Miyake, Mizuno et al. 2013, Van Laarhoven, Neitzel et al. 2015, Bogershausen, Gatinois et al. 2016, Yang, Tan et al. 2016), and *Kdm6a* plays a post-developmental role in mouse synaptic plasticity and cognition (Tang, Zeng et al. 2017).

We therefore examined *Kdm6a* in mouse brains. We first confirmed that *Kdm6a* escapes X chromosome inactivation in the XX mouse brain through RNA fluorescence *in situ* hybridization (RNA-FISH) (Panning 2004) in mouse primary cortical neurons. Isolated XX neuronal nuclei with *Xist* RNA coating of the inactive X chromosome, indicating X chromosome inactivation, showed *Kdm6a* labeling at two sites, marking its transcription from both the active and inactive X chromosomes (**Figure 3.17A**). In contrast, XY neurons showed only one site for transcription (**Figure 3.17A**). Immunolabeling of *Kdm6a* protein in the adult hippocampus of XX and XY mice with a well-characterized antibody (Wiedemuth, Thieme et al. 2018) showed a largely neuronal cytoplasmic staining pattern that was diffuse in both XX and XY mouse brains (**Figure 3.17B**).

We assessed whether two X chromosomes increased expression of *Kdm6a* protein and mRNA in mouse hippocampus. *Kdm6a* protein expression was significantly higher in XX mice than in XY mice as measured by two antibodies ($P < 0.05$, **Figure 3.17C and D**). To determine whether the second X chromosome primarily governed higher expression, we assessed *Kdm6a* mRNA in FCG and XY* mice. As anticipated (Berletch, Deng et al. 2013, Lei and Jiao 2018) hippocampal *Kdm6a* was significantly elevated in XX mice with testes and ovaries ($P < 0.001$, **Figure 3.17E**). The presence of neither hAPP nor the Y chromosome altered this primary X effect (**Figure 3.17F**).

***KDM6A* expression is elevated in the brains of women, and *KDM6A* genetic variation in humans associates with cognitive resilience**

We explored whether *KDM6A* mRNA was altered by sex in brains of individuals with and without AD. We queried gene expression from a public dataset (GSE 15222, **Tables 3.1 and 3.2**) accounting for age, postmortem interval and sex. *KDM6A* expression was significantly higher in pathologically confirmed AD cases relative to controls in the temporal cortex, an area affected in early AD ($P=3.64 \times 10^{-4}$, **Figure 3.18A**). This increase was independently confirmed in two other public datasets of human post-mortem gene expression in the temporal cortex, parahippocampal gyrus, and superior temporal gyrus (**Tables 3.1 and 3.3**). In contrast, regions typically affected later or spared in AD such as the cerebellum showed no changes (**Tables 3.1 to 3.3**). We then assessed *KDM6A* expression in brains of individuals identified as male or female in the GSE 15222 dataset. *KDM6A* expression was higher in females with ($P=4.83 \times 10^{-4}$, **Figure 3.18B**) and without AD ($P=9.79 \times 10^{-4}$, **Figure 3.18B**).

We then queried whether *KDM6A* expression, by proxy of a genetic variation, was associated with cognitive change over time. Using the Genotype-Tissue Expression Project (GTEx) online portal of gene expression across tissues of nearly 1000 individuals (Consortium, Laboratory et al. 2017), we searched for common variants associated with altered expression of *KDM6A*. The minor allele of one genetic variant, rs12845057, was associated with increased expression of *KDM6A* in the brain ($P=7.0 \times 10^{-6}$). Frequency of the minor allele (A) is about 14% globally and 7% in Europeans (Sherry, Ward et al. 2001). To test associations between the *KDM6A* variant and cognitive change, we queried the Alzheimer's Disease Neuroimaging Initiative (ADNI) dataset derived from a multi-site study of individuals with both whole genome sequencing and serial neuropsychological examinations ($n=778$) that is enriched for individuals with MCI, a transition phase to AD. The minor allele was distributed equally among categories of cognitively normal ($n=268$), MCI ($n=465$), and AD ($n=45$) individuals, indicating that it did not associate with disease risk (cohort demographics, **Table 3.4**). Next, we used linear mixed-effects

regression models to test for an association between the minor allele A of the *KDM6A* variant and cognitive change, accounting for baseline age, sex, education, and *APOE* ϵ 4 dose. Increasing dose of the minor allele of the *KDM6A* variant was significantly associated with less cognitive decline over time using the Mini-Mental State Examination (MMSE) ($\beta=0.141$, SE 0.035, $P=0.00005$, **Figure 3.18C**). This finding was consistent in another cognitive measure using the Alzheimer's Disease Assessment Scale (ADAS-cog), in overall function using the clinical dementia rating sum of boxes score (CDR), when assessing women only in all measures (**Figure 3.19**), and when assessing cognition in cognitively normal and in MCI individuals as subgroups (**Table 3.5**).

Kdm6a* knockdown in XX mouse neurons worsens, whereas *Kdm6a* overexpression in XY neurons attenuates A β toxicity *in vitro

We next turned to experiments with primary wildtype mouse neurons exposed to recombinant A β . The A β preparation was enriched for oligomers during the experimental time frame, based on our previous characterization (Cheng, Dubal et al. 2009). XY mouse neurons were more vulnerable to A β -induced toxicity, in a dose-dependent manner, compared to XX neurons, using both the 3-(4,5-dimethylthiazol-2-yl)-2,5-diphenyltetrazolium bromide (MTT) ($P<0.001$, **Figure 3.20A**) and lactate dehydrogenase (LDH) ($P<0.01$, **Figure 3.21**) assays. In parallel with *in vivo* findings, neurons derived from XY* mice with one X chromosome (XY and XO) were significantly more vulnerable to A β toxicity than those with two X chromosomes (XX and XXY) ($P<0.001$, **Figure 3.20B and C**). The protective effect of two X chromosomes was decreased by the Y chromosome ($P<0.05$, **Figure 3.20B**), indicating an X:Y interaction.

Given that *Kdm6a* escapes X chromosome inactivation in XX neurons, and is increased in XX compared to XY brains, we tested directly whether *Kdm6a* modulates neuronal susceptibility to A β toxicity *in vitro*. In XX mouse neurons, we decreased *Kdm6a* expression ($P<0.01$, **Figure 3.20D and E**) to that found in XY neurons via lentivirus-mediated knockdown. Knockdown of

Kdm6a in XX mouse neurons significantly worsened dose-dependent A β toxicity ($P<0.01$, **Figure 3.20F**), to a range observed in XY neurons. In XY mouse neurons, we increased *Kdm6a* expression to that found in XX neurons or higher ($P<0.01$, **Figure 3.20D and G**) via lentivirus-mediated overexpression. Overexpression of *Kdm6a* in XY mouse neurons significantly attenuated dose-dependent A β toxicity ($P<0.001$, **Figure 3.20H**), to a range observed in XX neurons.

***Kdm6a* attenuates male vulnerability to cognitive impairments in XY-hAPP mice**

We next determined whether increasing expression of *Kdm6a* attenuated male vulnerability to cognitive deficits in XY-hAPP mice. We gonadectomized XY non-transgenic and hAPP mice, injected lentivirus with (*Kdm6A*-OE) or without (control) the *Kdm6a* transgene bilaterally into the dentate gyrus, a region that affects spatial learning and memory, and analyzed mice behaviorally 1 month later (**Figure 3.22A**). Lentiviral-mediated overexpression of *Kdm6a* in XY males increased *Kdm6a* mRNA expression in the dentate gyrus ($P<0.05$, **Figure 3.22B**) to that expected in XX females. In finding the hidden platform of the Morris water maze, XY-hAPP-*Kdm6a*-OE mice showed significantly better performance than XY-hAPP control mice measured by latency ($P<0.001$, **Figure 3.22C**) and learning ($P<0.05$, **Figure 3.22D**), quantified by comparing the last day of training to the first. Similarly, XY-hAPP-*Kdm6a*-OE mice showed significantly better learning than did XY-hAPP control mice measured by distance ($P<0.001$, **Figure 3.22E and F**), although distance curves did not statistically differ. In a probe trial, XY-hAPP-*Kdm6A*-OE mice showed robust spatial memory retention, compared to XY-hAPP control mice ($P<0.01$, **Figure 3.22G and H**) performing similarly to unimpaired non-transgenic mice. With the visible platform, hAPP mice swam marginally faster with longer distance than non-transgenic mice; however, overexpression of *Kdm6a* did not alter either measure in either genotype (**Figure 3.5D and E**). Further, increasing *Kdm6a* expression in XY mice did not alter hAPP-induced

hyperactivity in the open field task and increased time spent in open arms in the elevated plus maze in hAPP mice (**Figure 3.23**).

DISCUSSION

Our data suggest a role for sex chromosomes in countering deficits and toxicity related to AD in both sexes of mice. A second X chromosome decreased mortality and brain dysfunction in gonadectomized male and female hAPP mice, without altering soluble A β or co-pathogenic proteins. A second X chromosome conferred resilience, in part, through the candidate gene *Kdm6a*, a histone demethylase that escapes X chromosome inactivation, causing higher expression in cells with two X's compared to one X. Genetic variation of *KDM6A* linked to its increased brain expression was associated with slower cognitive decline in an aging population of individuals, including those with MCI.

Dissection of sex differences and their mechanistic underpinnings with powerful genetic tools provides opportunities to understand disease and unravel new sex-based pathways (Sampathkumar, Bravo et al. 2019). Male sex is a major, underappreciated risk factor for rapid progression to death in AD (Heyman, Wilkinson et al. 1987, Stern, Tang et al. 1997, Claus, van Gool et al. 1998, Lapane, Gambassi et al. 2001, Ueki, Shinjo et al. 2001), as confirmed by our meta-analysis (Fig. 1), and in other neurodegenerative conditions (Sejvar, Holman et al. 2005, Buter, van den Hout et al. 2008, Kihira, Yoshida et al. 2008, Forsaa, Larsen et al. 2010). These findings do not contradict the fact that more women have AD due to their longevity (Hebert, Scherr et al. 2001) and their increased risk or incidence after age 85 (Jorm and Jolley 1998, Mielke, Vemuri et al. 2014, Buckley, Mormino et al. 2018, Dubal 2020), which together contribute to a higher lifetime risk of AD in women compared to men (Brookmeyer and Abdalla 2018). When men get AD they die faster (Heyman, Wilkinson et al. 1987, Stern, Tang et al. 1997, Claus, van Gool et al. 1998, Lapane, Gambassi et al. 2001, Ueki, Shinjo et al. 2001). The male brain may be

biologically older and more vulnerable, an idea supported by epigenetic (Horvath, Gurven et al. 2016) and metabolic studies (Goyal, Blazey et al. 2019) of humans.

In aging and preclinical AD, male sex may increase the likelihood of abnormalities favoring transition to clinical dementia. Men show significantly worse memory function (Buckley, Mormino et al. 2018) and cognitive decline than do women (Cerhan, Folsom et al. 1998, Jack, Wiste et al. 2015, Casaletto, Elahi et al. 2019), implying less compensation for similar subclinical brain pathology measured by positron emission tomography imaging of amyloid (Jack, Wiste et al. 2015, Buckley, Mormino et al. 2018). In studies of AD biomarkers (Jack, Bennett et al. 2016), men show increased neurodegeneration (Jack, Therneau et al. 2016, Jack, Wiste et al. 2017), a precursor for dementia. These findings could underlie earlier onset and increased incidence or prevalence of MCI observed in men from many (Koivisto, Reinikainen et al. 1995, Ganguli, Dodge et al. 2004, Caracciolo, Palmer et al. 2008, Petersen, Roberts et al. 2010, Roberts, Geda et al. 2012) although not all (Kivipelto, Helkala et al. 2001, Solfrizzi, Panza et al. 2004, Di Carlo, Lamassa et al. 2007) populations.

Recent studies of aging and AD [reviewed in (Dubal 2020)] indicate similar amyloid amounts in the brain (Jack, Wiste et al. 2015, Jansen, Ossenkoppele et al. 2015, Jack, Wiste et al. 2017, Buckley, Mormino et al. 2018, Hohman, Dumitrescu et al. 2018) and cerebrospinal fluid (CSF) (Hohman, Dumitrescu et al. 2018) between men and women, similar overall tau burden (Buckley, Mormino et al. 2019), but increased CSF and regional tau in women with high amyloid (Hohman, Dumitrescu et al. 2018, Buckley, Mormino et al. 2019). Likewise, AD pathology is similar between the sexes, up until older ages (Jansen, Ossenkoppele et al. 2015), when both pathology and risk of AD increases in women. Each sex may respond differently to comparable amounts of pathogenic proteins, a possibility observed in mice (Kodama, Guzman et al. 2020), which may explain why with similar tau loads, men show less neuro-structural preservation (Ossenkoppele, Lyoo et al. 2020) and more cognitive impairment (Digma, Madsen et al. 2020).

Congruent with human observations, soluble A β and amyloid deposition were similar between the sexes in our mice until very old age and did not explain male vulnerability at the neuronal or cognitive level. Other AD mouse models show very high amounts of A β with increased mortality in female mice (Wang, Tanila et al. 2003, Hirata-Fukae, Li et al. 2008, Halford and Russell 2009, Carroll, Rosario et al. 2010), and are thus incongruent with our mouse findings. Since no single model of AD fully recapitulates human AD, a disease with a wide clinical spectrum, we conducted cellular viability, cognitive, behavioral, synaptic, and mortality studies that collectively showed worse outcomes in primary neurons and gonadectomized male mice, a sex bias that persisted in our hAPP mice regardless of age at hormone depletion, mouse strain, or genetic background. Our mouse studies focused on hAPP/A β -dependent abnormalities, representing a specific component of AD, a complex disease comprising multiple pathogenic proteins and risk factors.

We used gonadectomy to equate gonadal hormones between the sexes and simulate human reproductive aging, an approach distinctly different from previous studies of sex in AD-related models (Dubal, Broestl et al. 2012). Gonadectomy enables direct comparison of the sexes without confounding, activational (short-acting) effects of ovarian and testicular hormones. This is of value because ovarian hormones modulate A β , network dysfunction and cognitive deficits in female hAPP mice (Pike 2017, Broestl, Worden et al. 2018). Our experiments did not test the activational effects of hormonal treatments [reviewed in (Pike 2017, Broestl, Worden et al. 2018)].

Sex chromosomes largely governed sex differences in vulnerability to mortality, cognitive dysfunction, molecular impairments, and cellular dysfunction in the FCG mouse model. The XY genotype in hAPP mice that developed with ovaries or testes worsened measures, compared to the XX genotype that developed with ovaries or testes. Similarly, we recently found that sex chromosomes influenced mortality in mice during normal aging (Davis, Lobach et al. 2019), suggesting action on fundamental pathways converging in aging and disease. The lack of a second X chromosome, rather than the presence of a Y chromosome, caused male disadvantage

in animal and cellular models of AD in the XY* model. The presence of only one X chromosome (in XO females and XY males) consistently worsened hAPP/A β -related mortality, cognitive deficits, and cellular viability in both males and females, compared to two X chromosomes (in XX females and XXY males). The Y chromosome, the Y chromosome gene *Sry*, testes, or some combination of these decreased mortality in hAPP mice with one, but not two X chromosomes. XY-hAPP males (+*Sry*) survived longer than did XY-hAPP females (–*Sry*) or XO-hAPP females (–*Sry*) indicating a potential protective role of the *Sry* protein or of testicular development itself in the XY, but not XX, genotype. Given that the X and Y chromosomes share homologous genes in pseudoautosomal regions, select Y genes may partially compensate for the lack of a second X chromosome.

Many factors influencing neural function reside on the X chromosome (Skuse 2005). Two X chromosomes could confer neural advantage through increased X dose arising from baseline escape of the inactive X chromosome. Whereas XY and XX organisms express one active X due to X chromosome inactivation in females, select factors like the *Kdm6a* gene escape. *Kdm6a* is a histone demethylase that robustly and consistently escapes X chromosome inactivation in female mice and humans (Greenfield, Carrel et al. 1998, Berletch, Ma et al. 2015) and is enriched in the brain (Vawter, Evans et al. 2004, Xu, Deng et al. 2008, Lei and Jiao 2018). The second X chromosome increased *Kdm6a* expression, independent of gonads or the Y chromosome, in our mice. This is important because the Y paralog of *Kdm6a*, UTY (Greenfield, Scott et al. 1996) has high homology to *Kdm6a* (Gazova, Lengeling et al. 2019) but a nearly inactive histone demethylation domain (Shpargel, Sengoku et al. 2012, Walport, Hopkinson et al. 2014). The presence of UTY in XY neurons and mice did not modify *Kdm6a*-mediated attenuation of AD-related toxicity *in vitro* or *in vivo*.

KDM6A expression in human brain was higher in females compared to males and in those with AD compared to controls. Because *KDM6A* loss of function mutations cause intellectual disability in humans (Lederer, Grisart et al. 2012, Miyake, Koshimizu et al. 2013, Miyake, Mizuno

et al. 2013, Van Laarhoven, Neitzel et al. 2015, Yang, Tan et al. 2016) and *Kdm6a* elevation caused neural and cognitive resilience in our mouse studies, it is interesting to speculate that increased *KDM6A* in AD could be a protective, compensatory response.

A common genetic variant in an intergenic region near *KDM6A*, rs12845057, was associated with greater expression in human brain. The minor allele frequency varies across populations and about 13% of females and 6.5% of males carry it globally (Sherry, Ward et al. 2001). In the current study of the ADNI cohort, increasing the minor allele dose was associated with cognitive resilience in individuals undergoing longitudinal testing over a decade, a finding consistent across clinical measures and when we assessed females only. Our analysis in males, who carry half the frequency, was likely limited by statistical power. In our subgroup analyses by clinical diagnosis, individuals with MCI showed the most resilience associated with the *KDM6A* minor allele, suggesting that increased *KDM6A* could modify clinical trajectory during the transitional period from MCI to AD. While the ADNI cohort includes longitudinal data and multi-site investigation, its limitations include a study of predominantly non-Hispanic, Caucasian populations within the United States. How broadly our findings extend to other populations remains to be determined.

In the current study, modestly increasing *Kdm6a* expression in XY mouse primary neurons and hippocampus of XY-hAPP mice attenuated hAPP/A β neurotoxicity and cognitive impairment. These findings suggest that minor elevation in *Kdm6a* transcription was sufficient to functionally increase neural resilience and partially reverse deficits in the XY-hAPP mice. Whether this requires histone demethylase activity is currently unknown. *Kdm6a* may act differently across cell types and biological systems. Whereas *Kdm6a* deletion in hippocampus impairs synaptic plasticity and cognition in mice (Tang, Zeng et al. 2017), its deletion in immune CD4⁺ T cells ameliorates the neuroimmune response in a mouse model of autoimmune encephalomyelitis (Itoh, Golden et al. 2019). Thus, downstream actions of *Kdm6a* may be cell type specific.

Our study has several caveats and limitations. Our experiments do not exclude other potential contributions of X- or Y-based biological functions. A second X chromosome could contribute resilience through other baseline X escapee genes, epigenetic diversity derived from parent-of-X origin, or reactivation of the silent X chromosome. Furthermore, we did not study how the Y chromosome, its *Sry* gene, or testicular development contributed to a decreased mortality in hAPP mice with one X chromosome. Last, there are limitations to modeling AD in mice, including in each mouse model we used. Thus, we investigated several models and approaches including mouse primary neurons, hAPP mice, human brain tissue expression data, and human cognitive data, and included several AD-related measures to increase the potential relevance of our findings. Collectively, these results imply that a second X chromosome, or genes that an X chromosome harbors, could contribute to counteracting AD vulnerability in both sexes.

MATERIALS AND METHODS

Study design

The objectives of our study were to probe the association of sex-based mortality risk in AD using meta-analysis; investigate whether sex chromosomes modify vulnerability related to AD in mice using molecular, behavioral, cellular, neurogenetic, and behavioral approaches, and test in mice whether an X chromosome factor decreased male vulnerability related to AD. We used experimental models of AD (mice and their primary neurons) and human databases of both brain tissue expression and of clinical, cognitive performance. All animal studies were approved by the Institutional Animal Care and Use Committee of the University of California, San Francisco and conducted in compliance with National Institute of Health guidelines. For animal experiments, all studies were conducted in a blinded manner and included male and female mice across the lifespan in multiple cohorts at the ages and background strains indicated. Mouse studies used littermate controls along with randomization of mice, and experimentalists were blinded to the genotypes of mice. In mouse studies, exclusion criteria (greater than 2 SDs above or below the

mean) were defined *a priori* to ensure unbiased exclusion of outliers. We used transgenic mouse models of sex biology crossed with hAPP mice and also used mouse primary neurons exposed to varying doses of A β . We assessed several outcome measures including mortality, cognition, cell death, pathology, RNA and protein measures, and biochemistry. Cell culture treatments were carried out with vehicle or synthetic A β 1-42 peptide previously characterized by atomic force microscopy, and relative neurotoxicity was assessed with MTT and LDH assays.

Our findings showing a statistical effect of the second X chromosome in contributing resilience across measures in mice and mouse primary neurons led us to study *Kdm6a*, an X-linked gene that escapes inactivation in mice and humans. We established that *Kdm6a* escapes X-chromosome inactivation in mouse primary neurons using RNA-FISH. We then queried *KDM6A* expression in humans using established databases of brain tissues including the Mayo Clinic Brain Bank and Mount Sinai School of Medicine Brain Bank (RNA sequencing), Gene Expression Omnibus (RNA microarray), and GTEx. We examined clinical and cognitive trajectories using the ADNI database to assess the relevance of our findings to the human condition. Last, we tested whether elevating the expression of *Kdm6a* causally contributed resilience to AD-related deficits in mouse primary neurons and hAPP mice using lentiviral gene delivery methods.

Statistical analyses

Statistical analyses were carried out with GraphPad Prism (version 5.0) for t-tests, and log-rank tests for survival analyses. For FCG-hAPP mouse and XY*-hAPP mouse survival statistical analysis, Cox proportional hazards models were applied to determine main effects and a multivariate Cox model was used to test interactions of main variables on survival. R (nmlr package) was used for analyses of variance ANOVAs, post-hoc tests, and for meta-analysis. Differences between two means were assessed by two-tailed t-tests for all experiments unless indicated otherwise in a replication cohort. Differences among multiple means were assessed by two-way ANOVA. A mixed model ANOVA was used for analyses of Morris water maze data and

included effects of repeated measures. Only significant *P*-values were stated for two-way ANOVA results. Unless indicated otherwise, multiple comparisons of post-hoc t-tests were corrected for with the Bonferroni-Holm (step-wise Bonferroni) procedure to control for a family-wise error rate of $\alpha=0.05$. Linear mixed effects models were fit in R (Team 2019) using the standard lme4 (Bates, Mächler et al. 2014) package. In mouse studies, exclusion criteria (greater than 2 SDs above or below the mean) were defined *a priori* to ensure unbiased exclusion of outliers. Error bars represent \pm SEM. Null hypotheses were rejected at or below a *P*-value of 0.05. All analyses for *KDM6A* human studies were performed using R version 3.5.2 unless otherwise stated. We used linear mixed-effects modeling with random intercepts to test whether the genetic variant identified via GTEx as a modifier of *KDM6A* expression in brain also affected cognitive and clinical changes in the ADNI cohort. We covaried for baseline age, sex, education, and *APOE* ϵ 4 dose.

Meta-analysis of Human Mortality in studies of Alzheimer’s disease worldwide

We performed a meta-analysis of longitudinal population studies reporting risk of male mortality, compared to female mortality, in individuals with Alzheimer’s Disease (AD). Keywords “Alzheimer’s disease and mortality” were used on a search of PubMed and retrieved publications from 1985–July 25, 2015. Papers that included Hazard Ratios (HRs), or values that could be calculated into HRs (i.e. beta coefficients), standard error (or 95% confidence intervals), and information on survival or mortality following disease presentation (or other specified time point) were included. Hazard ratios reported as female mortality were inverted to derive male mortality. Papers that examined less than 100 individuals (except in early onset AD), only one sex, animal models, non-dementia populations, molecular markers, drug trials, or environmental effects were excluded from analyses. Data that assessed mortality associated with AD in cross sectional analyses of all deaths, such as death record studies without information about disease onset, were excluded. Only those papers that defined the time variable as age of onset of disease or duration of disease (starting from age of onset) were included; thus, papers whose Cox

proportional hazards model defined the time variable beginning from the date of diagnosis or study start point were excluded. Meta-analysis was performed using R (R-package “metaphor” and “meta”) (Viechtbauer 2010) with a random effects model using the Knapp-Hartung(-Sidik-Jonkman) adjustment (Hedges and Vevea 1998, Hartung and Knapp 2001, Hartung and Knapp 2001, Sidik and Jonkman 2002); Wald confidence intervals were fit for the relative risk of death between males and females.

Mice for *in vivo* studies: Mortality, Behavioral, and Biochemical Studies

Mice for *in vivo* studies were on a congenic C57BL/6J background and kept on a 12-h light/dark cycle with *ad libitum* access to food and water, unless indicated otherwise. The standard housing group was five mice per cage except for single housing during water maze studies. Cognitive and behavioral studies were carried out during the light cycle. Hemizygous hAPP-J20 (Mucke, Masliah et al. 2000) and J9 (Mucke, Masliah et al. 2000) mice express a mutant form of the human amyloid precursor protein with the Swedish (K670N/M671L) and Indiana (V717F) mutations, under control of the platelet-derived growth factor (PDGF) β -chain promoter (Rockenstein, McConlogue et al. 1995); hAPP and A β in brain tissues are approximately 50% lower in hAPP-J9 mice than hAPP-J20 mice (Mucke, Masliah et al. 2000). In one experiment to assess effects of a mixed genetic background, we analyzed littermates from the F1 offspring of C57BL/6J hAPP-J20 males and FVB/N nontransgenic (NTG) females (**Figure S1**). For all other breeding and experiments, mice were on a congenic C57BL/6J background. hAPP mice of either the J20 or J9 lines were generated by crossing hAPP males with NTG C57BL/6J females. Four Core Genotypes (FCG) mice (Mahadevaiah, Odorisio et al. 1998, Mucke, Masliah et al. 2000, Arnold and Chen 2009) were derived from males with *SRY* (testis-determining gene) deleted from the Y chromosome and inserted as a transgene onto an autosome (chromosome 3). Female hAPP-J20 mice were crossed with male FCG mice. XY* male mice (Eicher, Hale et al. 1991, Arnold 2009) harbor an altered pseudoautosomal region on the Y chromosome that recombines

abnormally with the X chromosome. Female hAPP-J20 mice were crossed with male XY* mice. Just after birth, pups from both crosses were fostered with FVB/N mothers since hAPP mothers often neglected and/or ate their newborn litters. Male and female mice were gonadectomized following sexual differentiation and after reaching reproductive maturity at approximately 75 days, unless indicated otherwise. In all cohorts, survival was assessed following weaning at approximately 21 days up until the age indicated; mice used for breeding were excluded from analyses. All cognitive, behavioral, and molecular experiments were conducted in a blinded manner on age-matched and genotype-balanced littermate offspring from the matings. Mice were analyzed from multiple cohorts.

Lentivirus production and stereotaxic injection

Lysine-specific demethylase 6a (*Kdm6a*) knockdown was achieved using a piLenti-siRNA lentiviral plasmid (Applied Biological Materials, catalog number: i037814) with the target sequence 5'-GCCACGTTGGTCATACTATACTGGGCATG-3' (sh-Kdm6a-3359). A similar construct with a scramble siRNA sequence (5'-GGGTGAACTCACGTCAGAA-3') (Applied Biological Materials, catalog number: LV015-G) was used as a control. To upregulate *Kdm6a* expression, a sequence encoding *Kdm6a* (NCBI Reference Sequence: NM_009483.2; 4275 bp) was inserted between the *Ascl* and *Bmt1* restriction sites of the pSicoR lentiviral backbone (pSicoR-EF1a-Blast-T2A-EGFP) obtained from the UCSF viracore (catalog number: MP394). *Kdm6a* cDNA is ~4kb. In order to reduce the total construct size, the blasticidin insert was deleted and replaced by the *Kdm6a* cDNA. Active lentiviral particles were produced by cotransfecting 293FT cells with a lentiviral transfer plasmid, a vector genome plasmid, a gag-pol packaging plasmid and an envelope plasmid (VSV-pseudotyped third-generation packaging plasmids). Lipofectamine™ 2000 Transfection Reagent or HiGenofect™ Transfection Reagent (C&M Biolabs, Cat. CM0202) was used as a transfection reagent to increase transfection efficiency. Viruses were purified by ultracentrifugation for 2 hours at 25,000 rpm in a Beckman Coulter L-80 Ultracentrifuge. The titer

(Tu/ml) of the lentivirus produced was determined using Clontech's Lenti-X qRT-PCR Titration Kit (Cat. 631235). Three- to four-month old NTG and hAPP-J20 mice were anaesthetized using isofluorane at 2-3% and placed in a stereotaxic frame. Lentiviral vectors (4-5 μ l per hemisphere) were stereotactically injected bilaterally into the dentate gyrus of the hippocampus using the coordinates, AP=-2.1, ML= \pm 1.7 and DV=1.9. Mice were allowed to wake up completely after surgery before being returned to their home cage. All behavioral assays were conducted 3-5 weeks after lentiviral injections.

Behavioral studies

All studies were carried out in a blinded manner. Arenas, objects, or chambers were cleaned with 70% alcohol between testing sessions in all tasks except the water maze.

Morris Water Maze

Testing was carried out as described (Dubal, Yokoyama et al. 2014, Dubal, Zhu et al. 2015). Briefly, the water maze pool (diameter, 122 cm) contained white, opaque water ($21^{\circ}\pm 1^{\circ}\text{C}$) with a square, 14 cm² platform submerged 2 cm below the surface. Prior to hidden platform training, mice underwent two pre-training trials by swimming through a channel to mount a hidden rescue platform. During hidden platform training, the platform location remained constant and the drop location varied between trials. Mice received either one or two training sessions, consisting of two to six trials each, daily for four to seven days, as indicated. The maximum time allowed per trial was 60 seconds. For the probe trial, the platform was removed and the mice were allowed 60 seconds to swim. Following probe testing, mice were tested for their ability to find the platform when marked with a visible cue (15 cm pole placed on the platform).

Passive Avoidance

Testing was carried out as described (Dubal, Zhu et al. 2015). Briefly, the apparatus consisted of a two-compartment dark/light shuttle box separated by a guillotine door, with a shock grid floor in the dark chamber (Gemini, Avoidance System, San Diego Instruments). During training, mice were placed in the lit chamber for acclimation. After 15 seconds, the door between the two chambers was raised, and latency to enter the dark chamber was recorded. Immediately after mice entered the dark chamber, the door closed and a foot shock was delivered (0.35 mA, 2 s). Ten seconds after the shock, mice were removed and returned to their home cage. Twenty-four hours after training, latency to enter the dark chamber was measured over a maximum time period of 300 or 500 seconds, as indicated. For some cohorts, mice were retested on subsequent days following training to measure forgetting of fear memory.

Novel Place Recognition

Testing was carried out as described (Cisse, Halabisky et al. 2011). Briefly, mice were acclimated to the testing room for 1 hour before testing, which was performed in a square white chamber (40 x 40 cm) under dim lighting. On the first day, mice were habituated to the arena for 10 min. Twenty-four hours later, mice were presented with two identical objects placed equidistant from each other and from the surrounding chamber walls. During this training session, mice showed a similar preference for each of the objects. For the test session 24 hours later, one of the objects was moved to a new location and mice were allowed to explore for 10 minutes. Frequency of object interactions and time of object exploration were manually scored from videos and analyzed.

Contextual Fear Conditioning

Testing was carried out as described (Dubal, Yokoyama et al. 2014). Briefly, mice were tested for context memory for the location where they received a foot shock using a trace fear

conditioning paradigm. Mice were first acclimated to the testing chamber for 12 minutes, 24 hours before training. During training, mice were placed into the chamber for 12 minutes. Baseline freezing activity was recorded for 4 minutes. Then, a series of 4 cycles (100 seconds each) of the following was presented: 20 second silence, 20 second tone, 18 second silence, 2 second 0.30 mA foot shock, and 40 second silence. Twenty-four hours later, mice were returned to the same chamber for 3 minutes without receiving shocks, and the time they spent freezing was recorded as a measurement of context memory. Mice were then tested for context-independent cued conditioning 2 hours after context testing. For this purpose, mice were placed into a new dark chamber with a new odor (2% acetic acid), and the time they spent freezing was recorded. First, baseline freezing was recorded for 3 minutes. Then, a series of 4 cycles (100 seconds each) of the following was presented: 20 second silence, 20 second tone and 60 second silence.

Openfield

Testing was carried out as described (Dubal, Yokoyama et al. 2014, Dubal, Zhu et al. 2015). Briefly, mice were acclimated to the room for 30 minutes and allowed to explore the open field for 10-15 minutes, as indicated in figure legends. Total activity in the open field (clear plastic chamber, 41 x 30 cm) was detected by beam breaks and measured with an automated Flex-Field/Open Field Photobeam Activity System (San Diego Instruments).

Elevated Plus Maze

Testing was carried out as described (Dubal, Yokoyama et al. 2014, Dubal, Zhu et al. 2015). Briefly, mice were habituated to the testing room for 1 hour before testing. Dim light was maintained in the testing room for both habituation and testing. Mice were placed in the center of an elevated plus maze facing an open arm and allowed to explore for 10 minutes. Total time spent and distance traveled in open and closed arms was recorded using Kinder Scientific Elevated Plus Maze and MotorMonitor™ system.

Protein extraction and western blot analysis for hAPP and p-tau

Hippocampus was dissected and lysed with ice-cold lysis buffer (1X PBS, pH 7.4, 1 mM DTT, 0.5 mM EDTA, 0.5% Triton, 0.1M phenylmethyl sulfonyl fluoride (PMSF), protease inhibitor mixture (Roche), and phosphatase inhibitors 2 and 3 (Sigma Aldrich)), sonicated for 10 minutes, heated at 95 °C for 10 minutes, and centrifuged for 10 minutes at 10,000 rpm. Protein concentration was assessed using a BCA assay (Thermo Fisher). 20 µg of total protein were loaded into 4-12% gradient Bis-Tris gels (BioRad), and electroblotted onto 0.45 µm nitrocellulose membranes (GE Life Sciences). Membranes were blocked with blocking solution (5% milk in TBST (1X TBS, 0.05% Tween 20)) for 1 hour at room temperature. Primary antibodies were incubated overnight at 4 °C. Membranes were then washed with TBST, and incubated for 1 hour at room temperature with fluorescent secondary antibodies (LI-COR) at a dilution of 1:10,000 and 1:15,000. After washing, membranes were developed with LI-COR Odyssey. Western blot signal was quantified using ImageStudio software. Expression of GAPDH was used as a loading normalization control. The following primary antibodies were used: mouse anti-hAPP (8e5; 1:1,500, Elan pharmaceuticals), rabbit anti-tau (1:5,000; Millipore), mouse anti-p-tau (PHF-1; 1:2,500, gift from Peter Davies) and mouse anti-GAPDH (1:10,000; Millipore).

Protein extraction and western blot analysis of Kdm6a

Hippocampus was dissected and lysed with ice-cold RIPA buffer (50 mM Tris-HCl, pH 7.4, 150 mM NaCl, 0.5% sodium deoxycholate, 0.05% TritonX-100, 0.1% SDS, protease inhibitor mixture (Roche), and phosphatase inhibitors 2 and 3 (Sigma Aldrich)), rotated at 4 °C for 30 minutes, centrifuged for 20 minutes at 12,000 rpm. Protein concentration was assessed using a BCA assay (ThermoFisher). 40 µg of total protein were loaded into 7.5% Tris-HCl gels (BioRad), and electroblotted onto 0.2 µm PVDF membranes (Roche). Membranes were blocked with

blocking solution (5% skim milk in PBST (1X PBS, 0.05% Tween 20)) for 30 minutes at room temperature. Primary antibodies were incubated overnight at 4 °C. Membranes were then rinsed with MilliQ H₂O and incubated for 1 hour at room temperature with HRP-conjugated secondary antibodies (BioRad) at a dilution of 1:20,000. After three 5 min washes in PBST, membranes were exposed via enhanced chemiluminescence (SuperSignal™ West Pico PLUS, ThermoFisher) and X-ray film (CL-Xposure™, ThermoFisher). Films were digitally scanned at a high resolution (minimum 600dpi) on an Epson photo scanner and western blot signal was quantified using ImageStudio software. Expression of GAPDH was used as a loading normalization control. The following primary antibodies were used: rabbit anti-KDM6A/UTX (1:1,000; Abcam and GeneTex) and mouse anti-GAPDH (1:10,000; Millipore).

A β ELISA

Enzyme-linked immunoabsorbant assays (ELISAs) were carried out as described (Dubal, Zhu et al. 2015) (Fig. 2, figure legend) and results were replicated using manufacturer's directions (Immunobiological Laboratories) and used for further measurements (fig. S6). Briefly, hippocampus was dissected, homogenized, and sonicated in ice-cold lysis buffer, protease and phosphatase inhibitors. Following the addition of guanidine, samples were re-homogenized and analyzed for human A β 1-42 by ELISA.

Immunohistochemistry

Immunohistochemistry and analyses were carried out as described (Palop, Jones et al. 2003, Dubal, Zhu et al. 2015) on floating 30 μ m sections obtained with a sliding microtome (calbindin, 3D6) or on either 40 μ m (NeuN, Kdm6a, DAPI) or 50 μ m sections obtained from a cryostat (GFP, NeuN). Primary antibodies were rabbit anti-calbindin (1:20,000; Swant), rabbit anti-GFP (1:10,000; Abcam), mouse anti-NeuN (1:1000; Millipore), rabbit anti-KDM6A/UTX (1:100;

Abcam), and mouse biotinylated anti-3D6 (1:500; Elan Pharmaceuticals). Binding of the non-biotinylated antibody was detected with biotinylated donkey anti-rabbit (1:1000; Jackson ImmunoResearch) followed by incubation with avidin-biotin/peroxidase (Vector Laboratories). Sections were then developed with 3,3'-diaminobenzidine tetrahydrochloride (Sigma-Aldrich). Binding of GFP, NeuN, and Kdm6a antibodies were detected using Alexa Fluor fluorescent secondary antibodies (1:1000; Life Technologies). Sections were then mounted with VECTASHIELD Hardset containing DAPI (VECTOR Laboratories) and captured using a digital inverted fluorescent microscope with spinning disk confocal (Micro-Manager, Nikon Ti). Images were contrasted in ImageJ so that background levels and cell bodies were visible to the human eye. Some punctate spots may have become saturated to achieve visibility. All other images were captured with a digital microscope (AxioCam, Carl Zeiss) and percent area calculations were performed with the Bioquant software package (BIOQUANT Image Analysis Corporation) as described (Palop, Jones et al. 2003). The average percent area of the hippocampus covered by A β -immunoreactive deposits was determined in three coronal sections 500 μ m apart (approximate distances from Bregma: -1.0, -1.5, and -2.0 mm) in each mouse and quantified as described (Dubal, Zhu et al. 2015).

Primary cell cultures

Cortices were isolated between postnatal days 0-2 from male and female neurons derived from congenic C57BL/6J NTG or XY* mice (Eicher, Hale et al. 1991, Arnold 2009) and used to establish primary neuronal cultures as described (Cheng, Dubal et al. 2009). Cells were plated at 1 million cells/mL in either 24 or 96 well plates for subsequent maturation and treatment. All treatments were carried out on day 7-8 *in vitro* in neurobasal media with B-27 supplement (NBA/B27) unless otherwise stated. All cell culture reagents were purchased from Gibco.

Fluorescent *in situ* hybridization (FISH)

Cultured mouse cortical neurons were dissociated using trypsin. All culture media from wells was removed and 700 μ L of trypsin was added per well. Cells were incubated at 37 °C for 7 minutes. To stop the reaction, 2 mL of NBA with B27 was added to the trypsin. Cells were removed from wells, put into a 15 mL falcon tube, and centrifuged at 1000 rpm for 10 minutes. Supernatant was removed and cells were resuspended in 2 mL of media. To prepare slides for FISH, the trypsinized neurons were cytospun onto a glass slide with a Cytospin at 800 rpm for 3 minutes and then left to air dry for 2-3 minutes. FISH was performed as described (Panning 2004). Probes were generated using an Xist plasmid or BAC, for the Kdm6a probe, by random priming with the Invitrogen BioPrime™ Array CGH Genomic Labeling Module kit. Images were collected with an Olympus BX60 microscope 100x oil objective and a Hamamatsu ORCA-ER digital camera using Openlab 4.0.1 software, assembled using ImageJ, and levels adjusted to enhance contrast.

Transduction of Primary Cell Cultures with *Kdm6a* Lentivirus

Cortices were isolated from postnatal day 0-2 male and female C57BL/6 pups and used to establish primary cultures as previously described (Cheng, Dubal et al. 2009). At day *in vitro* (DIV) 4, male cultures were transduced with *Kdm6a* overexpression lentivirus at MOI=2 and female cultures were transduced with *Kdm6a* knockdown lentivirus at MOI=4. Male and female cultures were treated with A β oligomers on DIV 10 and 14 respectively. Cell death was assessed 24 hours later using the MTT assay.

Culture treatments and cell toxicity assays

Synthetic A β 1-42 peptide (rPeptide) was reconstituted in DMSO to 5 mM. A β peptide stock solution was prepared by further dilution with 1X PBS to 100 μ M and incubated at 4 $^{\circ}$ C for 24 hours and immediately used or stored at -80 $^{\circ}$ C until use (Klein 2002, Cheng, Dubal et al. 2009); vehicle was prepared with equivalent DMSO volume in 1X PBS (1:50 dilution). A β peptide concentration was assessed using protein assay (Bio-Rad). For cell culture treatments, culture medium was fully replaced with conditioned medium, prepared by diluting A β peptide stock solution in fresh NBA/B27 medium to final concentrations of 1 μ M, 2.5 μ M, and 5 μ M. Vehicle-only medium was prepared by diluting equivalent (DMSO/PBS) volumes in fresh NBA/B27 medium. Vehicle control medium was prepared with an equivalent volume and dilution of DMSO in culture media. Using the described A β preparation, A β assembles into primarily oligomeric forms stably over 24 hours (Cheng, Dubal et al. 2009), the duration of the cellular toxicity assays.

Cell toxicity was assessed 24 hours after addition of vehicle or A β by MTT or LDH assays as described (Aras, Hartnett et al. 2008). Briefly, MTT (Sigma) was added to cell culture media in 96 well plates at 0.5 mg/mL final concentration and incubated for 60-90 minutes at 37 $^{\circ}$ C. Upon medium removal, cells were lysed with 100 μ L of DMSO and absorbance was measured at 560 nm. LDH assay was conducted following manufacturer instructions (Sigma Cytotoxicity Detection Kit). Briefly, 40 μ l of media in triplicate was taken from each 24-well of cultured cells and placed

into a separate 96-well plate. 40 μ l of LDH Assay mix was added, incubated in the dark for 20 minutes, and absorbance was measured at 490 nm (minus background at 690 nm). Lysis buffer was added to the original 24-well plate of cultured cells, incubated for 45 minutes at 37 °C, and previous steps were repeated to obtain the total LDH value. Fresh NBA media was used as blank wells.

For each genotype, mean absorbance from vehicle-treated cells was the reference to calculate toxicity for each individual sample. Relative neurotoxicity was then calculated for each genotype, as the differential between vehicle- and A β -treated cells.

***KDM6A* Human Studies**

Cohort Descriptions.

Mayo Clinic Brain Bank and Mount Sinai School of Medicine Brain Bank. We used RNA sequencing metadata from the Mayo Clinic (Allen, Carrasquillo et al. 2016) and Mount Sinai School of Medicine (Wang, Beckmann et al. 2018) Brain Banks to test whether *KDM6A* expression varied between pathologically confirmed AD cases and controls. We obtained data through the Accelerating Medicines Partnership - Alzheimer's Disease (AMP-AD) portal. Samples used in these analyses come from a variety of brain regions and include many regions implicated in AD such as parahippocampal cortex and superior temporal cortex. In aggregate, 343 individuals were included from these two brain banks; cohort characteristics and sample distribution by region are available in **Table 3.3**. Data from the two brain banks' collective samples was reprocessed and harmonized using a consensus toolset at the Mount Sinai Icahn School of Medicine Minerva HPC system. The resulting data is accessible online through Synapse (www.synapse.org; ID: syn14237651). Technical details describing reprocessing, analysis, and results are also available online through Synapse.

GSE 15222. We next used RNA microarray expression data from the Gene Expression Omnibus (GEO, <https://www.ncbi.nlm.nih.gov/geo/>) to compare *KDM6A* expression in temporal cortex samples from pathologically confirmed AD cases and controls. This data was initially published in 2009 (Webster, Gibbs et al. 2009) but is now publicly available through GEO and identified as GSE15222. The dataset includes 211 individuals; cohort characteristics are provided in **table S2**. For additional information on sample processing and quality control steps, please see (Webster, Gibbs et al. 2009).

GTex. In order to explore the effects of variation in *KDM6A* expression during normal aging as well as neurodegenerative disease, we next identified a gene expression quantitative trait loci (eQTL) using publicly available data from the Genotype-Tissue Expression (GTEx) project. Briefly, GTEx provides gene sequencing and expression data from brain as well as other tissue types. All samples are free from known genetic disease. GTEx includes a variety of samples types, including brain tissue and provides both genotype and gene expression data. For additional information, please see <https://gtexportal.org/home/documentationPage#staticTextPublicationPolicy> or (Carithers, Ardlie et al. 2015, Consortium, Laboratory et al. 2017).

ADNI. Our study utilized genetic and longitudinal clinical data from the Alzheimer's Disease Neuroimaging Initiative (ADNI) to study the effects of the genetic variants identified by GTEx. ADNI is a multi-center prospective longitudinal cohort study designed to identify and track biomarkers of Alzheimer's disease (Petersen, Aisen et al. 2010, Saykin, Shen et al. 2010, Weiner, Veitch et al. 2012). The study data includes clinical characteristics, cognitive testing, genetic data, and neuroimaging data. ADNI diagnoses are assigned by an attending physician at each study site and must comply with set inclusion/exclusion criteria as well as cutoffs based on neuropsychological tests, the details of which are previously described (Petersen, Aisen et al.

2010, Bonham, Desikan et al. 2016). In this study, we focused our analyses on the Mini Mental Status Exam (MMSE) (Folstein, Folstein et al. 1975), a broad measure of cognitive status. We utilized all available samples with whole genome sequencing (WGS) data available and genetic data passing quality control for our genetic variants of interest. For additional information on processing and quality control of WGS data, please see (Saykin, Shen et al. 2015). Written and informed consent was obtained from all study participants and all research was IRB approved. Acknowledgements and funding for ADNI are provided in the Supplemental Acknowledgements section below.

Statistical Methods for Human *KDM6A* studies.

All analyses for *KDM6A* human studies were performed using R version 3.5.2 unless otherwise stated.

Mayo Clinic Brain Bank and Mount Sinai School of Medicine Brain Bank. As described on Synapse (www.synapse.org; ID: syn14237651), the effect of diagnosis on *KDM6A* expression was tested using linear regression controlling for sex and other biological and technical confounders that explained more than 1% of variance on the expression residuals. We did not explore whether *KDM6A* expression varied by sex as this metadata was not available on the Synapse portal.

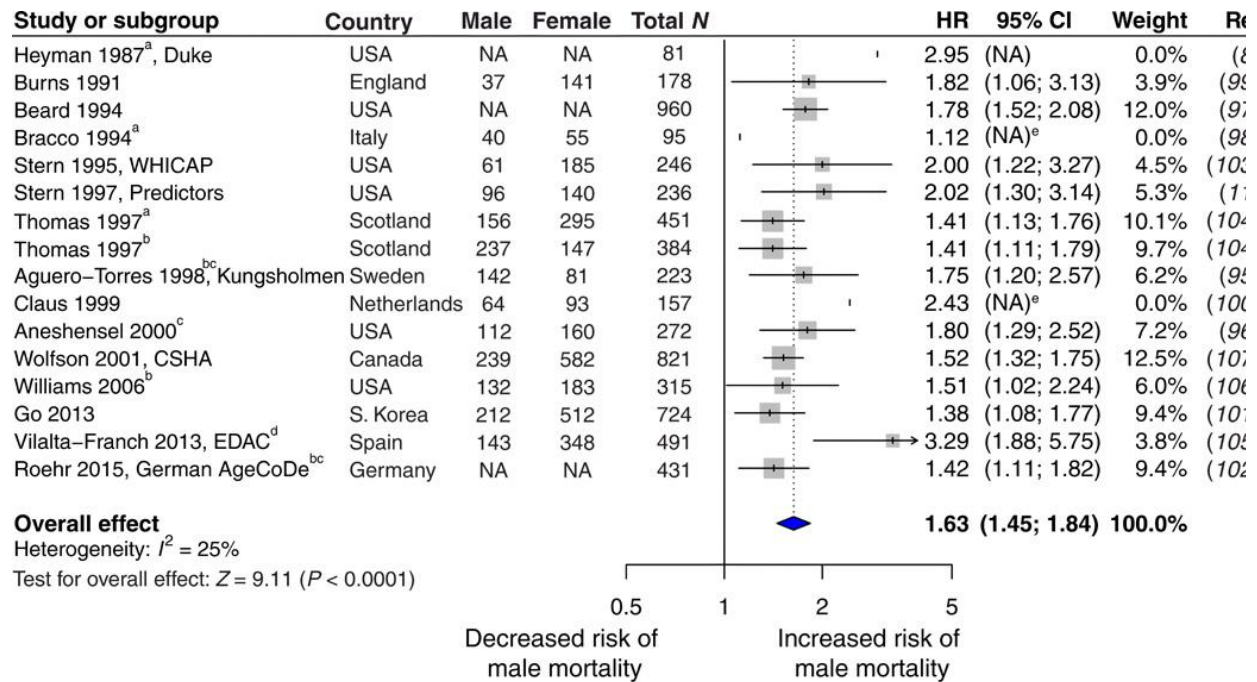
GSE 15222. We tested for differences in *KDM6A* expression by diagnosis and sex using linear regression controlling for age at death, postmortem interval, and sex. Similar to the analyses described above, we also examined whether greater age at death was associated with greater *KDM6A* expression in AD using the covariates listed above and controlling for diagnosis. Finally, we specifically examined if *KDM6A* expression varied within sex and diagnosis controlling for postmortem interval and age at death.

GTEx. The analytical methods used by *GTEx* are previously described and available to the public at (www.gtexp.org). Briefly, eQTLs are calculated using genotype data from WGS and gene expression data measured using RNA sequencing. *Cis*-eQTLs mapping and statistical testing was performed using FastQTL (Ongen, Buil et al. 2016). For additional information on *GTEx*, please see (Carithers, Ardlie et al. 2015, Consortium 2015). Methods for calculation of eQTLs are described in (Robinson and Oshlack 2010, Stegle, Parts et al. 2010, Wright, Sullivan et al. 2014, Ongen, Buil et al. 2016) and the link provided (<https://gtexpportal.org/home/documentationPage#staticTextAnalysisMethods>). Using the *GTEx* online portal (www.gtexpportal.org), we searched for genetic variants with a minor allele frequency (MAF) greater than 0.01 associated with altered *KDM6A* expression in human brain samples.

ADNI. We used linear mixed-effects modeling with random intercepts ('1|subject' in equation below specifies allowing a random intercept for each participant) to test whether the genetic variant identified via *GTEx* as a modifier of *KDM6A* expression in brain also impacted cognitive and clinical changes in the *ADNI* cohort. We covaried for baseline age, sex, education, and *APOE* $\epsilon 4$ dose. We modeled changes in MMSE score as follows:

$$\Delta \text{MMSE} = \beta_0 + \beta_1 \text{Age}_{\text{baseline}} \times \Delta t + \beta_2 \text{Sex}_{\text{female}} \times \Delta t + \beta_3 \text{Education}_{\text{baseline}} \times \Delta t + \beta_4 \text{APOE } \epsilon 4_{\text{dose}} \times \Delta t + \beta_5 \text{eQTL}_{\text{dose}} \times \Delta t + (1|\text{subject}) + \epsilon$$

FIGURES



NA, not available.

^aEarly-onset AD

^bStudies include dementia, vascular dementia, and/or AD with Lewy body dementia

^cAdditional statistical model(s) yielded similar results

^dCohort also studied in another publication, not included here

^eHR calculated from mortality data provided in paper

Figure 3.1. A meta-analysis of hazard ratios for male and female mortality in AD populations worldwide. Hazard ratios (HRs) and 95% CIs are shown in a forest plot for studies (8, 11, 95–107) reporting male risk, compared to female risk, for death in longitudinal (and not cross-sectional) analysis of individuals with AD. Overall HR with 95% CI shown in bold indicates increased risk of male mortality (male, HR 1.63, CI 1.45 to 1.84; $P < 0.0001$). WHICAP, Washington Heights-Inwood Columbia Aging Project; CSHA, Canadian Study of Health and Aging; EDAC, Evolution of Dementia of the Alzheimer-type and Caregiver burden; AgeCoDe, Aging, Cognition, and Dementia in Primary Care Patients.

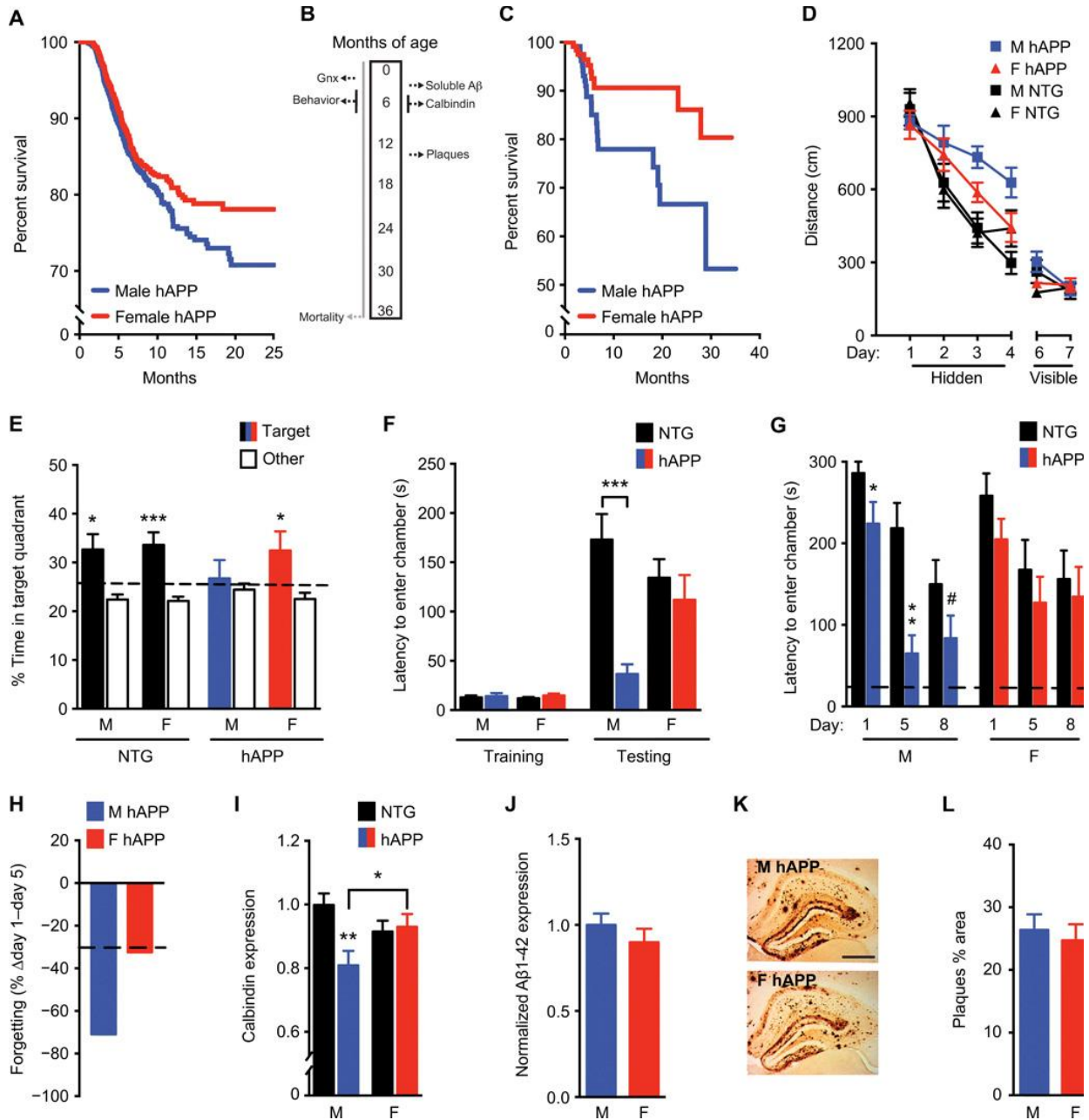


Figure 3.2 Male sex increases mortality, cognitive deficits, and synaptic protein abnormalities in hAPP mice. **(A)** Shown are Kaplan-Meier survival curves of male hAPP mice ($n = 1572$, blue) compared with female hAPP mice ($n = 1589$, red); all mice had intact gonads (log-rank test, $P < 0.001$). **(B)** All mice except those in (A) underwent gonadectomy (Gnx) at about 2.5 months of age; this was followed by behavioral testing conducted from 4 to 7 months of age and survival analysis conducted until 3 years of age. **(C)** Shown are Kaplan-Meier survival curves of male ($n = 116$) compared to female ($n = 123$) hAPP mice after gonadectomy (log-rank test, $P < 0.05$). **(D)** Shown are spatial learning curves of mice (age 4 to 7 months; $n = 10$ to 15 per group) tested in the Morris water maze during hidden platform training and when the platform was visible. Data points are daily average of total distance traveled to reach the platform over four trials. Mixed-model ANOVA for hidden training: female hAPP versus male hAPP mice, $P < 0.05$. **(E)** A probe trial was conducted after hidden platform learning and removal of the escape platform. Percentage of time mice spent in the target quadrant of the maze, indicating memory for

platform location, versus the average time spent in the other three quadrants is shown; * $P < 0.05$; *** $P < 0.001$. The dashed line represents chance performance (25%). (F) Shown is passive avoidance, fear memory of mice (age 3 to 3.5 months; $n = 7$ to 10 per group) reflected by latency to enter the dark chamber during training and testing 1 day after an electric shock to the foot. Two-way ANOVA: hAPP effect, $P < 0.01$; hAPP by sex interaction, $P < 0.05$. (G) Forgetting of passive avoidance memory in a separate cohort of mice (age 5 to 6 months; $n = 10$ to 12 per group), reflected by latency to enter a dark chamber 1, 5, and 8 days after a foot shock, was measured. The dashed line represents latency to enter the dark chamber during training, which did not differ among groups. (H) Percentage loss of fear memory from days 1 to 5 is shown. The dashed line represents the average for nontransgenic (NTG) animals. (I) Shown is quantitation of calbindin immunoreactivity in mouse dentate gyrus (age 5 to 7 months; $n = 11$ to 14 mice per group). Two-way ANOVA: hAPP effect, $P < 0.05$; hAPP by sex interaction, $P < 0.05$. Means are relative to NTG male control mice, arbitrarily defined as 1. (J) Soluble A β 1-42 amounts in the mouse hippocampus determined by enzyme-linked immunosorbent assay (ELISA) are shown (age 3 months; $n = 8$ to 11 mice per group). (K) Representative immunostaining of hippocampal A β deposits in coronal brain sections from a male (top, M) and female (bottom, F) hAPP mouse (age 14.5 to 15 months). Scale bar, 200 μm ; magnification, $\times 4$. (L) Quantitation of percentage area covered by A β deposits in hAPP mice (age 14.5 to 15 months; $n = 11$ per group). Behavioral studies in male and female NTG and hAPP mice were performed across seven independent cohorts including in fig. S4. # $P = 0.06$; * $P < 0.05$; ** $P < 0.01$; *** $P < 0.001$ [Bonferroni-Holm for (F), (G), and (I)]. Data are presented as means \pm SEM.

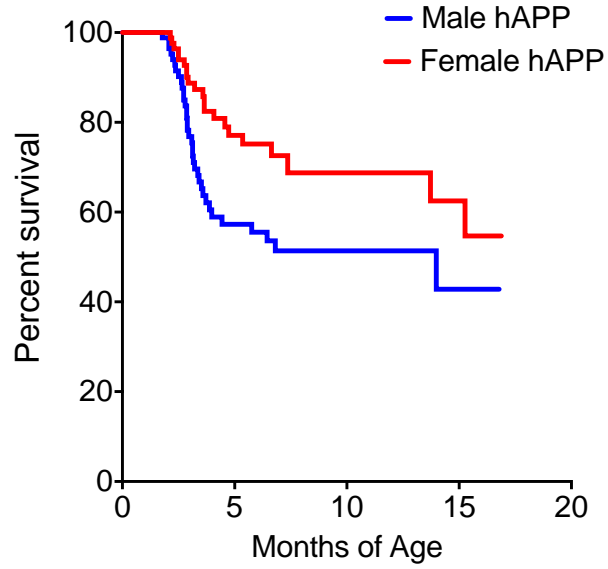


Figure 3.3. Male and female hAPP mouse mortality on a mixed genetic background. Kaplan-Meier curves show that male hAPP mice (n=87) (line J20) show decreased lifespan compared to female hAPP mice(n=88) on a mixed F1 generation background strain of C57BL/6J crossed with FVB/N. Log-rank test, $P < 0.05$.

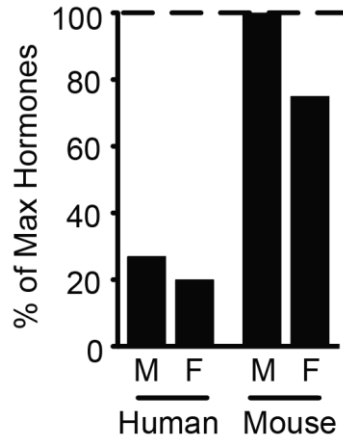


Figure 3.4. Human and mouse gonadal hormones in aging. Reduction of bioactive gonadal hormones in aged humans (up to about 80 years) but not aged mice (up to 24 months). Dashed line indicates maximum gonadal hormone concentrations reached during young life-stages (adapted from review (Dubal, Broestl et al. 2012)).

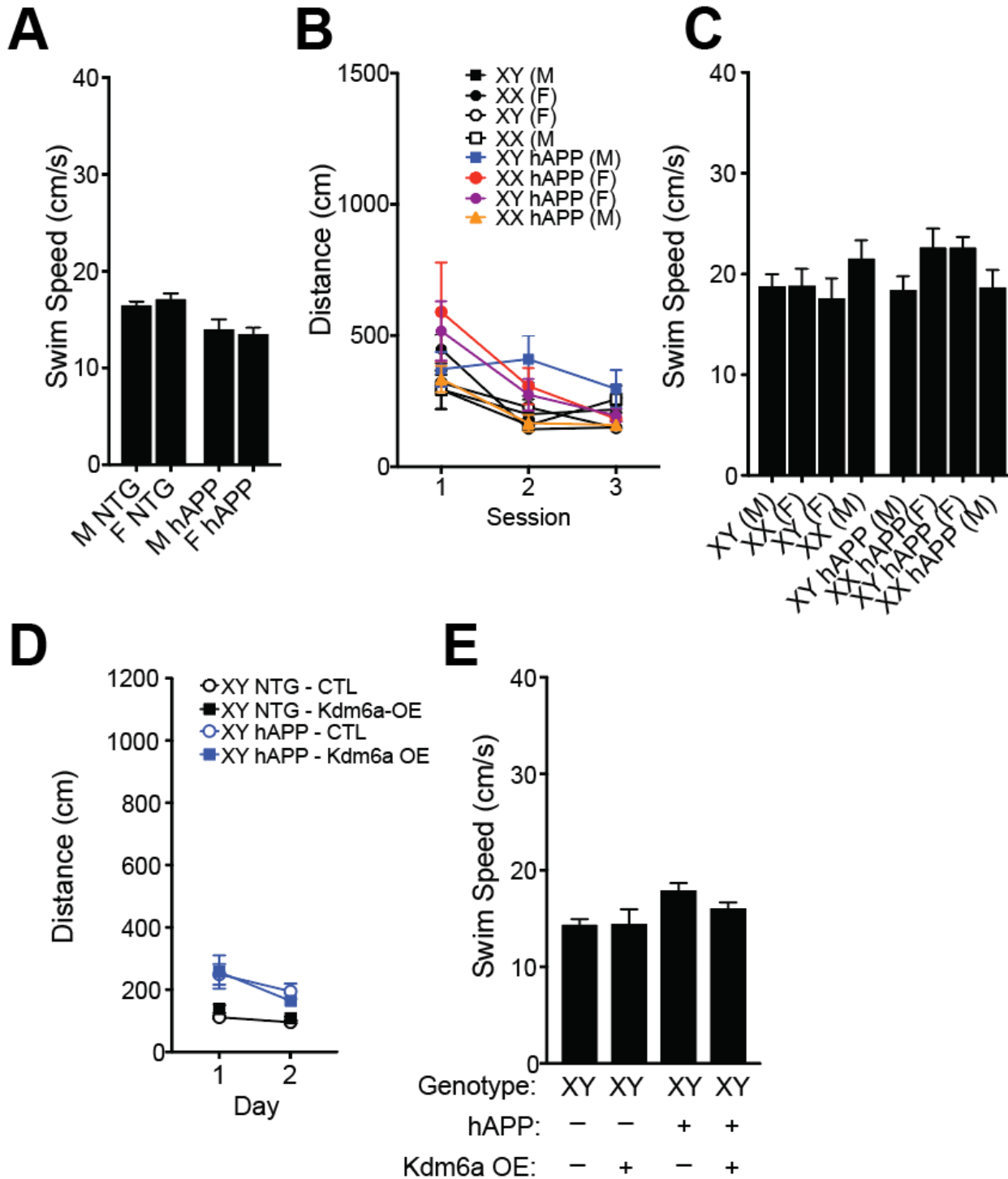


Figure 3.5. Swim speeds and visible platform performance of mice in a water maze test. Morris water maze swim speeds and visible platform performance did not differ between male and female mice or with Kdm6a overexpression within the NTG or hAPP genotypes. (A) hAPP mice swam slower than NTG mice, and male mice swam with equivalent speed to females within each genotype (age 3-7 months; n=7-15 per group). ANOVA: hAPP effect P<0.0001; sex genotype effect P<0.93; interaction P<0.40. Data is related to **Figure 3.2**. (B) All experimental groups derived from FCG mice crossed with hAPP mice (age 3-5 months; n=5-6 per group)

showed similar distances traveled in the Morris water maze when the platform was visible in session 3. ANOVA: hAPP effect $P < 0.59$; sex genotype effect $P < 0.09$; interaction $P < 0.13$. **(C)** All experimental groups derived from FCG mice crossed with hAPP mice (age 3-5 months; $n = 5-6$ per group) showed similar swim speeds. ANOVA: hAPP effect $P < 0.24$; sex genotype effect $P < 0.62$; interaction $P < 0.08$) Data points in **(B)** are averages of two trials. Data is related to **Figure 3.13**. **(D)** hAPP mice swam slightly greater distances in the Morris water maze compared to NTG when platform was visible on Day 2 (age 5-5.5 months; $n = 7-15$ per group). ANOVA: hAPP effect $P < 0.0001$; Kdm6a effect $P < 0.56$; interaction $P < 0.15$. Data is related to **Figure 3.22**. **(E)** hAPP mice swam slightly faster in the Morris water maze compared to NTG mice but overexpression of Kdm6a had no effect (age 5-5.5 months; $n = 7-15$ per group). ANOVA: hAPP effect $P < 0.01$; Kdm6a effect $P < 0.31$; interaction $P < 0.25$. Data is related to **Figure 3.22**. Data are mean \pm SEM.

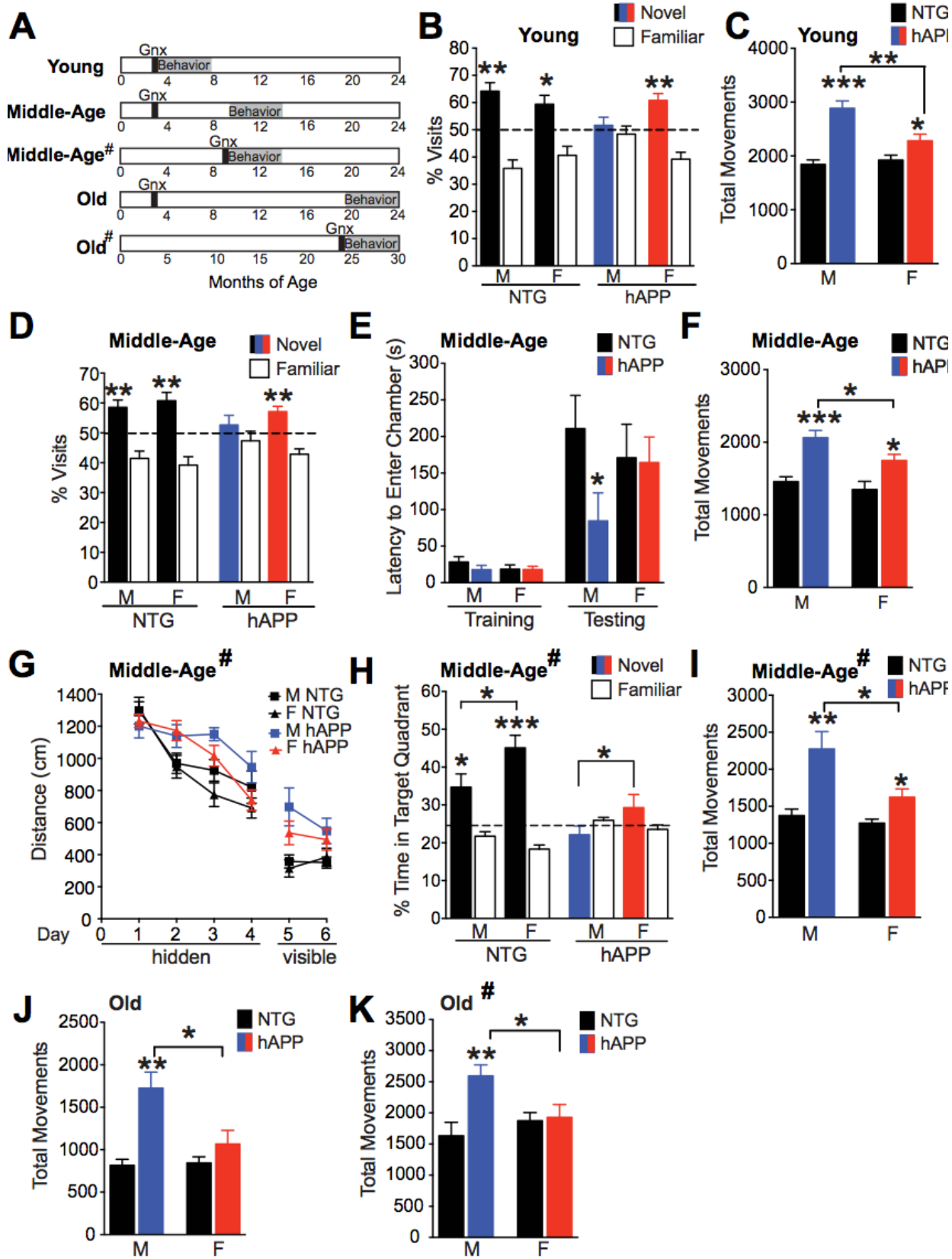


Figure 3.6. Male sex and cognitive deficits under several conditions. Mice from transgenic line J20 were gonadectomized at different times and tested across the lifespan in multiple cohorts. **(A)** Experimental paradigm shows mice underwent gonadectomy at young, middle or old life stages followed by testing and survival studies. #=Gonadectomy at middle-age or old life-stage as indicated. **(B–C)** Cognitive and behavioral tests of young male and female, NTG and hAPP mice undergoing gonadectomy at young age. **(B)** Novel place recognition (spatial learning and memory) in mice (age 4.5-5.5 months; n=11-15 per group) as reflected by the percentage of visits made to the object in the novel location. Dashed line = average preference for each of the objects during training across all groups. **(C)** Total number of movements by mice (age 4-6 months; n=12-15 per group) during exploration of an open field for 15 minutes. Two-way ANOVA: hAPP effect $P<0.0001$, sex effect $P<0.05$, hAPP by sex interaction $P<0.01$. **(D–F)** Cognitive and behavioral tests of middle age male and female, NTG and hAPP mice that underwent gonadectomy when young. **(D)** Novel place recognition in mice (age 14-14.5 months; n=8-15 per group) as reflected by the percentage of visits made to the object in the novel location. Dashed line = average preference for each of the objects during training across all groups. **(E)** Passive avoidance memory reflected by latency to enter the dark chamber during training, and then during testing 24h after receiving a shock in the dark chamber (age 10.5-11 months; n=6-12 per group). **(F)** Total number of movements by mice (age 10.5 months; n=10-12 per group) during exploration of an open field for 15 minutes. Two-way ANOVA: hAPP effect $P<0.0001$, sex effect $P<0.05$. **(G–I)** Cognitive and behavioral tests of middle age male and female, NTG and hAPP mice that underwent gonadectomy at middle age. **(G)** Spatial learning curves of male and female, NTG and hAPP mice (age 14 months, n=9-13 per group) tested in the Morris water maze. Data points represent the daily average of total distance traveled to reach the platform over six trials. Mixed model ANOVA: M-hAPP vs. F-hAPP, $P<0.05$. **(H)** Probe trial 2 hours after completion of hidden platform learning. Percentage of time mice spent in the target quadrant and other three quadrants. Dashed line = performance expected based on chance. **(I)** Total number of movements by mice (age 13.5-14 months; n=6-15 per group) during exploration of an open field for 15 minutes. Two-way ANOVA: hAPP effect $P<0.0001$, sex effect $P<0.01$, hAPP by sex interaction $P=0.05$. **(J)** Total number of movements by mice (age 27 months; n=6-11 per group), gonadectomized at young age, during exploration of an open field for 15 minutes. Two-way ANOVA: hAPP by sex interaction $P<0.05$. **(K)** Total number of movements made by mice (age 20-36 months; n=6-15 per group), gonadectomized at old age, during exploration of an open field for 15 minutes. Two-way ANOVA: hAPP effect $P<0.01$, hAPP by sex interaction $P<0.05$. For all data, * $P<0.05$, ** $P<0.01$, *** $P<0.001$ vs. NTG (Bonferroni-Holm), dashed line (one-sample t-tests), or as indicated by bracket (Bonferroni-Holm). Data represent mean \pm SEM.

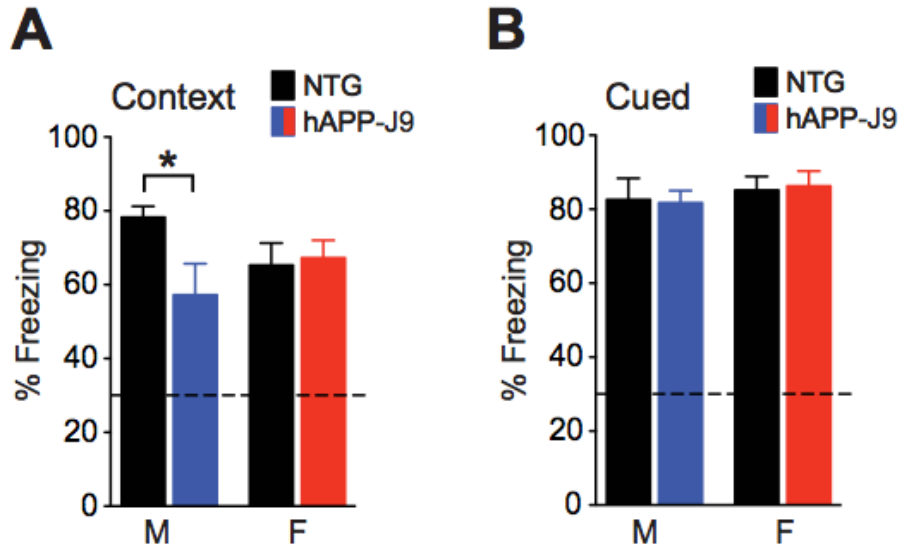


Figure 3.7. Male sex worsens cognition in another transgenic hAPP line. **A,B** Mice from transgenic line J9 (Mucke, Masliah et al. 2000) (n=4-9 per group; age 8-11 months) were gonadectomized and then tested in a fear conditioning task. Percent time mice spent freezing (**A**) in the same context in which training occurred; Two-way ANOVA: hAPP effect $P < 0.05$, hAPP by sex interaction $P < 0.05$; $*P = 0.05$ as indicated by bracket (Bonferroni-Holm); and then (**B**) in a different context but with the same auditory cues. Dashed line = baseline freezing. Data represent mean \pm SEM.

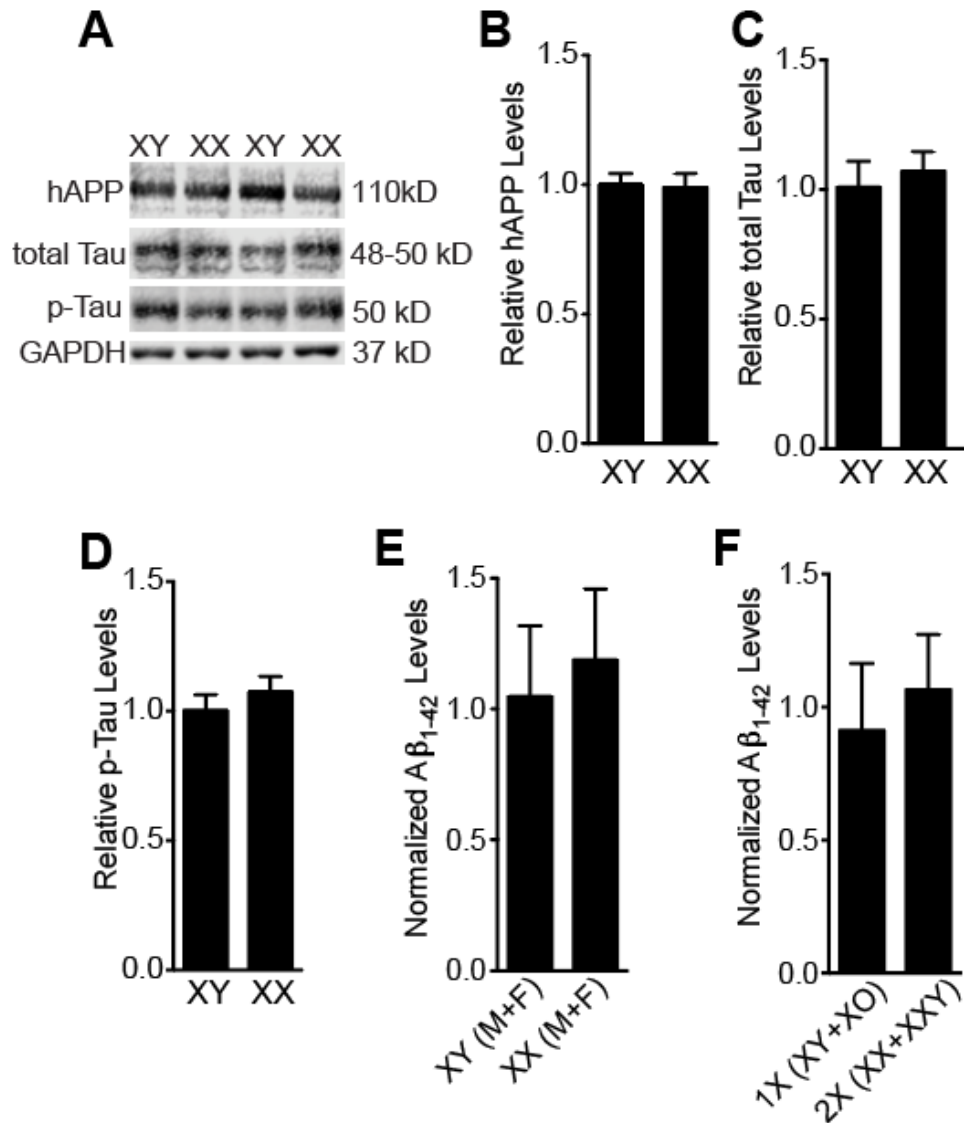


Figure 3.8. A β and related proteins in XX-and XY-hAPP mice crossed with FCG and XY* models. A β , tau, and p-tau did not differ between XX and XY hAPP mice, regardless of gonadal type or X chromosome dose. **(A)** Western blot image for hippocampal hAPP, total Tau and p-Tau and GAPDH of individual, gonadectomized hAPP transgenic mice derived from the fluorescence gel shown in full in **Figure 3.9**. Bands represent individual mouse samples and not technical replicates. **(B-D)** Quantitation of hippocampal expression of **(B)** hAPP, **(C)** total tau and **(D)** p-Tau respectively, upon normalization using GAPDH as loading control in gonadectomized hAPP mice (age 3-4 months; n=9-11 mice per group). **(E,F)** Relative A β 1-42 in the hippocampus of hAPP mice (age 3-4 months; n=8-11 mice per group) determined by ELISA in **(E)** hAPP-FCG mice XX (M+F) vs. XY (M+F) and **(F)** hAPP-XY* mice 2X (XX+XXY) vs. 1X (XO+XY). Data represent mean \pm SEM.

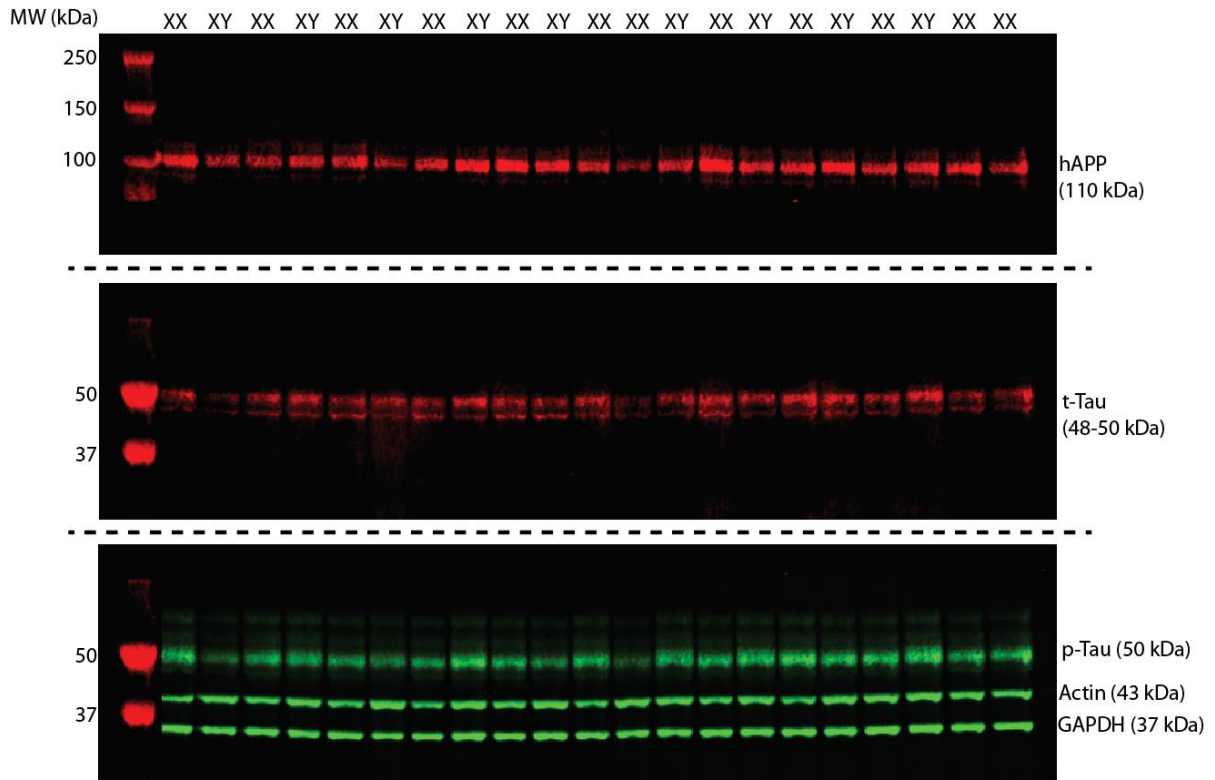


Figure 3.9. Western blot image of hAPP, t-Tau, p-Tau, and loading controls. Full western blot of proteins and loading controls in XX and XY hippocampal homogenates from which representative bands are shown in black and white in fig. S6A. Secondary antibody labeling with green and red fluorescence distinguished between t-Tau and p-Tau. Quantitation of bands in fluorescence or black and white yielded equivalent data. Dotted lines indicate where the gel was cut.

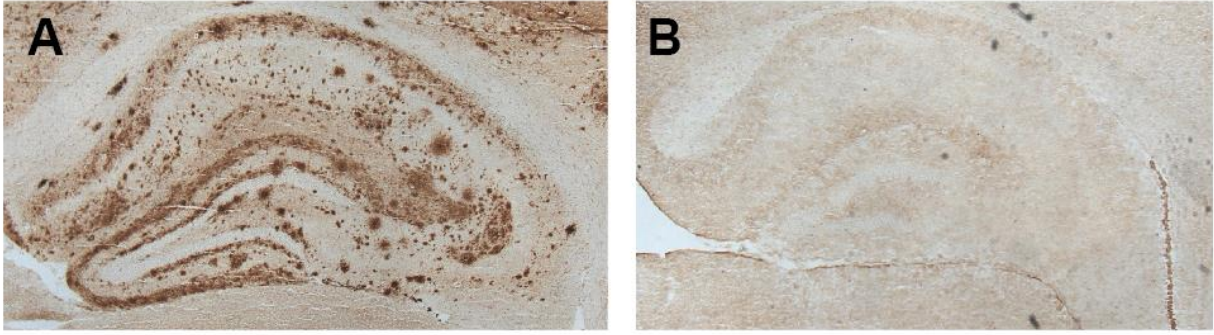


Figure 3.10. 3D6 immunostaining specificity for A β plaques. Immunostaining of mouse hippocampus with 3D6 antibody in a (A) hAPP-J20 section and (B) NTG control. Magnification=4X.

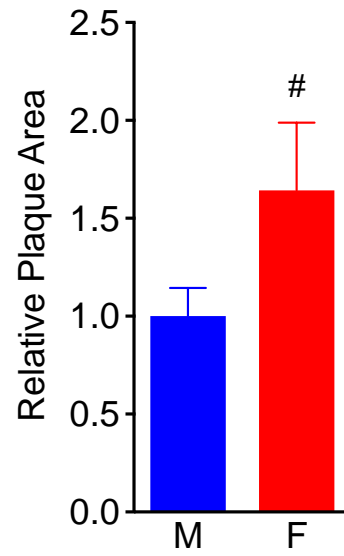


Figure 3.11. A β plaque area in very old female hAPP mice. Relative area of A β deposits in hippocampus of hAPP mice tended to be higher in females at very old age. #P<0.07 (age 24-27 months; n=6-9 per group). Data represent mean \pm SEM.

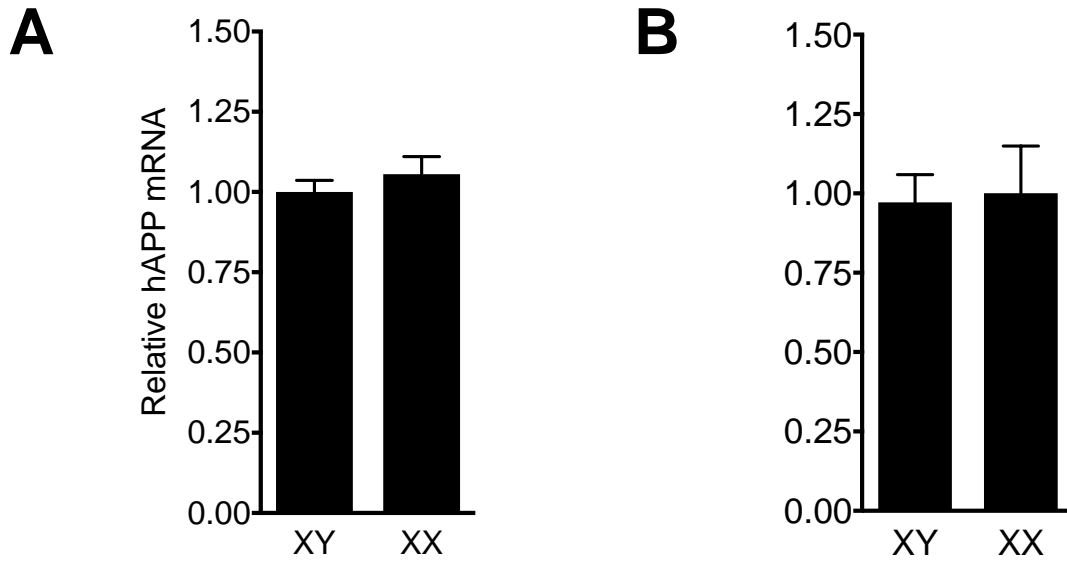


Figure 3.12. hAPP mRNA expression with and without gonadectomy. Relative hAPP mRNA expression in hAPP mice (age 3-4 months; n=10-12 per group) in (A) XY and XX genotype mice with gonads intact and (B) XY and XX genotype mice following gonadectomy shows that expression did not differ between sexes in either condition. Data represent mean \pm SEM.

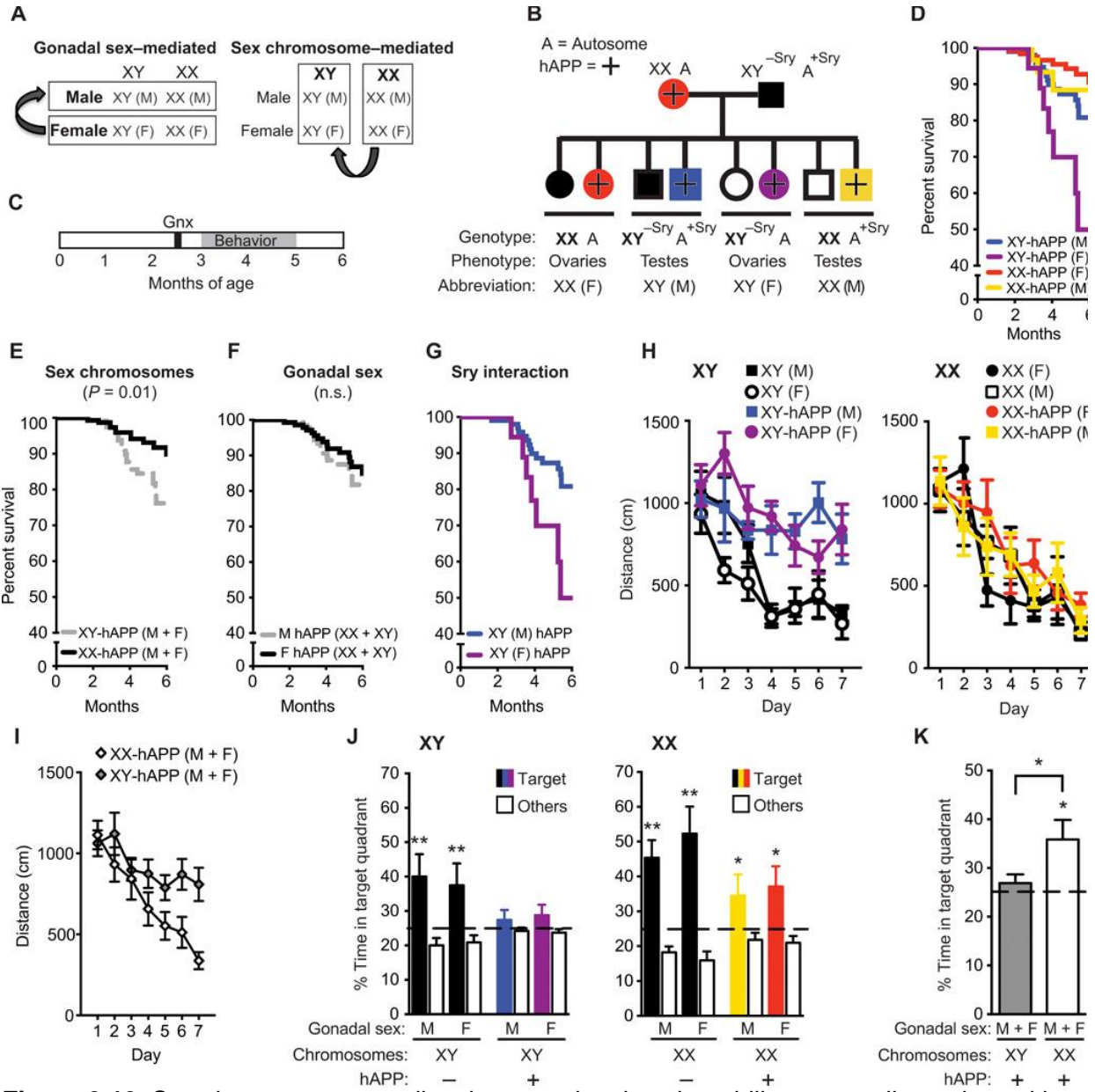


Figure 3.13. Sex chromosomes mediate increased male vulnerability to mortality and cognitive impairments in hAPP mice. **(A)** Strategy to identify the cause of sexual dimorphism using the FCG mouse model. **(B)** Diagram of the cross between hAPP and FCG transgenic mice is presented. FCG mice harbor a transposition of the *Sry* gene from the Y chromosome onto an autosome (A, autosome). Progeny include XX and XY mice, each with either ovarian (F) or testicular (M) development and with or without hAPP expression (hAPP, +). **(C)** Experimental strategy: All mice underwent gonadectomy at about 2.5 months of age, followed by behavioral testing and survival studies at 3 to 6 months of age. **(D to G)** In the Kaplan-Meier survival curves, **(D)** all groups of hAPP mice showed **(E)** a main effect of sex chromosomes on mortality (XY, HR 2.49, CI 1.21 to 5.14, $P < 0.01$) and **(F)** no main effect of gonadal sex on mortality ($P = 0.45$). **(G)** An interaction between sex chromosomes and gonadal sex indicated lower mortality in XY (male, M) compared to XY (female, F) mice (XY-M, HR 0.18, CI 0.03 to 0.92, and $P < 0.05$). Analyses were by Cox proportional hazards for all groups: (XY-M: $n = 101$; XX-F: $n = 122$; XY-F: $n = 18$; XX-M: $n = 31$). **(H and I)** Spatial learning curves from the eight

genotypes of mice tested altogether in the Morris water maze (age 3 to 5 months; $n = 5$ to 6 per group) show that **(H)** XY-hAPP mice (M or F) traveled longer distances to find the target platform, enabling escape from the water maze, than did XX-hAPP mice (M or F). This is highlighted in **(I)**, where all XY-hAPP (M + F) mice were compared with all XX-hAPP (M + F) mice. XX or XY mice without hAPP (M or F) learned similarly well. Data points are daily averages of total distance traveled to reach the platform over four trials. Mixed-model ANOVA: XX-hAPP versus XY-hAPP, $P < 0.01$. **(J and K)** A probe trial, during which the escape platform in the target quadrant was removed, tested for memory of the platform location in the eight genotypes of mice. Percentage of time spent in the target quadrant, indicating memory of the platform location, versus the average time spent in the other three quadrants showed that **(J)** XY-hAPP (M or F) mice did not favor the target quadrant, whereas XX-hAPP (M or F) mice did. The greater impairment of learning and memory in XY-hAPP mice is highlighted in **(K)** where all XY-hAPP (M + F) mice are compared with all XX-hAPP (M + F) mice. The dashed line represents chance performance. These findings were replicated in an independent cohort **(Figure 3.14)**. * $P < 0.05$; ** $P < 0.01$ versus chance performance of 25% (one-sample t tests) or as indicated by bracket (t test). Data are presented as means \pm SEM. n.s., not significant.

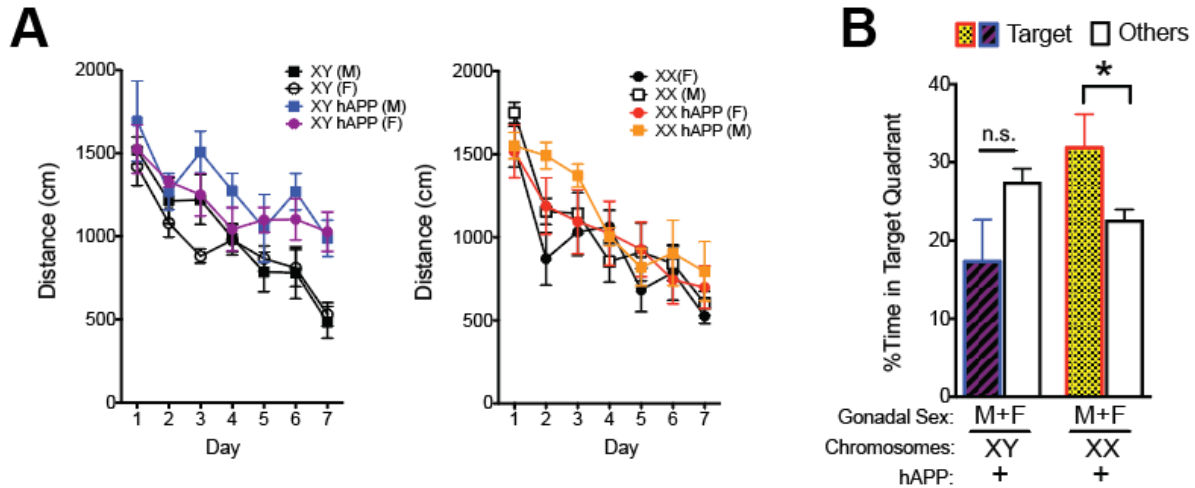


Figure 3.14. Independent, replicate water maze cohort of FCG mice crossed with hAPP mice. FCG mice were crossed with hAPP mice to produce four sex genotypes, with and without hAPP. **(A)** Spatial learning curves from the 8 genotypes of mice tested all together in the water maze (age 3-6 months; $n=4-7$ per group) show that XY-hAPP (M +F) mice traveled longer distances to find the target platform than XX-hAPP (M+F) mice. Mixed model ANOVA: XY-hAPP vs. XY-NTG, $P<0.001$; XX-hAPP vs. XX-NTG, $P<0.2$. **(B)** Probe trial after completion of hidden platform learning shows that XX-hAPP mice (M+F) remember the target. Data show that sex chromosomes mediated male hAPP vulnerability in Morris water maze. $*P<0.05$. Data represent means \pm SEM.

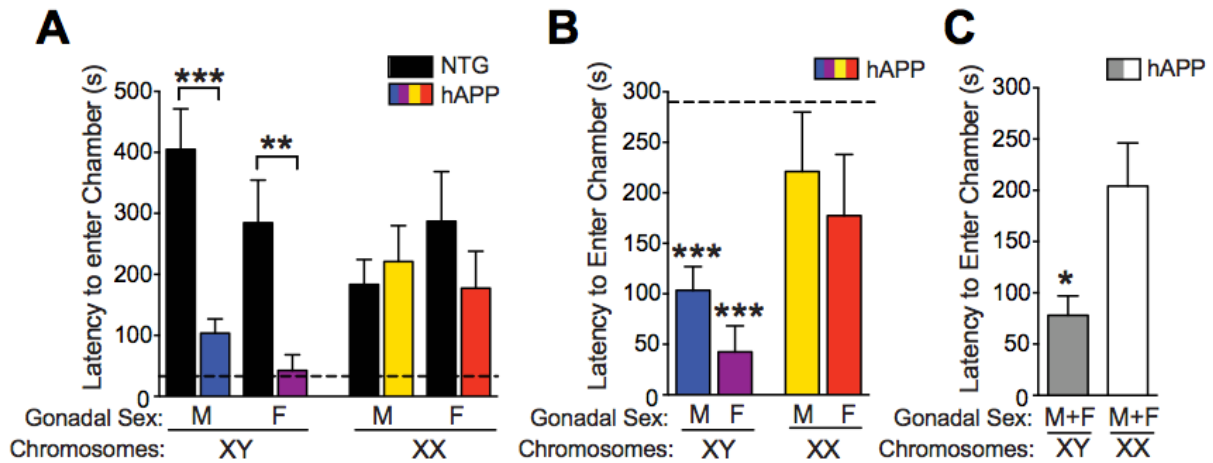


Figure 3.15. Sex chromosomes and fear memory impairment in male hAPP mice. Testing in the passive avoidance task (age 3.5-7 months; n=5-11 per group) for fear memory reflected by latency to enter the dark chamber 24-h following a shock showed that sex chromosomes mediated male vulnerability to impairments of memory in hAPP mice. **(A)** XY-hAPP mice (M and F), but not XX-hAPP mice (M and F) exhibited shorter latencies than NTG mice. Two-way ANOVA: hAPP effect $P < 0.0001$; $**P < 0.01$, $***P < 0.001$ (Bonferroni-Holm). Dashed line=latency to enter dark chamber during training which did not differ among the groups. **(B)** XY-hAPP mice (M or F) exhibited shorter latencies than XX-hAPP mice (M or F). Two-way ANOVA: sex chromosome effect, $P < 0.05$; $***P < 0.001$ vs. NTG average (dashed line) by one-sample t-tests. **(C)** XY-hAPP (M+F) compared with XX-hAPP (M+F). $*P < 0.05$ (t-test). Data represent mean \pm SEM.

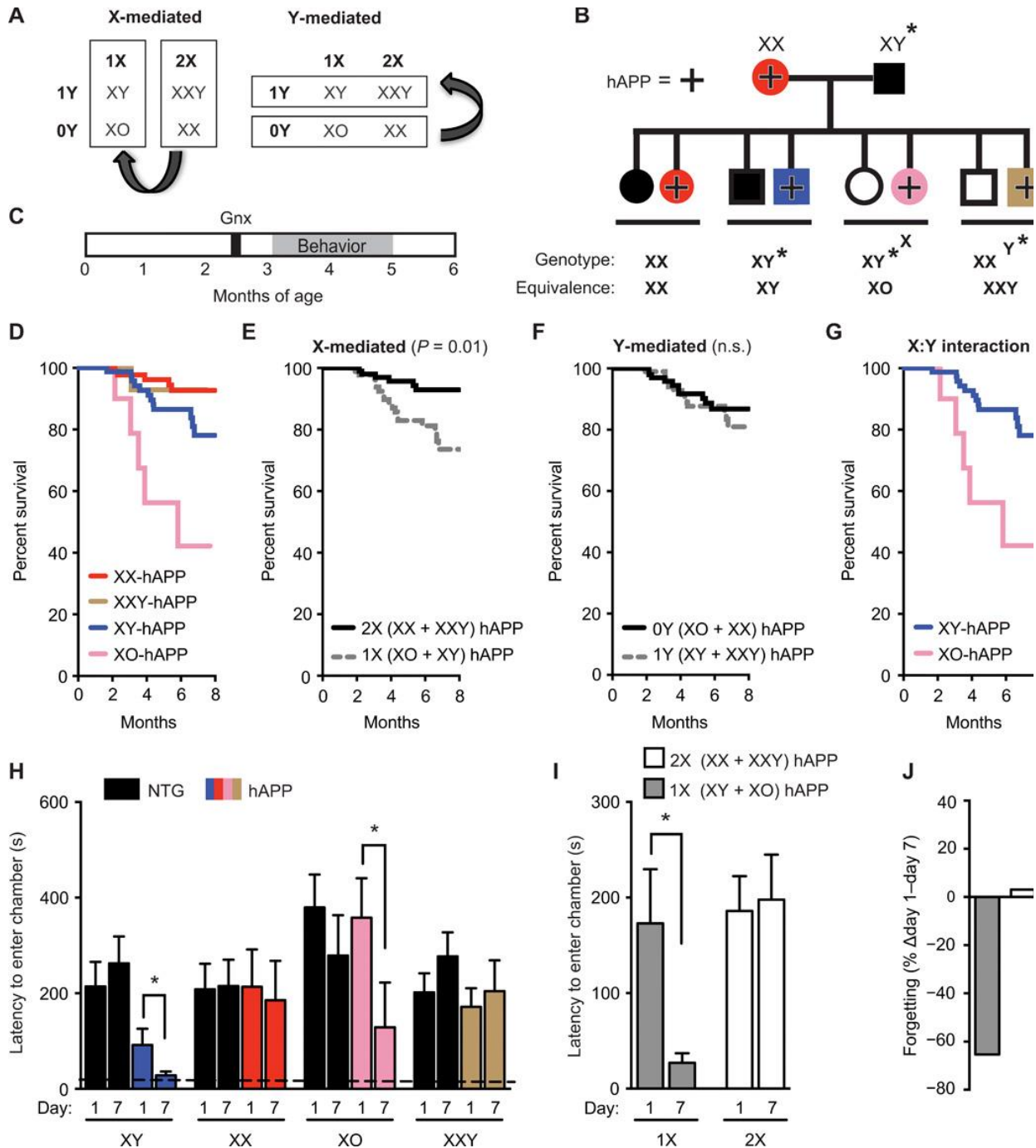


Figure 3.16. A second X chromosome confers resilience against AD-related cognitive impairments in XY (male) and XO (female) hAPP mice. **(A)** Strategy to identify whether the sex chromosome effect depends on the X or Y chromosome. **(B)** Diagram of mouse cross used in this experiment. hAPP females (XX, hAPP) were crossed with XY* males that harbored an altered pseudoautosomal region on the Y chromosome, allowing abnormal crossover with the X chromosome during meiosis (33, 34). The cross resulted in offspring of eight genotypes, each of the sex chromosome genotypes, with or without hAPP. The equivalent number of X and Y chromosomes for each genotype is shown. **(C)** Experimental strategy: All mice underwent gonadectomy at 2.5 months of age followed by behavioral testing and survival studies between 3 and 6 months of age. **(D to G)** In the Kaplan-Meier survival curves in **(D)**, all hAPP mice show

(E) a main effect of X chromosome dose on mortality (2X, HR 0.2, $P < 0.01$, CI 0.12 to 0.75) and (F) no main effect of a Y chromosome on mortality ($P = 0.53$). (G) An interaction between X and Y chromosomes showed lower mortality in the presence of Y (or male gonadal type) when X dose = 1 (XY versus XO, HR 0.23, $P < 0.01$, CI 0.08 to 0.64). Analyses were by Cox proportional hazards for all groups (XY: $n = 79$, XX: $n = 88$; XO: $n = 10$; XXY: $n = 15$ mice). (H to J) Shown is testing of mice in the passive avoidance task, measured by latency to enter the dark chamber 1 and 7 days after a foot shock (age 3 to 5 months; $n = 4$ to 16 per group). (H) Abnormal loss of fear memory in hAPP mice of XY and XO genotypes is shown. Two-way repeated measures ANOVA: X dose effect, $P < 0.05$. The dashed line represents latency to enter the dark chamber during training, which did not differ among the groups. (I) Greater loss of fear memory in hAPP mice with 1X compared to 2X chromosomes is presented. (J) Percent loss of fear memory in hAPP mice with 1X compared to 2X chromosomes is shown. * $P < 0.05$ as indicated by bracket (Bonferroni-Holm). Data are presented as means \pm SEM.

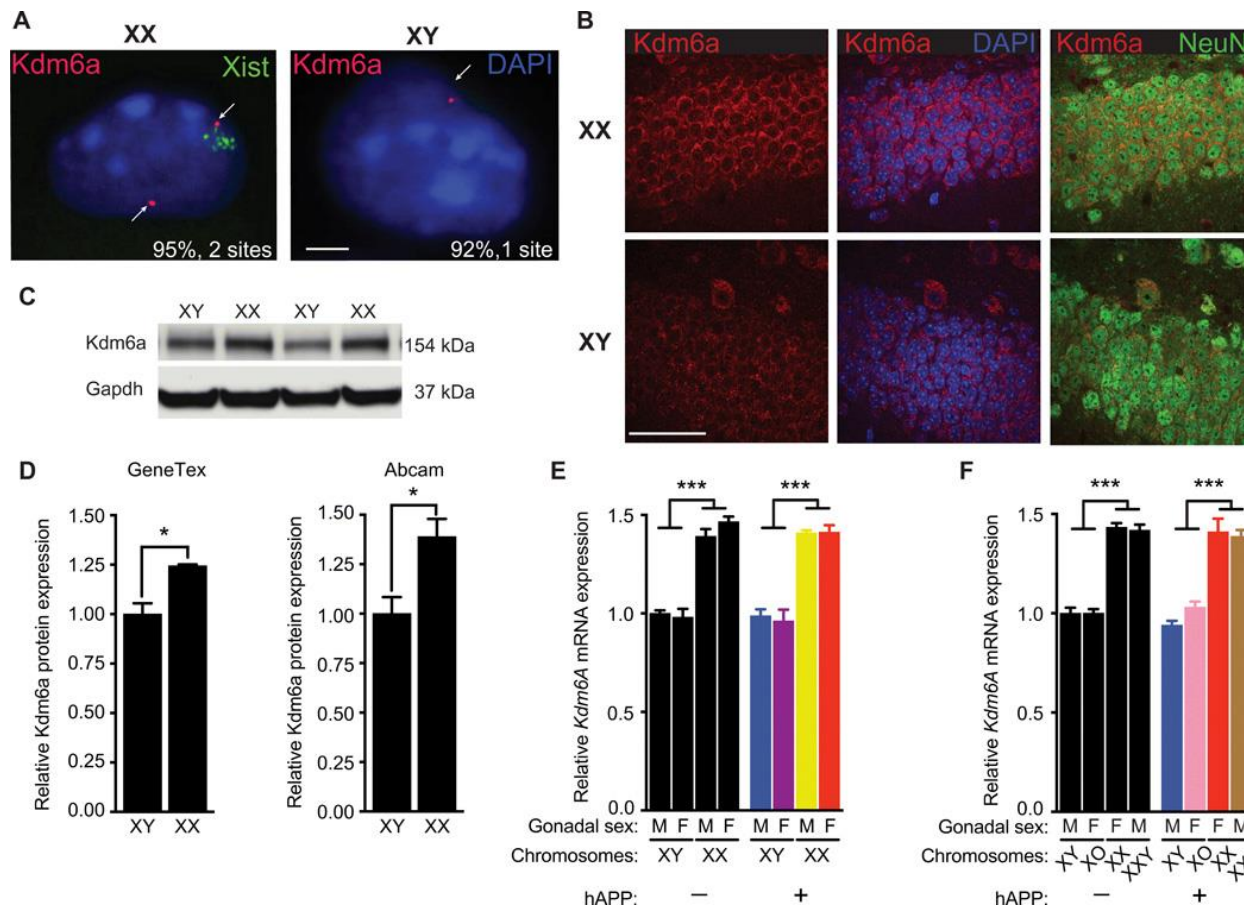


Figure 3.17. A second X chromosome elevates *Kdm6a* expression independent of gonads or the Y chromosome in mice. **(A)** Representative fluorescence in situ hybridization images for *Kdm6a* and *Xist* (RNA FISH) expression in XX (top) and XY (bottom) primary mouse neuronal nuclei. *Kdm6a* is shown in red, *Xist* is shown in green, and 4',6-diamidino-2-phenylindole (DAPI) nuclear stain is shown in blue. Nascent *Kdm6a* transcripts appear as red fluorescent puncta at the site of transcription (indicated by white arrows). *Xist* RNA remains associated with the inactive X chromosome and is detected only in XX cells. Inset numbers indicate the percentage of nuclei with two sites of nascent *Kdm6a* accumulation in XX cells and one site in XY cells ($n = 100$ cells). Scale bar, 2 μm . **(B)** Representative confocal images of *Kdm6a* staining (left), *Kdm6a* with DAPI staining (middle), and *Kdm6a* with Neuronal nuclei (NeuN) staining (right) in the hippocampal dentate gyrus region of a gonadectomized nontransgenic (NTG) female XX mouse (top row) and a gonadectomized NTG male XY mouse (bottom row). *Kdm6a* is shown in red, DAPI nuclear stain is shown in blue, and NeuN is shown in green. Scale bar, 50 μm ; magnification, $\times 100$. **(C and D)** Western blot representative image **(C)** and subsequent quantification **(D)** of *Kdm6a* protein expression in the hippocampus of gonadectomized NTG XX female and XY male mice. Bands represent individual mouse samples. **(C)** Representative images show samples bound by the GeneTex antibody, and **(D)** quantification is given for both GeneTex and Abcam rabbit anti-*Kdm6a* antibodies; *Kdm6a* was normalized using glyceraldehyde phosphate dehydrogenase (GAPDH) as a loading control. Means are relative to NTG XY male control mice, arbitrarily defined as 1 (age 3.4 to 3.6 months; $n = 3$ mice per group). Gonadectomized NTG XX female mice show higher *Kdm6a* protein expression. Two-tailed t test, $*P < 0.05$. **(E and F)** Hippocampal *Kdm6a* mRNA expression in **(E)** FCG mice (age 3.5 to 5.5 months; $n = 6$ to 26 mice per group) and **(F)** XY* mice (age 5.5 to 7.5 months; $n = 4$ to 17 mice per group) with and without hAPP, shown relative to XY male mice without hAPP.

Two-way ANOVA: sex chromosome effect, $***P < 0.001$ and X dose effect, $***P < 0.001$. Data are presented as means \pm SEM in (D) to (F). $*P < 0.05$; $***P < 0.001$ (Bonferroni-Holm).

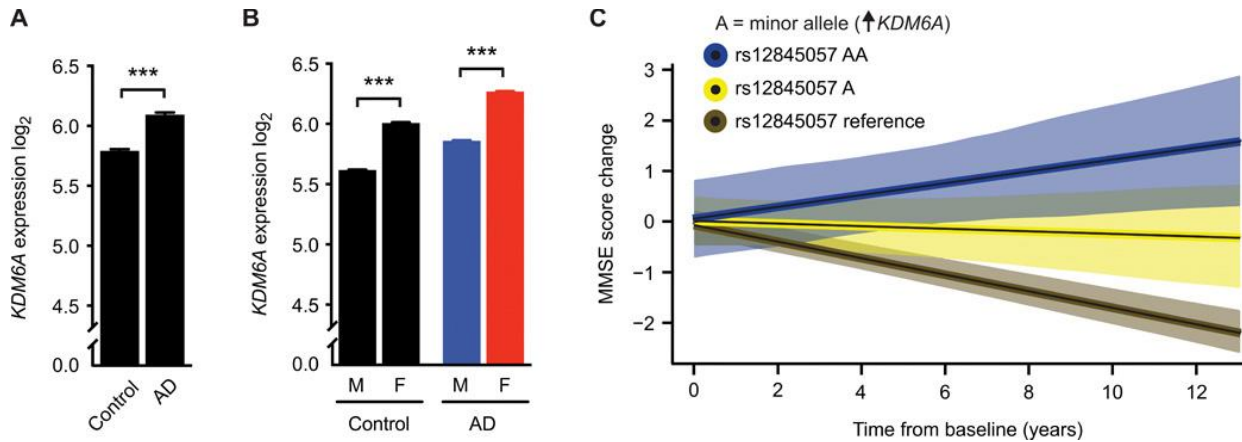


Figure 3.18. *KDM6A* genetic variation associates with cognitive resilience in humans. **(A)** Shown is human *KDM6A* RNA expression via RNA sequencing and microarray in the temporal and parahippocampal cortex of individuals without (control, $n = 135$) and with AD ($n = 86$) ($***P = 3.64 \times 10^{-4}$). **(B)** Shown is human *KDM6A* RNA expression via RNA sequencing and microarray in individuals identified as male (M) or female (F) without (M, $n = 75$; F, $n = 60$; $***P = 9.79 \times 10^{-4}$) and with AD (M, $n = 37$; F, $n = 49$; $***P = 4.83 \times 10^{-4}$). Expression data were analyzed by linear models accounting for effects of postmortem interval and age at death. **(C)** Shown is cognitive change with 95% CIs in 778 individuals of the ADNI cohort (cognitively normal, 268; MCI, 465; AD, 45), who carried two alleles (AA, blue, $n = 8$ all female), one allele (A, yellow, $n = 78$), or no allele (noncarriers, reference, brown, $n = 692$) for the rs12845057 variant of the *KDM6A* gene associated with increased *KDM6A* RNA expression in brain (**Table 3.4**). Cognition was measured by the MMSE score. Increasing dose of the minor allele was associated with slower rates of cognitive decline over time ($\beta = 0.141$, SE 0.035, $P = 0.00005$). Cognitive data were analyzed by linear models accounting for effects of baseline age, sex, education, and *APOE* ϵ 4 dose. Data are presented as means \pm SEM in **(A)** and **(B)**. $***P < 0.001$ (Bonferroni-Holm).

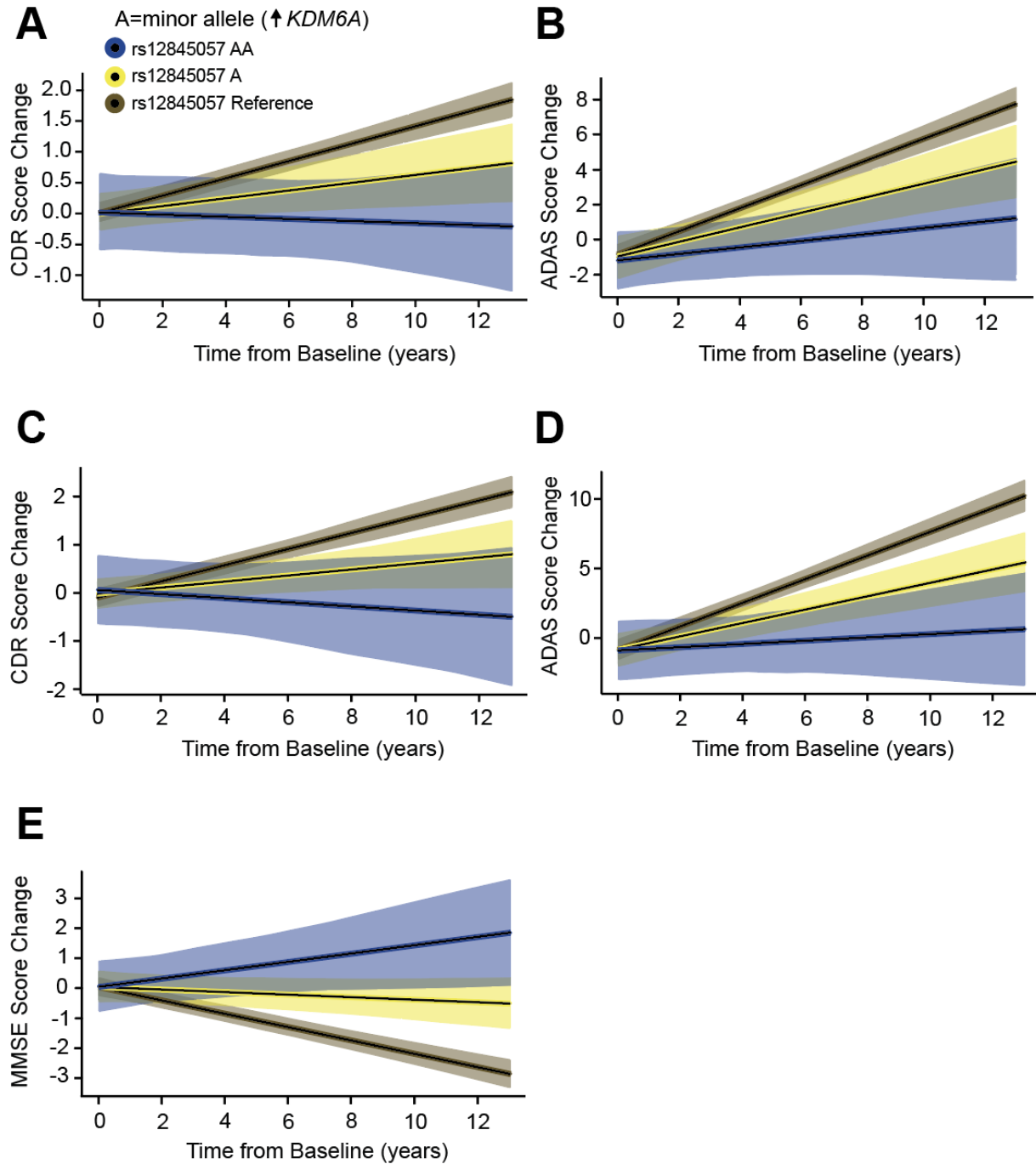


Figure 3.19. *KDM6A* variant, other clinical exam scores, and assessment of women only. Performance of individuals with increasing dose of the minor allele of the rs12845057 variant of *KDM6A* associated with less cognitive decline using other clinical exam scores of dementia and Alzheimer’s disease in men and women, and also in women only. **(A,B)** Men and Women with clinical exam scores measured by **(A)** Clinical Dementia Rating sum of boxes (CDR) scores ($\beta = -0.079$, SE 0.02, $P = 0.001$) and **(B)** Alzheimer’s Disease Assessment Scale (ADAS) scores ($\beta = -0.239$, SE 0.08, $P = 0.003$). **(C–E)** Women only with clinical exam scores measured by **(C)** CDR ($\beta = -0.105$, SE 0.03, $P = 0.0004$), **(D)** ADAS ($\beta = -0.364$, SE 0.097, $P = 0.0002$), and **(E)** Mini Mental State Exam (MMSE) scores ($\beta = 0.180$, SE 0.043, $P = 0.00003$). All individuals

are ADNI participants with rs12845057 genotypes available. Increasing dose of the minor allele A associated with less decline in all cognitive or clinical score measures in men and women, and also in women only. For CDR and ADAS measures, higher score = lower function. For MMSE measures, higher score = higher cognition. The lines indicate slope of cognitive change and shaded areas correspond to 95% confidence intervals.

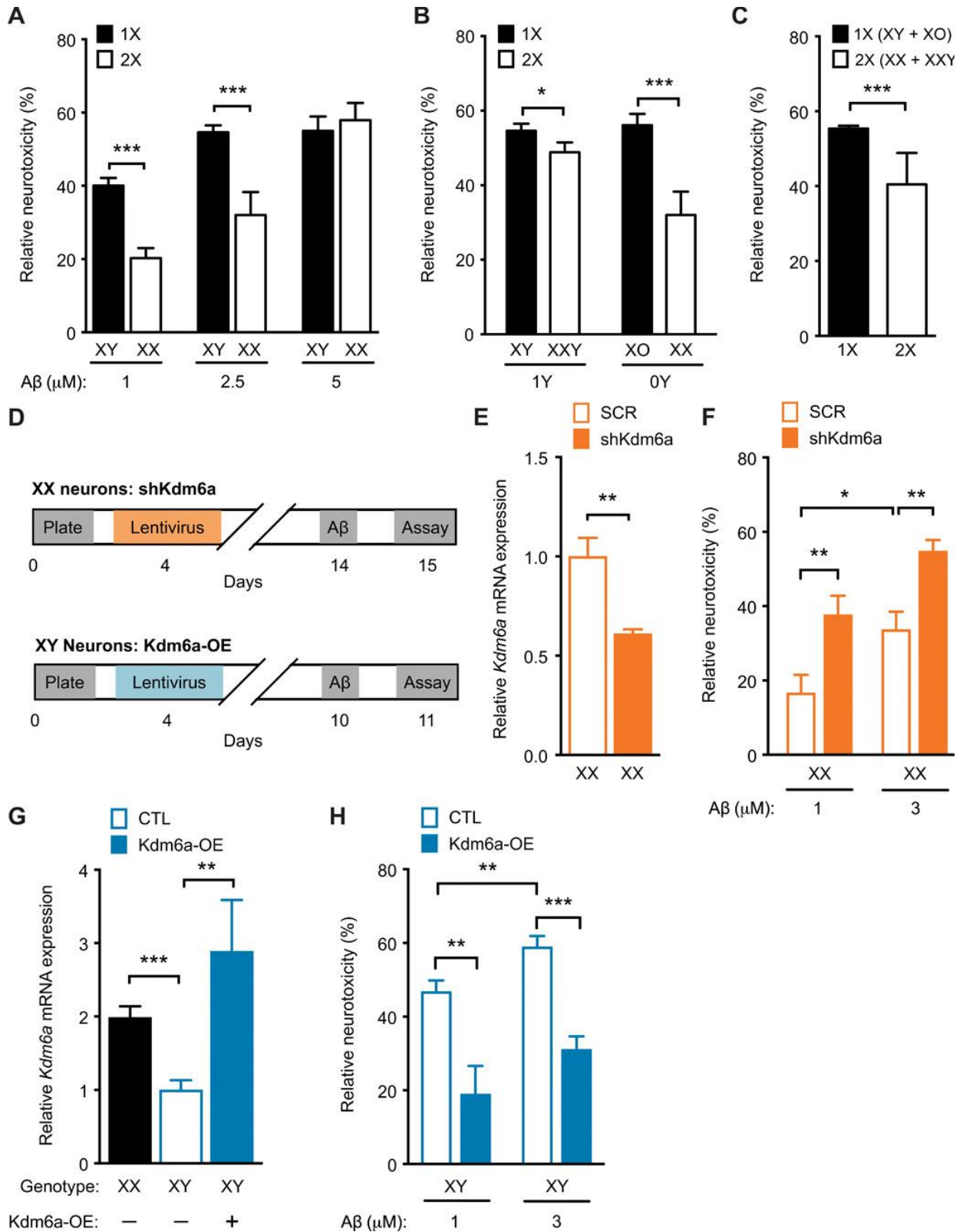


Figure 3.20. *Kdm6a* knockdown in XX mouse neurons worsens, whereas *Kdm6a* overexpression in XY neurons attenuates Aβ toxicity in vitro. (**A to C**) Vulnerability of mouse primary neurons was tested by the MTT assay. For each genotype, cell toxicity was calculated

as a percentage of the corresponding vehicle-treated group, 24 hours after treatment with increasing doses of A β . **(A)** Mouse primary cortical XY neurons showed greater vulnerability than did XX neurons after exposure to vehicle or increasing doses of A β ($n = 8$ to 40 wells per experimental group from 8 to 10 pups per genotype, from four independent litters). Two-way ANOVA: sex chromosome effect, $P < 0.01$; A β dose effect, $P < 0.001$; interaction, $P < 0.05$. **(B)** Toxicity of A β in neurons of varying X and Y chromosome dosage derived from littermate pups of XY* males crossed with nontransgenic (NTG) females, with genotypes roughly equivalent to XO, XX, XY, and XX, exposed to vehicle or A β (2.5 μ M) ($n = 15$ to 45 wells per experimental group from 7 to 10 pups per genotype, from four independent litters). Two-way ANOVA: X effect, $P < 0.0001$; Y effect, not significant; X by Y interaction, $P < 0.05$. **(C)** Main effect of X chromosome dose shows increased A β toxicity in neurons with 1X (XO and XY combined) compared to those with 2X chromosomes (XX and XXY combined). **(D)** Experimental strategy of lentivirus-mediated knockdown of *Kdm6a* in XX mouse primary cortical neurons (top) and *Kdm6a* overexpression in XY mouse primary cortical neurons (bottom). **(E)** Shown is *Kdm6a* mRNA expression in neurons transfected with lentivirus expressing scrambled (SCR) or short hairpin (sh) *Kdm6a* for knockdown expressed relative to XX SCR ($n = 5$ to 6 wells per experimental group from eight XX pups, from two litters). Two-tailed t test, ** $P < 0.01$. **(F)** Shown is A β toxicity in XX neurons treated with SCR or sh*Kdm6a* and exposed to vehicle or A β (1 and 3 μ M); knockdown of *Kdm6a* worsened A β toxicity ($n = 24$ to 25 wells per experimental group from 14 XX pups, from three independent litters). Two-way ANOVA: *Kdm6a* effect, $P < 0.001$; A β effect, $P < 0.001$; *Kdm6a* by A β interaction, $P = 0.99$. **(G)** *Kdm6a* mRNA expression in neurons transfected with lentivirus expressing control (CTL) or overexpressing *Kdm6a* (*Kdm6a*-OE), shown relative to control XY neurons ($n = 3$ to 8 wells per experimental group from 12 XY pups, from two independent litters). One-way ANOVA, $P < 0.001$. **(H)** Shown is A β toxicity in XY neurons transfected with lentivirus expressing control or overexpressing *Kdm6a* (*Kdm6a* OE) and exposed to vehicle or A β (1 and 3 μ M); overexpression of *Kdm6a* attenuated A β toxicity ($n = 12$ to 13 wells per experimental group from 26 XY pups, from three independent litters). Two-way ANOVA: *Kdm6a* effect, $P < 0.001$; A β effect, $P = 0.01$; *Kdm6a* by A β interaction, $P = 0.99$. * $P < 0.05$; ** $P < 0.01$; *** $P < 0.001$ (Bonferroni-Holm). Data are presented as means \pm SEM.

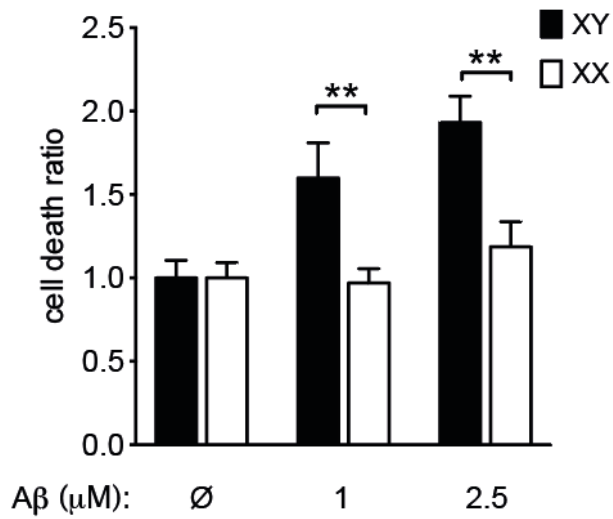


Figure 3.21. Cell death induced by A β toxicity and assessed by LDH release assay. Toxicity in neurons derived from littermate pups of wild type males (XY) and females (XX), exposed to vehicle (Ø) or A β (1 μ M or 2.5 μ M). Toxicity was assessed by LDH assays: the OD values were normalized to absolute lysate LDH activity and ratios of cell death were calculated relative to vehicle treated cells per genotype (n=9–15 wells per experimental group from 3–5 pups per genotype, from 3 independent litters). Two-way ANOVA: Sex effect $P < 0.0001$, dose effect $P < 0.001$, sex by dose interaction $P < 0.001$. One tailed t-test Bonferroni-Holm corrected $**P < 0.01$. Data represent means \pm SEM

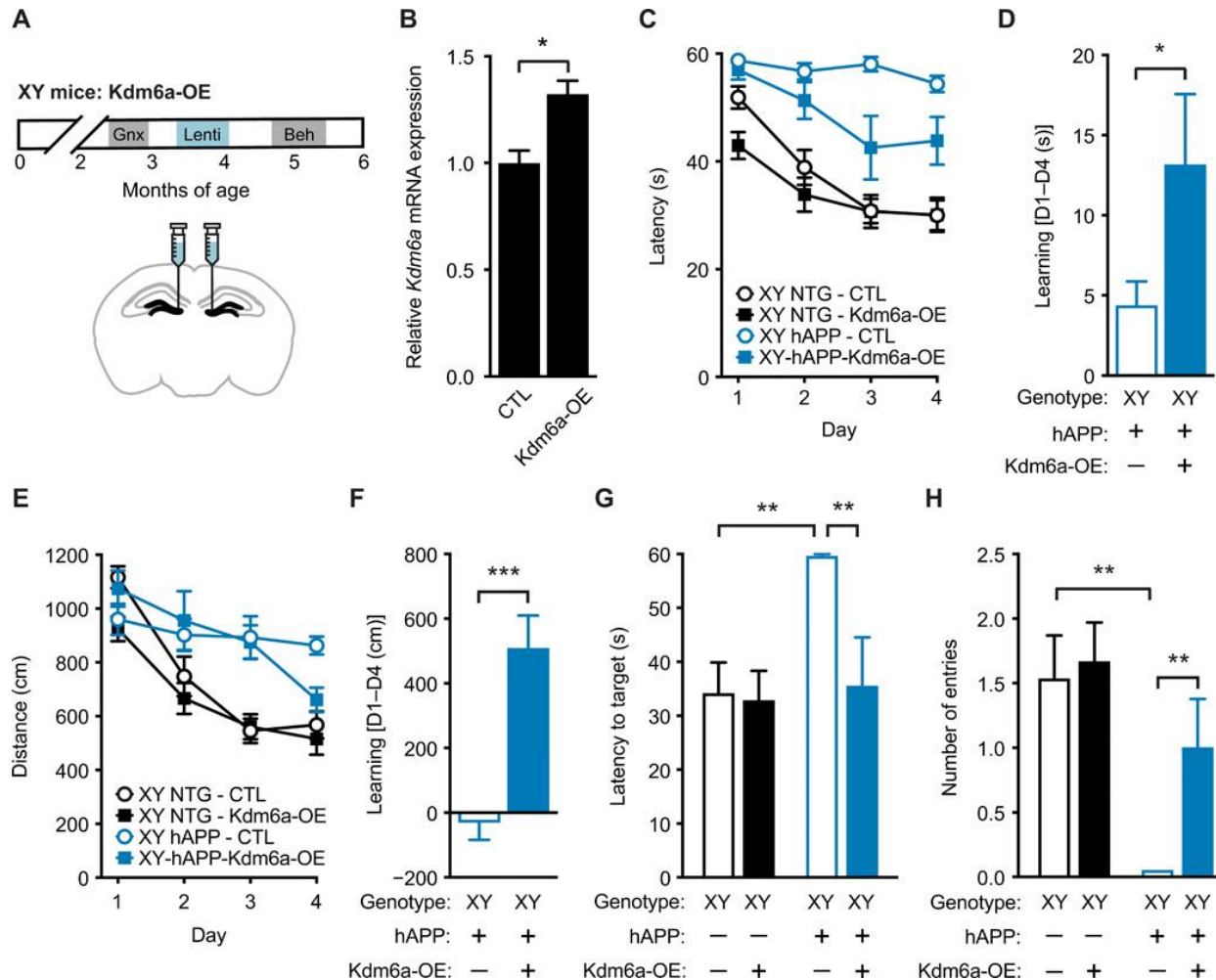


Figure 3.22. *Kdm6a* overexpression in hippocampus attenuates male vulnerability to cognitive impairments in XY-hAPP mice. **(A)** Experimental strategy: XY mice were gonadectomized and injected with lentivirus expressing control or overexpressing *Kdm6a* (*Kdm6a* OE) into the dentate gyrus of the hippocampus; animals were then tested on behavioral tasks. **(B)** Shown is *Kdm6a* mRNA expression measured in dentate gyrus of mice injected with lentivirus expressing control or overexpressing *Kdm6a* (*Kdm6a* OE) ($n = 3$ mice per experimental group), relative to XY control; t test, $*P < 0.05$. **(C to F)** Spatial learning task results for the four experimental groups of XY mice tested in the Morris water maze (age 5 to 5.5 months; $n = 7$ to 15 per group). XY-hAPP-*Kdm6a*-OE mice exhibited **(C)** decreased latency to find the target escape platform (mixed-model ANOVA: XY-hAPP-CTL versus XY-hAPP-*Kdm6a*-OE, $P < 0.001$) and **(D)** a better learning index of latency during hidden platform training, measured by the difference in performance of each mouse at day 4 from average group performance on day 1 (D1 to D4). **(E)** XY-hAPP-*Kdm6a*-OE mice did not travel a statistically decreased distance to find the target platform but **(F)** showed better learning in the distance traveled during hidden platform training. **(G and H)** Probe trial results 24 hours after completion of hidden platform learning, indicating spatial memory of the escape platform location, showed that XY-hAPP-*Kdm6a*-OE mice had attenuated spatial deficits including decreased **(G)** latency to target platform and **(H)** increased number of entries into the target zone, compared to XY-hAPP-CTL mice. $*P < 0.05$; $**P < 0.01$; $***P < 0.001$ [Bonferroni-Holm for **(G)** and **(H)**]. Data are presented as means \pm SEM.

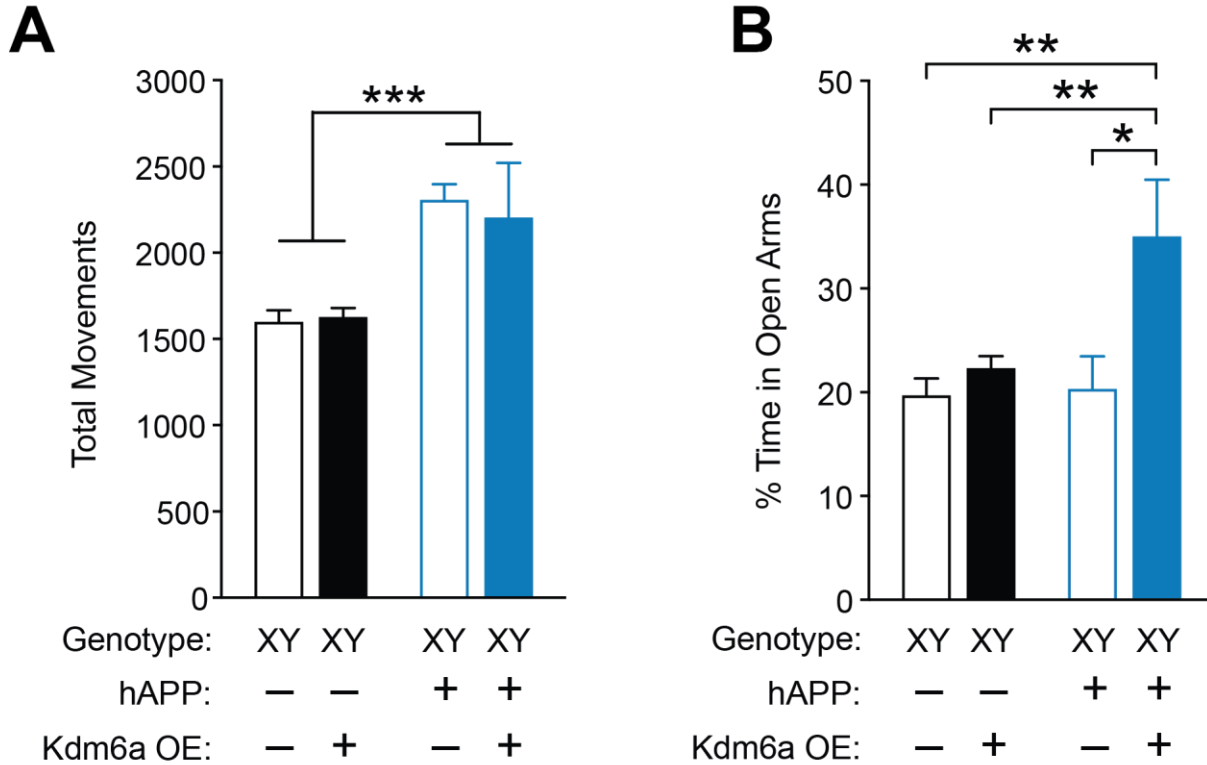


Figure 3.23. Kdm6a overexpression and other behavioral tasks in male XY-hAPP mice. Kdm6a was overexpressed in the dentate gyrus of male XY-hAPP mice. **(A)** Total number of movements by genotype during exploration of openfield for 10 minutes (age 5-5.5 months; n=7-22 per group). XY-hAPP mice had a significantly higher total number of movements compared to XY-NTG, regardless of viral manipulation of Kdm6a in the dentate gyrus. Two-way ANOVA: hAPP effect $***P < 0.0001$, Kdm6a OE effect n.s., hAPP by Kdm6a OE interaction n.s. **(B)** Percentage time spent in the open arms of the elevated plus maze by genotype during 10-minute exploration period (age 5-5.5 months; n=8-22 per group). XY-hAPP-Kdm6a OE mice spent significantly more time in the open arms of the elevated plus maze compared to any other group. Two-way ANOVA: hAPP effect $P = 0.0075$, Kdm6a OE effect $P = 0.0007$, hAPP by Kdm6a OE interaction $P = 0.0150$; $*P < 0.05$, $**P < 0.01$ (Bonferroni-Holm). Data represent mean +SEM.

TABLES

Table 3.1. *KDM6A* in AD and Control Brain Tissues. Results from RNA expression analysis in pathologically confirmed AD cases and controls demonstrate differential expression of *KDM6A* in AD-specific regions with greater *KDM6A* expression in AD vs. Control. Differential expression analyses comparing AD cases to control demonstrated significant increases in areas impacted early in AD such as temporal cortex, parahippocampal gyrus, and superior temporal cortex controlling for age at death, sex, and postmortem interval. AD = Alzheimer’s disease; GSE 15222 – data from (122); Mayo = Mayo Clinic Brain Bank; MSSM = Mount Sinai School of Medicine Brain Bank; CI = confidence interval.

Analysis	Cohort	Tissue	Log Fold Change Expression	95% Lower Limit CI	95% Upper Limit CI	P-value
AD vs. Control	Mayo	Cerebellum	0.089	-0.024	0.20	0.12
	Mayo	Temporal Cortex	0.16	0.043	0.27	0.0068
	GSE 15222	Temporal Cortex	0.26	0.12	0.40	0.00036
	MSSM	Frontal Pole	0.026	-0.048	0.010	0.50
	MSSM	Superior Temporal Gyrus	0.090	0.0037	0.18	0.041
	MSSM	Parahippocampal Gyrus	0.14	0.059	0.23	0.00093
	MSSM	Inferior Frontal Gyrus	0.010	-0.073	0.094	0.81

Table 3.2. GSE 15222 Cohort Characteristics. Participant sex, postmortem interval, and age at death are provided by diagnostic grouping for GSE15222. Significant differences were observed between AD cases and controls with AD cases having lower average postmortem intervals and greater ages at death (both $P < 0.01$). For additional information, please see (122). AD = Alzheimer’s disease; SD = Standard Deviation.

	AD	Control	P-Value
N	86	135	
Males (%)	37 (43.0)	75 (55.6)	0.146
Postmortem Interval Mean Hours (SD)	7.59 (6.01)	10.77 (9.71)	0.007
Age at Death in Mean Years (SD)	84.03 (6.78)	80.32 (9.24)	<0.001

Table 3.3. Mayo and Mount Sinai Brain Bank Sample Characteristics. For each cohort, the total participant number is provided along with sample counts for each tissue type grouped by diagnosis and sex. For additional information, please see www.synapse.org under entry syn14237651. CBE=Cerebellum; FP=Frontal Pole; IFG=Inferior Frontal Gyrus; MAYO=Mayo Clinic Brain Bank Data (see syn14237651 for additional details); MSSM=Mount Sinai Brain Bank study (see syn14237651 for additional details); PHG=Parahippocampal Gyrus; STG=Superior Temporal Gyrus; TCX=Temporal Cortex.

Study	Total Cohort Size	Tissue Type	Sample Count by Diagnosis			
			AD		Control	
			Female	Male	Female	Male
Mayo	179	CBE	47	32	35	37
		TCX	49	31	35	36
MSSM	164	FP	63	27	23	22
		IFG	55	24	17	20
		PHG	47	18	18	20
		STG	57	28	20	17

Table 3.4. ADNI Cohort characteristics. Participant baseline age, baseline sex, baseline education, baseline MMSE score, *APOE* ϵ 4 dosage, rs12845057 genotype, and average follow up time (date accessed 3/11/2019) are shown for each diagnostic grouping. AD=Alzheimer's disease; CN=Clinically Normal Control; MCI=Mild Cognitive Impairment; MMSE=Mini Mental State Exam; SD=Standard Deviation.

	AD	MCI	CN	
N	45	465	268	P-Value
Age (Years; Mean (SD))	75.22 (9.30)	72.34 (7.48)	74.52 (5.51)	<0.001
Sex (Male; %)	28 (62.2)	274 (58.9)	131 (48.9)	0.02
<i>APOE</i> ϵ 4 Dose (%)				
0	12 (26.7)	249 (53.5)	194 (72.4)	
1	24 (53.3)	177 (38.1)	69 (25.7)	<0.001
2	9 (20.0)	39 (8.4)	5 (1.9)	
Education (Years; Mean (SD))	15.69 (2.70)	15.93 (2.83)	16.40 (2.68)	0.06
Baseline MMSE (Mean (SD))	22.78 (1.89)	27.90 (1.67)	29.09 (1.15)	<0.001
rs12845057 genotype (%)				
Reference	41 (91.1)	421 (90.5)	230 (85.8)	
A	4 (8.9)	38 (8.2)	36 (13.3)	0.19
AA	0 (0)	6 (1.3)	2 (0.7)	
Follow up time (Years; Mean (SD))	2.37 (1.39)	5.73 (2.75)	7.33 (3.08)	<0.001

	Female	Male	
N	345	433	P-Value
Age (Years; Mean (SD))	72.40 (7.41)	73.94 (6.72)	0.002
<i>APOE</i> ϵ 4 Dose (%)			
0	203 (58.8)	252 (58.2)	
1	123 (35.7)	147 (33.9)	0.42
2	19 (5.5)	34 (7.9)	
Education (Years; Mean (SD))	15.48 (2.67)	16.56 (2.77)	<0.001
rs12845057 genotype (%)			
Reference	289 (83.8)	403 (93.1)	
A	48 (13.9)	30 (6.9)	<0.001
AA	8 (2.3)	0 (0)	
Diagnosis (%)			
AD	17 (4.9)	28 (6.5)	
MCI	137 (39.7)	131 (30.3)	0.2
CN	191 (55.4)	274 (63.3)	
Follow up time (Years; Mean (SD))	6.03 (3.08)	6.13 (3.03)	0.65

Table 3.5. Longitudinal and Subgroup Analyses in the ADNI Cohort. Results from analyses in the ADNI cohort and subgroup analyses separated by clinical diagnosis and sex demonstrate that carrying the rs12845057 variant in *KDM6A* was associated with slower changes in clinical impairment (CDR) and decreased cognitive changes (MMSE and ADAS) (Figure 6C, fig. S13). In subgroup analyses separated by clinical diagnosis, these changes are most robustly demonstrated in those diagnosed with MCI. In subgroup analyses separated by sex, significant relationships were observed in females diagnosed as CN and MCI. AD=Alzheimer's Disease; ADAS=Alzheimer's Disease Assessment Scale (cognitive); CDR=Clinical Dementia Rating Scale Sum of Boxes Score; CN=Cognitively Normal; MCI=Mild Cognitive Impairment; MMSE=Mini Mental Status Exam.

	All Dx		AD		MCI		CN	
	β (SE)	P-value	β (SE)	P-value	β (SE)	P-value	β (SE)	P-value
Male & Female Combined								
CDR	-0.079 (0.024)	1.20E-03	-0.576 (0.615)	3.49E-01	-0.018 (0.047)	6.97E-01	-0.067 (0.021)	1.85E-03
ADAS	-0.239 (0.080)	2.88E-03	-0.491 (1.594)	7.58E-01	-0.460 (0.154)	2.85E-03	0.088 (0.085)	3.01E-01
MMSE	0.141 (0.035)	5.03E-05	-0.735 (0.924)	4.27E-01	0.218 (0.067)	1.28E-03	0.069 (0.031)	3.06E-02
Male								
CDR	-0.023 (0.044)	5.92E-01	-0.898 (0.642)	1.62E-01	0.019 (0.096)	8.40E-01	0.056 (0.038)	1.37E-01
ADAS	0.038 (0.014)	7.90E-01	-2.495 (2.062)	2.26E-01	-0.181 (0.295)	5.40E-01	0.269 (0.158)	8.88E-02
MMSE	0.062 (0.062)	3.17E-01	1.247 (1.122)	2.66E-01	0.117 (0.135)	3.83E-01	-0.067 (0.054)	2.16E-01
Female								
CDR	-0.105 (0.030)	4.00E-04	-1.026 (1.208)	4.00E-01	-0.049 (0.055)	3.75E-01	-0.133 (0.026)	2.77E-07
ADAS	-0.364 (0.097)	1.81E-04	0.081 (2.670)	9.76E-01	-0.651 (0.188)	5.47E-04	-0.248 (0.098)	1.11E-02
MMSE	0.180 (0.043)	2.66E-05	-2.974 (1.659)	7.30E-02	0.275 (0.082)	7.69E-04	0.130 (0.034)	9.61E-04

Chapter 4 – Future Directions

SUMMARY

This thesis demonstrates the importance of two X chromosomes in mouse longevity and neurodegeneration as well as highlights an important epigenetic regulator and XCI escapee gene, Kdm6a, in rescuing AD-related deficits in XY male mice and neuronal cultures. While this work expands our understanding of sex biology there are many questions left remaining that warrant further investigation, several of which I explore in this chapter. I propose further inquiries into the XX-ovarian connection and increased longevity seen in FCG mice, the downstream effects of Kdm6a signaling in mice and humans, and the possibility of inactive X chromosome reactivation in aging and neurodegeneration.

Four Core Genotypes Lifespan

One important caveat of our work regarding longevity is that, unlike human populations, the female advantage in lifespan is not always observed in mice of different substrains and populations (Austad 2011). In the aforementioned study, even within the C57Bl6 substrain there wasn't a consensus on the directionality of the sex difference in lifespan (Austad 2011). Underlying this observation are likely the environmental differences in animal facilities, including diet, bedding, housing density, and ambient humidity and temperature. This explanation is bolstered by a follow-up study by the same group where genotype and husbandry techniques were standardized across multiple testing sites with multiple cohorts; when conditions were standardized the female advantage was evident with female mice living longer than male mice (Austad and Fischer 2016). Our findings would be similarly bolstered if the FCG model were bred on a mixed background that better reflects the genetic diversity seen in humans and by replicating the study across multiple animal facilities and cohorts.

It remains to be determined whether the female lifespan advantage observed in our FCG colony is more influenced by the presence of a second X chromosome, or the lack of a Y chromosome. The absence of differences in lifespan between the two XY groups may be the results of non-SRY Y chromosome gene expression. These inquiries would be answered by doing a similar lifespan study using the XY* model. As of this writing, I am unaware of any published data exploring the normal lifespan curves of XY* mice. It remains to be determined if male XXY mice that result from the XY* model have a lifespan curve closer to XX(T) or XY(T). If XXY is more similar to XX(T) it would suggest that the presence of a second X plays a more prominent role in overall lifespan. If the XXY mice have a lifespan more similar to XY(T) we might determine that it is the lack of a Y chromosome that benefits XX(T) animals. This would suggest that non-SRY Y chromosome genes might be detrimental to longevity. Unfortunately, this model would not add much to the observed XX-ovary interaction. It would be informative to assess longevity in XXY(O) female mice using the sex chromosome trisomy mouse model (Chen, Williams-Burris et al. 2013) to test if the presence of non-SRY Y linked genes has an impact on the XX-ovary interaction.

Our observation of XX-ovary interaction is especially interesting with the well-established link between gonadectomy and increased longevity in a variety of species (Berman and Kenyon 2006, Min, Lee et al. 2012, Hoffman, Creevy et al. 2013). We could further explore these observations by gonadectomizing post-development FCG mice and measuring their lifespan. This experiment would allow us to determine if the XX(O) increased longevity is due to organizational effects of ovaries on an XX background or if the activational effects of ovary-induced hormone production is necessary for the XX-ovary interaction. It would also test whether, in the absence of activational effects of hormones, XX(T) mice would have a lifespan closer to that seen in XX(O) mice. If gonadectomy abolishes the improved lifespan seen in XX(O) or all XX mice, the follow-up could determine if gonadectomy followed by administration of gonadal hormones rescues the increased lifespan. These studies would help to narrow the cause of this beneficial XX-ovarian interaction.

Further Characterization of Kdm6a Expression and Role in Neurodegeneration

We found that the presence of the second X chromosome increased *Kdm6a* expression – and *Kdm6a* overexpression rescued AD-related deficits in XY mice and neurons. While *Kdm6a*-KD was performed *in vitro*, it would be interesting to determine its effects *in vivo* in female hAPP mice to see if *Kdm6a*-KD exacerbates hAPP-induced deficits, and to what degree. It's possible that the deficits induced by hAPP expression are significant enough that knocking-down *Kdm6a* wouldn't result in a greater deficit in females. Females may also express compensatory mechanisms such that decreased *Kdm6a* expression wouldn't further deficits. All *Kdm6a* work thus far has been done with lentiviral stereotaxic injection methods; using a *Kdm6a*-cre line may overcome some of the drawbacks of lentiviral methods, specifically *Kdm6a*-KD in XX mice and neurons. While tamoxifen has been known to have estrogen receptor agonist/antagonist actions, recent studies support its use in studying sex differences of the aging brain (Chucair-Elliott, Ocanas et al. 2019) and show that it has no effect on overall behavior and neurogenesis (Rotheneichner, Romanelli et al. 2017). Furthermore, in conjunction with *Xist*-deletion mice, one could selectively delete *Kdm6a* expression from the inactive X, allowing assessment of removing *Kdm6a*-escape expression from XX females. This approach would be more precise and wouldn't be subject to lentiviral effectiveness, differences in imprinting, or the effects of a total deletion.

We additionally observed that *Kdm6a* appears to be located in the cytoplasm of neurons in the mouse hippocampus. A similar observation has been made by at least one other group using cell lines (Wiedemuth, Thieme et al. 2018). These observations suggest that in addition to its histone H3K27 demethylation activity in the nucleus, *Kdm6a* may have other functions outside the nucleus. To determine if *Kdm6a*-OE-induced resilience to AD-related deficits is due to its nuclear vs. cytoplasmic localization, one could generate *Kdm6a* mutants of predicated nuclear localization and nuclear export sequences. If *Kdm6a*-OE resilience is abolished when nuclear localization sequences are mutated, it would suggest that *Kdm6a*'s function within the nucleus

that confers its protective effect. Likewise, it would suggest its cytoplasmic functions confer its protective effect if Kdm6a-OE resilience is abolished when nuclear export sequences are mutated. It is also possible that Kdm6a-OE's protective effect is due to a combination of its nuclear and cytoplasmic functions, in which case a decrease in its effectiveness, but not totally abolishment, would be observed in both mutants. Characterization of these mutant forms of Kdm6a would be necessary to confirm that the mutation had its intended effects.

It's possible that Kdm6a's function is cell-type specific. While little work has been done with regards to Kdm6a's cell-type expression in the brain, one study in the rat CNS showed it was predominately expressed by neurons, followed by astrocytes, with little to no expression in microglia (Smith, Kimyon et al. 2014). The lentiviral overexpression used in the previous chapter was not neuron-specific and it's possible that Kdm6a overexpression occurred in non-neuronal cells of the hippocampus and contributed to the observed phenotype. It would therefore be informative to conduct a comprehensive single cell RNA-sequencing of male and female mouse hippocampi to identify what XCI-escapee and Kdm6a subpopulation expression looks like and which cell populations were most effected by lentiviral overexpression.

We also identified an intergenic genetic variant in humans that is associated with greater Kdm6a expression in the brain and reduced cognitive decline, rs12845057. Increased *KDM6A* expression in AD brains, in isolation, is ambiguous, since the direction of gene expression change does not reveal its biologic influence on disease. This relationship could be determined by using iPSCs with variable dose of the rs12845057 SNP. iPSCs could then be differentiated into neurons and their survival assessed using the A β toxicity assay or other cellular AD models. Determining the directionality of *KDM6A* expression's association with resilience in human cells could both bolster our findings in mice, as well as provide a new therapeutic target for treatment of AD. It would also be interesting to determine the frequency of this variant in more genetically diverse populations. Establishing the frequency of rs12845057 in more genetically diverse populations would help determine its relevancy in assessment of AD vulnerability and possible treatments.

Underlying Mechanisms of Protective Effects of Kdm6a Overexpression

It is important to note that while *KDM6A* escapes XCI, the Y chromosome harbors a paralogue of *KDM6A*, *UTY* (Greenfield, Carrel et al. 1998) that shares 87% homology (Gazova, Lengeling et al. 2019). However, unlike *KDM6A*, *UTY* contains a nearly inactive catalytic domain for histone demethylation (Shpargel, Sengoku et al. 2012, Walport, Hopkinson et al. 2014). While these proteins could potentially interact, the presence of *Uty* in XY neurons and mice did not alter the ability of increased *Kdm6a* to attenuate AD-related toxicity *in vitro* or *in vivo*. This observation suggests that the effects of *Kdm6a*-OE are likely due to its demethylase activity. However, it remains to be determined if the protective effects conferred by *Kdm6a* overexpression are in fact due to its histone demethylase function or other mechanisms. It is known that *Kdm6a* has demethylase independent functions, as established by studies using a catalytically dead mutant that doesn't phenocopy a full deletion in mouse development (Agger, Cloos et al. 2007, Lee, Villa et al. 2007, Faralli, Wang et al. 2016). Therefore, future studies should establish whether it is *Kdm6a*'s demethylase-dependent or independent functions that confer its protective effects.

Overexpression of a catalytically dead *Kdm6a* could be used to test the importance of its demethylase activity to its protective effects. If AD-related deficits are rescued in XY hAPP mice and neurons with the demethylase-dead *Kdm6a*-OE then it can be concluded that *Kdm6a*-mediated resilience is due to demethylase-independent functions. Similarly, if no rescue is found it suggests that previously observed rescue effects of *Kdm6a*-OE are due to its demethylase-dependent activity. In these experiments, it is important to also measure H3K27me3 protein levels relative to histone H3 levels to determine if *Kdm6a*-OE increases H3K27me3 and if demethylase-dead *Kdm6a*-OE abolishes this change. If changes are attributed to H3K27 demethylation activity, an important follow-up would then be to perform high throughput methods, such as ChIP-seq, to determine which parts of the genome are most likely regulated by *Kdm6a*'s demethylase activity. To determine non-histone demethylation activity, neutron-encoded (Neucode) stable

incorporation of labeled amino acids (SILAC) in culture (Overmyer, Tyanova et al. 2018) combined with methyl-Lysine enrichment (Hartel, Chew et al. 2019) and mass spectrometry would provide an unbiased method to identify proteins that show Kdm6a-dependent methylation. To obtain a catalogue of Kdm6a's demethylation targets, XX and XO KDM6A knock out neurons would be analyzed. XX and XY neurons could then be compared to identify targets that may underlie male/female differences in susceptibility to A β toxicity. If it's determined that resilience is conferred by demethylase-independent functions, a next step would be to determine what other proteins Kdm6a interacts with using mass spectrometry of Flag-tagged Kdm6a immunoprecipitation to determine its interactome. Such methods could also be used to compare the interactome of Kdm6a in XX vs. XY neurons to determine sex-specific and dose-specific partners.

It is likely that Kdm6a, whether through demethylase dependent or independent functions, is a regulator of autosomal genes and that it is these downstream genes and cellular functions that lead to the observed rescue of AD-related deficits in Kdm6a-OE. One group in China has identified a downstream target of Kdm6a, serotonin receptor 5b (5-Htr5b), a G-coupled protein receptor (GPCR). Overexpression of 5-Htr5b rescues observed hippocampal-dependent memory deficits and neuronal dysregulation in Kdm6a-KO mice and cultured hippocampal neurons (Tang, Zeng et al. 2017, Tang, Mi et al. 2020). It's possible that the rescue of deficits in Kdm6a overexpression were due to increased 5-Htr5b expression. Future studies would benefit from including an analysis of 5-Htr5b expression in our system and experimentation to determine if increased 5-Htr5b is sufficient to rescue observed hAPP and A β deficits.

Xi Reactivation in Aging and Neurodegeneration

In addition to the role of individual XCI escapee genes, it is possible that parts or the entirety of the inactive X may undergo reactivation. Biallelic expression of X-linked genes may also occur due to the partial or whole reactivation of the Xi chromosome itself, known to occur in

females during stem cell reprogramming and generation of germ cells. It has been speculated, but not conclusively shown, that Xi reactivation can occur with aging. It is widely known that genomic instability including loss of repressive epigenetic marks occurs with aging (Villeponteau 1997, Lopez-Otin, Blasco et al. 2013). A loss of repressive marks on the Xi would presumably lead to Xi reactivation. This reactivation may play a role in the female aging phenotype in ways that could be both protective and detrimental. Loss of XCI has been shown to occur in cancer (Agrelo and Wutz 2010, Yildirim, Kirby et al. 2013) but it is possible that reactivation of Xi may be beneficial under certain circumstances. Compared to other chromosomes, the X chromosome is rich with genes important for brain development and many mental disability disorders are X-linked (Zechner, Wilda et al. 2001, Ropers and Hamel 2005). Few studies so far have focused on Xi reactivation with age and those that do have been descriptive and explore neither possible downstream effects, nor upstream mechanisms (Wareham, Lyon et al. 1987, Bennett-Baker, Wilkowski et al. 2003, Schoeftner, Blanco et al. 2009). For example, a 2003 study by Bennett-Baker et al. showed that, in both mouse kidney and spleen, aging resulted in increased expression of *Atp7a* from the inactive X, a gene known to be normally silenced in adult mice (Bennett-Baker, Wilkowski et al. 2003). Another paper reported that telomere shortening, a process known to occur in aging, results in reduced repression of the inactive X (Schoeftner, Blanco et al. 2009). Despite these findings, the role of Xi-reactivation in the brain has not been thoroughly explored. Our lab has bred a unique mouse model that enables us to definitively identify gene expression from the X_a vs. the X_i. It involves crossing the previously mentioned female *Xist*^{Δ/+} C57Bl/6J (*M. musculus*) with a wildtype male from a different subspecies, CAST/EiJ (*M. castaneus*). This crossing enables the determination of the origin of each X-linked transcript using established as well as *de novo* SNPs that distinguish the *M. musculus* and *M. castaneus* genomes (**Figure 4.1**). Females with the maternal skewing caused by the *Xist* deletion should only express X-linked SNPs from their maternal, *M. musculus* X. Any X-linked *M. castaneus* SNPs identified would be indicative of genes which escape XCI. Single cell RNA-sequencing (scRNA-seq) of various cell

populations in the brain would be most informative for our lab. As a positive control of Xi reactivation, pharmacologic methods of reactivating the inactive X chromosome could be used.

If age-related stress does indeed cause reactivation of the Xi, an increase in the number of genes being expressed from the Xi as shown by SNP read counts from the Xi of *Xist*^{Δ/+} Bl6xEiJ mouse brains and cultures would be found. It may be that reactivation is only seen in aged mice or only upon specific age-related stress induction. In this case, the results will provide a clue as to which age-related pathways may cause reactivation, providing another line of investigation. Alternatively, it may be that XCI is maintained throughout aging, even as other repressive marks on the epigenome are lost. Or Xi reactivation may be a process that occurs in some subset animals but not all and is variable across the lifespan. It is also possible that loss of Xi repression is ultimately detrimental to females and does not confer resilience. Regardless of the outcome, elucidating changes in X-linked gene expression from the inactive X during aging will inform our understanding of sex differences in aging and its underlying molecular pathways.

FIGURES

Figure 4

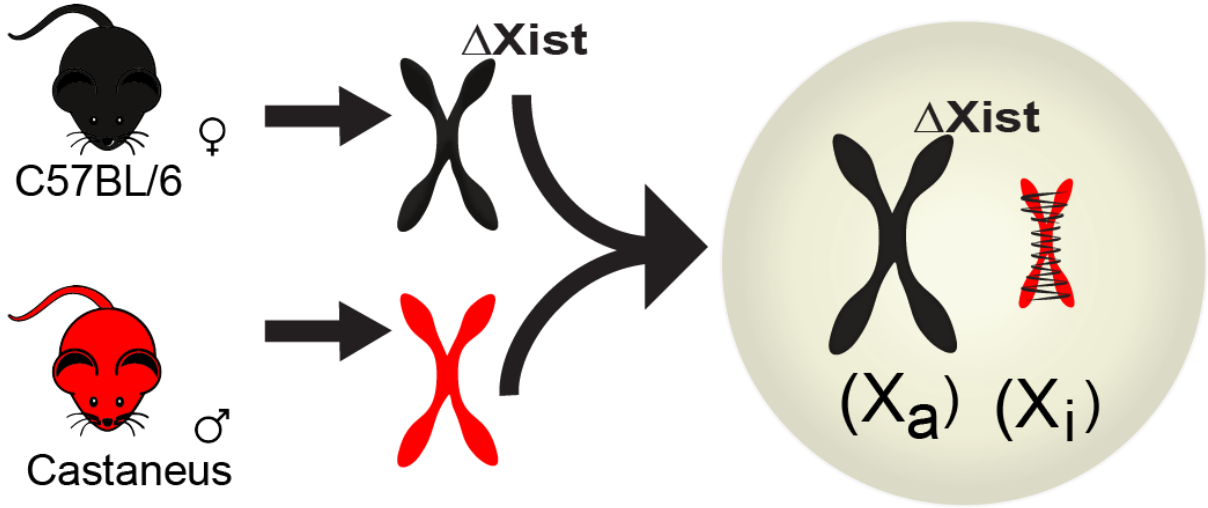


Figure 4.1. Diagram of female $Xist^{\Delta/+}$ C57BL/6J (*M. musculus*) crossed with wildtype male from CAST/EiJ (*M. castaneus*) and the resultant skewed offspring.

References

- Agger, K., P. A. Cloos, J. Christensen, D. Pasini, S. Rose, J. Rappsilber, I. Issaeva, E. Canaani, A. E. Salcini and K. Helin (2007). "UTX and JMJD3 are histone H3K27 demethylases involved in HOX gene regulation and development." Nature **449**(7163): 731-734.
- Agrelo, R. and A. Wutz (2010). "Context of change--X inactivation and disease." EMBO Mol Med **2**(1): 6-15.
- Allen, M., M. M. Carrasquillo, C. Funk, B. D. Heavner, F. Zou, C. S. Younkin, J. D. Burgess, H. S. Chai, J. Crook, J. A. Eddy, H. Li, B. Logsdon, M. A. Peters, K. K. Dang, X. Wang, D. Serie, C. Wang, T. Nguyen, S. Lincoln, K. Malphrus, G. Bisceglia, M. Li, T. E. Golde, L. M. Mangravite, Y. Asmann, N. D. Price, R. C. Petersen, N. R. Graff-Radford, D. W. Dickson, S. G. Younkin and N. Ertekin-Taner (2016). "Human whole genome genotype and transcriptome data for Alzheimer's and other neurodegenerative diseases." Sci Data **3**: 160089.
- Aras, M. A., K. A. Hartnett and E. Aizenman (2008). "Assessment of cell viability in primary neuronal cultures." Curr Protoc Neurosci **Chapter 7**: Unit 7 18.
- Arnegard, M. E., L. A. Whitten, C. Hunter and J. A. Clayton (2020). "Sex as a Biological Variable: A 5-Year Progress Report and Call to Action." J Womens Health (Larchmt) **29**(6): 858-864.
- Arnold, A. P. (2004). "Sex chromosomes and brain gender." Nature reviews. Neuroscience **5**(9): 701-708.
- Arnold, A. P. (2009). "Mouse models for evaluating sex chromosome effects that cause sex differences in non-gonadal tissues." Journal of neuroendocrinology **21**(4): 377-386.
- Arnold, A. P. and X. Chen (2009). "What does the "four core genotypes" mouse model tell us about sex differences in the brain and other tissues?" Front Neuroendocrinol **30**(1): 1-9.
- Austad, S. N. (2011). Chapter 23 - Sex Differences in Longevity and Aging. Handbook of the Biology of Aging (Seventh Edition). E. J. Masoro and S. N. Austad. San Diego, Academic Press: 479-495.

Austad, S. N. and K. E. Fischer (2016). "Sex Differences in Lifespan." Cell Metab **23**(6): 1022-1033.

Balaton, B. P. and C. J. Brown (2016). "Escape Artists of the X Chromosome." Trends Genet **32**(6): 348-359.

Balaton, B. P., A. M. Cotton and C. J. Brown (2015). "Derivation of consensus inactivation status for X-linked genes from genome-wide studies." Biol Sex Differ **6**: 35.

Barrett, E. L. and D. S. Richardson (2011). "Sex differences in telomeres and lifespan." Aging Cell **10**(6): 913-921.

Bates, D., M. Mächler, B. Bolker and S. Walker (2014). "lme4: Linear mixed-effects models using Eigen and S4." Journal of Statistical Software **67**.

Beery, A. K. and I. Zucker (2011). "Sex bias in neuroscience and biomedical research." Neurosci Biobehav Rev **35**(3): 565-572.

Bennett-Baker, P. E., J. Wilkowski and D. T. Burke (2003). "Age-associated activation of epigenetically repressed genes in the mouse." Genetics **165**(4): 2055-2062.

Berletch, J. B., X. Deng, D. K. Nguyen and C. M. Disteche (2013). "Female bias in RhoX6 and 9 regulation by the histone demethylase KDM6A." PLoS Genet **9**(5): e1003489.

Berletch, J. B., W. Ma, F. Yang, J. Shendure, W. S. Noble, C. M. Disteche and X. Deng (2015). "Escape from X inactivation varies in mouse tissues." PLoS Genet **11**(3): e1005079.

Berletch, J. B., F. Yang and C. M. Disteche (2010). "Escape from X inactivation in mice and humans." Genome Biol **11**(6): 213.

Berman, J. R. and C. Kenyon (2006). "Germ-cell loss extends *C. elegans* life span through regulation of DAF-16 by kri-1 and lipophilic-hormone signaling." Cell **124**(5): 1055-1068.

Bogershausen, N., V. Gatinois, V. Riehmer, H. Kayserili, J. Becker, M. Thoenes, P. O. Simsek-Kiper, M. Barat-Houari, N. H. Elcioglu, D. Wieczorek, S. Tinschert, G. Sarrabay, T. M. Strom, A. Fabre, G. Baynam, E. Sanchez, G. Nurnberg, U. Altunoglu, Y. Capri, B. Isidor, D. Lacombe, C. Corsini, V. Cormier-Daire, D. Sanlaville, F. Giuliano, K. H. Le Quan Sang, H. Kayirangwa, P.

Nurnberg, T. Meitinger, K. Boduroglu, B. Zoll, S. Lyonnet, A. Tzschach, A. Verloes, N. Di Donato, I. Touitou, C. Netzer, Y. Li, D. Genevieve, G. Yigit and B. Wollnik (2016). "Mutation Update for Kabuki Syndrome Genes KMT2D and KDM6A and Further Delineation of X-Linked Kabuki Syndrome Subtype 2." Hum Mutat **37**(9): 847-864.

Bonham, L. W., R. S. Desikan, J. S. Yokoyama and I. Alzheimer's Disease Neuroimaging (2016). "The relationship between complement factor C3, APOE epsilon4, amyloid and tau in Alzheimer's disease." Acta Neuropathol Commun **4**(1): 65.

Broestl, L., K. Worden, A. J. Moreno, E. J. Davis, D. Wang, B. Garay, T. Singh, L. Verret, J. J. Palop and D. B. Dubal (2018). "Ovarian Cycle Stages Modulate Alzheimer-Related Cognitive and Brain Network Alterations in Female Mice." eNeuro **5**(6).

Bronikowski, A. M., J. Altmann, D. K. Brockman, M. Cords, L. M. Fedigan, A. Pusey, T. Stoinski, W. F. Morris, K. B. Strier and S. C. Alberts (2011). "Aging in the natural world: comparative data reveal similar mortality patterns across primates." Science **331**(6022): 1325-1328.

Brookmeyer, R. and N. Abdalla (2018). "Estimation of lifetime risks of Alzheimer's disease dementia using biomarkers for preclinical disease." Alzheimers Dement **14**(8): 981-988.

Brooks, R. C. and M. G. Garratt (2017). "Life history evolution, reproduction, and the origins of sex-dependent aging and longevity." Ann N Y Acad Sci **1389**(1): 92-107.

Buckley, R. F., E. C. Mormino, R. E. Amariglio, M. J. Properzi, J. S. Rabin, Y. Y. Lim, K. V. Papp, H. I. L. Jacobs, S. Burnham, B. J. Hanseeuw, V. Dore, A. Dobson, C. L. Masters, M. Waller, C. C. Rowe, P. Maruff, M. C. Donohue, D. M. Rentz, D. Kirn, T. Hedden, J. Chhatwal, A. P. Schultz, K. A. Johnson, V. L. Villemagne, R. A. Sperling, I. Alzheimer's Disease Neuroimaging, B. Australian Imaging, a. Lifestyle study of and S. Harvard Aging Brain (2018). "Sex, amyloid, and APOE epsilon4 and risk of cognitive decline in preclinical Alzheimer's disease: Findings from three well-characterized cohorts." Alzheimers Dement **14**(9): 1193-1203.

Buckley, R. F., E. C. Mormino, J. S. Rabin, T. J. Hohman, S. Landau, B. J. Hanseeuw, H. I. L. Jacobs, K. V. Papp, R. E. Amariglio, M. J. Properzi, A. P. Schultz, D. Kirn, M. R. Scott, T. Hedden,

M. Farrell, J. Price, J. Chhatwal, D. M. Rentz, V. L. Villemagne, K. A. Johnson and R. A. Sperling (2019). "Sex Differences in the Association of Global Amyloid and Regional Tau Deposition Measured by Positron Emission Tomography in Clinically Normal Older Adults." JAMA Neurol **76**(5): 542-551.

Buter, T. C., A. van den Hout, F. E. Matthews, J. P. Larsen, C. Brayne and D. Aarsland (2008). "Dementia and survival in Parkinson disease: a 12-year population study." Neurology **70**(13): 1017-1022.

Callahan, M. J., W. J. Lipinski, F. Bian, R. A. Durham, A. Pack and L. C. Walker (2001). "Augmented senile plaque load in aged female beta-amyloid precursor protein-transgenic mice." Am J Pathol **158**(3): 1173-1177.

Caracciolo, B., K. Palmer, R. Monastero, B. Winblad, L. Backman and L. Fratiglioni (2008). "Occurrence of cognitive impairment and dementia in the community: a 9-year-long prospective study." Neurology **70**(19 Pt 2): 1778-1785.

Carithers, L. J., K. Ardlie, M. Barcus, P. A. Branton, A. Britton, S. A. Buia, C. C. Compton, D. S. DeLuca, J. Peter-Demchok, E. T. Gelfand, P. Guan, G. E. Korzeniewski, N. C. Lockhart, C. A. Rabiner, A. K. Rao, K. L. Robinson, N. V. Roche, S. J. Sawyer, A. V. Segre, C. E. Shive, A. M. Smith, L. H. Sobin, A. H. Undale, K. M. Valentino, J. Vaught, T. R. Young, H. M. Moore and G. T. Consortium (2015). "A Novel Approach to High-Quality Postmortem Tissue Procurement: The GTEx Project." Biopreserv Biobank **13**(5): 311-319.

Carrel, L. and H. F. Willard (2005). "X-inactivation profile reveals extensive variability in X-linked gene expression in females." Nature **434**(7031): 400-404.

Carroll, J. C., E. R. Rosario, S. Kreimer, A. Villamagna, E. Gentschein, F. Z. Stanczyk and C. J. Pike (2010). "Sex differences in beta-amyloid accumulation in 3xTg-AD mice: role of neonatal sex steroid hormone exposure." Brain Res **1366**: 233-245.

Casaletto, K. B., F. M. Elahi, A. M. Staffaroni, S. Walters, W. R. Contreras, A. Wolf, D. Dubal, B. Miller, K. Yaffe and J. H. Kramer (2019). "Cognitive aging is not created equally: differentiating unique cognitive phenotypes in "normal" adults." Neurobiol Aging **77**: 13-19.

Cerhan, J. R., A. R. Folsom, J. A. Mortimer, E. Shahar, D. S. Knopman, P. G. McGovern, M. A. Hays, L. D. Crum and G. Heiss (1998). "Correlates of cognitive function in middle-aged adults. Atherosclerosis Risk in Communities (ARIC) Study Investigators." Gerontology **44**(2): 95-105.

Chen, S., Y. Li, S. Zhi, Z. Ding, Y. Huang, W. Wang, R. Zheng, H. Yu, J. Wang, M. Hu, J. Miao and J. Li (2020). "lncRNA Xist Regulates Osteoblast Differentiation by Sponging miR-19a-3p in Aging-induced Osteoporosis." Aging Dis **11**(5): 1058-1068.

Chen, X., S. M. Williams-Burris, R. McClusky, T. C. Ngun, N. Ghahramani, H. Barseghyan, K. Reue, E. Vilain and A. P. Arnold (2013). "The Sex Chromosome Trisomy mouse model of XXY and XYY: metabolism and motor performance." Biol Sex Differ **4**(1): 15.

Cheng, J. S., D. B. Dubal, D. H. Kim, J. Legleiter, I. H. Cheng, G. Q. Yu, I. Teseur, T. Wyss-Coray, P. Bonaldo and L. Mucke (2009). "Collagen VI protects neurons against Abeta toxicity." Nat Neurosci **12**(2): 119-121.

Cheng, Z., C. Luo and Z. Guo (2020). "lncRNA-XIST/microRNA-126 sponge mediates cell proliferation and glucose metabolism through the IRS1/PI3K/Akt pathway in glioma." J Cell Biochem **121**(3): 2170-2183.

Chin, J., J. J. Palop, J. Puolivali, C. Massaro, N. Bien-Ly, H. Gerstein, K. Scearce-Levie, E. Masliah and L. Mucke (2005). "Fyn kinase induces synaptic and cognitive impairments in a transgenic mouse model of Alzheimer's disease." J Neurosci **25**(42): 9694-9703.

Chucair-Elliott, A. J., S. R. Ocanas, D. R. Stanford, N. Hadad, B. Wronowski, L. Otalora, M. B. Stout and W. M. Freeman (2019). "Tamoxifen induction of Cre recombinase does not cause long-lasting or sexually divergent responses in the CNS epigenome or transcriptome: implications for the design of aging studies." Geroscience **41**(5): 691-708.

Cisse, M., B. Halabisky, J. Harris, N. Devidze, D. B. Dubal, B. Sun, A. Orr, G. Lotz, D. H. Kim, P. Hamto, K. Ho, G. Q. Yu and L. Mucke (2011). "Reversing EphB2 depletion rescues cognitive functions in Alzheimer model." Nature **469**(7328): 47-52.

Claus, J. J., W. A. van Gool, S. Teunisse, G. J. Walstra, V. I. Kwa, A. Hijdra, B. Verbeeten, Jr., J. H. Koelman, L. J. Bour and B. W. Ongerboer De Visser (1998). "Predicting survival in patients with early Alzheimer's disease." Dement Geriatr Cogn Disord **9**(5): 284-293.

Clutton-Brock, T. H. and K. Isvaran (2007). "Sex differences in ageing in natural populations of vertebrates." Proc Biol Sci **274**(1629): 3097-3104.

Colchero, F., R. Rau, O. R. Jones, J. A. Barthold, D. A. Conde, A. Lenart, L. Nemeth, A. Scheuerlein, J. Schoeley, C. Torres, V. Zarulli, J. Altmann, D. K. Brockman, A. M. Bronikowski, L. M. Fedigan, A. E. Pusey, T. S. Stoinski, K. B. Strier, A. Baudisch, S. C. Alberts and J. W. Vaupel (2016). "The emergence of longevous populations." Proc Natl Acad Sci U S A **113**(48): E7681-E7690.

Consortium, G. T. (2015). "Human genomics. The Genotype-Tissue Expression (GTEx) pilot analysis: multitissue gene regulation in humans." Science **348**(6235): 648-660.

Consortium, G. T., D. A. Laboratory, G. Coordinating Center -Analysis Working, G. Statistical Methods groups-Analysis Working, G. g. Enhancing, N. I. H. C. Fund, Nih/Nci, Nih/Nhgri, Nih/Nimh, Nih/Nida, N. Biospecimen Collection Source Site, R. Biospecimen Collection Source Site, V. Biospecimen Core Resource, B. Brain Bank Repository-University of Miami Brain Endowment, M. Leidos Biomedical-Project, E. Study, I. Genome Browser Data, E. B. I. Visualization, I. Genome Browser Data, U. o. C. S. C. Visualization-Ucsc Genomics Institute, a. Lead, D. A. Laboratory, C. Coordinating, N. I. H. p. management, c. Biospecimen, Pathology, Q. T. L. m. w. g. e, A. Battle, C. D. Brown, B. E. Engelhardt and S. B. Montgomery (2017). "Genetic effects on gene expression across human tissues." Nature **550**(7675): 204-213.

Corre, C., M. Friedel, D. A. Vousden, A. Metcalf, S. Spring, L. R. Qiu, J. P. Lerch and M. R. Palmert (2016). "Separate effects of sex hormones and sex chromosomes on brain structure and

function revealed by high-resolution magnetic resonance imaging and spatial navigation assessment of the Four Core Genotype mouse model." Brain Struct Funct **221**(2): 997-1016.

Csankovszki, G., B. Panning, B. Bates, J. R. Pehrson and R. Jaenisch (1999). "Conditional deletion of Xist disrupts histone macroH2A localization but not maintenance of X inactivation." Nat Genet **22**(4): 323-324.

Davies, W., A. Isles, R. Smith, D. Karunadasa, D. Burrmann, T. Humby, O. Ojarikre, C. Biggin, D. Skuse, P. Burgoyne and L. Wilkinson (2005). "Xlr3b is a new imprinted candidate for X-linked parent-of-origin effects on cognitive function in mice." Nat Genet **37**(6): 625-629.

Davis, E. J., I. Lobach and D. B. Dubal (2019). "Female XX sex chromosomes increase survival and extend lifespan in aging mice." Aging Cell **18**(1): e12871.

Deeb, S. S. (2005). "The molecular basis of variation in human color vision." Clin Genet **67**(5): 369-377.

Di Carlo, A., M. Lamassa, M. Baldereschi, M. Inzitari, E. Scafato, G. Farchi and D. Inzitari (2007). "CIND and MCI in the Italian elderly: frequency, vascular risk factors, progression to dementia." Neurology **68**(22): 1909-1916.

Digma, L. A., J. R. Madsen, R. A. Rissman, D. M. Jacobs, J. B. Brewer, S. J. Banks and I. Alzheimer's Disease Neuroimaging (2020). "Women can bear a bigger burden: ante- and post-mortem evidence for reserve in the face of tau." Brain Commun **2**(1): fcaa025.

Du, S., N. Itoh, S. Askarinam, H. Hill, A. P. Arnold and R. R. Voskuhl (2014). "XY sex chromosome complement, compared with XX, in the CNS confers greater neurodegeneration during experimental autoimmune encephalomyelitis." Proc Natl Acad Sci U S A **111**(7): 2806-2811.

Dubal, D. B. (2020). Sex Difference in Alzheimer's disease: an updated, balanced and emerging perspective on differing vulnerabilities. Sex Differences in Neurology and Psychiatry. R. Lanzberger, G. S. Kranz and I. Savic, Elsevier: in press.

Dubal, D. B., L. Broestl and K. Worden (2012). "Sex and gonadal hormones in mouse models of Alzheimer's disease: what is relevant to the human condition?" Biology of sex differences **3**(1): 24.

Dubal, D. B., J. S. Yokoyama, L. Zhu, L. Broestl, K. Worden, D. Wang, V. E. Sturm, D. Kim, E. Klein, G. Q. Yu, K. Ho, K. E. Eilertson, L. Yu, O. M. Kuro, P. L. De Jager, G. Coppola, G. W. Small, D. A. Bennett, J. H. Kramer, C. R. Abraham, B. L. Miller and L. Mucke (2014). "Life extension factor klotho enhances cognition." Cell Rep **7**(4): 1065-1076.

Dubal, D. B., L. Zhu, P. E. Sanchez, K. Worden, L. Broestl, E. Johnson, K. Ho, G. Q. Yu, D. Kim, A. Betourne, O. M. Kuro, E. Masliah, C. R. Abraham and L. Mucke (2015). "Life extension factor klotho prevents mortality and enhances cognition in hAPP transgenic mice." J Neurosci **35**(6): 2358-2371.

Dunford, A., D. M. Weinstock, V. Savova, S. E. Schumacher, J. P. Cleary, A. Yoda, T. J. Sullivan, J. M. Hess, A. A. Gimelbrant, R. Beroukhim, M. S. Lawrence, G. Getz and A. A. Lane (2017). "Tumor-suppressor genes that escape from X-inactivation contribute to cancer sex bias." Nat Genet **49**(1): 10-16.

Eicher, E. M., D. W. Hale, P. A. Hunt, B. K. Lee, P. K. Tucker, T. R. King, J. T. Eppig and L. L. Washburn (1991). "The mouse Y* chromosome involves a complex rearrangement, including interstitial positioning of the pseudoautosomal region." Cytogenetics and cell genetics **57**(4): 221-230.

Elmaleh, D. R., M. R. Farlow, P. S. Conti, R. G. Tompkins, L. Kundakovic and R. E. Tanzi (2019). "Developing Effective Alzheimer's Disease Therapies: Clinical Experience and Future Directions." J Alzheimers Dis **71**(3): 715-732.

Faralli, H., C. Wang, K. Nakka, A. Benyoucef, S. Sebastian, L. Zhuang, A. Chu, C. G. Palii, C. Liu, B. Camellato, M. Brand, K. Ge and F. J. Dilworth (2016). "UTX demethylase activity is required for satellite cell-mediated muscle regeneration." J Clin Invest **126**(4): 1555-1565.

Ferrini, R. L. and E. Barrett-Connor (1998). "Sex hormones and age: a cross-sectional study of testosterone and estradiol and their bioavailable fractions in community-dwelling men." Am J Epidemiol **147**(8): 750-754.

Folstein, M. F., S. E. Folstein and P. R. McHugh (1975). "'Mini-mental state'. A practical method for grading the cognitive state of patients for the clinician." J Psychiatr Res **12**(3): 189-198.

Forsaa, E. B., J. P. Larsen, T. Wentzel-Larsen and G. Alves (2010). "What predicts mortality in Parkinson disease?: a prospective population-based long-term study." Neurology **75**(14): 1270-1276.

Gaignard, P., S. Saviouroux, P. Liere, A. Pianos, P. Therond, M. Schumacher, A. Slama and R. Guennoun (2015). "Effect of Sex Differences on Brain Mitochondrial Function and Its Suppression by Ovariectomy and in Aged Mice." Endocrinology **156**(8): 2893-2904.

Ganesan, S., D. P. Silver, R. A. Greenberg, D. Avni, R. Drapkin, A. Miron, S. C. Mok, V. Randrianarison, S. Brodie, J. Salstrom, T. P. Rasmussen, A. Klimke, C. Marrese, Y. Marahrens, C. X. Deng, J. Feunteun and D. M. Livingston (2002). "BRCA1 supports XIST RNA concentration on the inactive X chromosome." Cell **111**(3): 393-405.

Ganguli, M., H. H. Dodge, C. Shen and S. T. DeKosky (2004). "Mild cognitive impairment, amnesic type: an epidemiologic study." Neurology **63**(1): 115-121.

Gatewood, J. D., A. Wills, S. Shetty, J. Xu, A. P. Arnold, P. S. Burgoyne and E. F. Rissman (2006). "Sex chromosome complement and gonadal sex influence aggressive and parental behaviors in mice." J Neurosci **26**(8): 2335-2342.

Gazova, I., A. Lengeling and K. M. Summers (2019). "Lysine demethylases KDM6A and UTY: The X and Y of histone demethylation." Mol Genet Metab **127**(1): 31-44.

Gendron, C. M., T. H. Kuo, Z. M. Harvanek, B. Y. Chung, J. Y. Yew, H. A. Dierick and S. D. Pletcher (2014). "Drosophila life span and physiology are modulated by sexual perception and reward." Science **343**(6170): 544-548.

Goyal, M. S., T. M. Blazey, Y. Su, L. E. Couture, T. J. Durbin, R. J. Bateman, T. L. Benzinger, J. C. Morris, M. E. Raichle and A. G. Vlassenko (2019). "Persistent metabolic youth in the aging female brain." Proc Natl Acad Sci U S A **116**(8): 3251-3255.

Greenfield, A., L. Carrel, D. Pennisi, C. Philippe, N. Quaderi, P. Siggers, K. Steiner, P. P. Tam, A. P. Monaco, H. F. Willard and P. Koopman (1998). "The UTX gene escapes X inactivation in mice and humans." Hum Mol Genet **7**(4): 737-742.

Greenfield, A., D. Scott, D. Pennisi, I. Ehrmann, P. Ellis, L. Cooper, E. Simpson and P. Koopman (1996). "An H-YDb epitope is encoded by a novel mouse Y chromosome gene." Nat Genet **14**(4): 474-478.

Halford, R. W. and D. W. Russell (2009). "Reduction of cholesterol synthesis in the mouse brain does not affect amyloid formation in Alzheimer's disease, but does extend lifespan." Proc Natl Acad Sci U S A **106**(9): 3502-3506.

Hartel, N., B. Chew, J. Qin, J. Xu and N. A. Graham (2019). "Deep protein methylation profiling by combined chemical and immunoaffinity approaches reveals novel PRMT1 targets." Mol Cell Proteomics.

Hartung, J. and G. Knapp (2001). "On tests of the overall treatment effect in meta-analysis with normally distributed responses." Stat Med **20**(12): 1771-1782.

Hartung, J. and G. Knapp (2001). "A refined method for the meta-analysis of controlled clinical trials with binary outcome." Stat Med **20**(24): 3875-3889.

Hebert, L. E., P. A. Scherr, J. J. McCann, L. A. Beckett and D. A. Evans (2001). "Is the risk of developing Alzheimer's disease greater for women than for men?" Am J Epidemiol **153**(2): 132-136.

Hedges, L. V. and J. L. Vevea (1998). "Fixed- and Random-Effects Models in Meta-Analysis." Psychological Methods **3**(4): 486-504.

Heyman, A., W. E. Wilkinson, B. J. Hurwitz, M. J. Helms, C. S. Haynes, C. M. Utley and L. P. Gwyther (1987). "Early-onset Alzheimer's disease: clinical predictors of institutionalization and death." Neurology **37**(6): 980-984.

Hirata-Fukae, C., H. F. Li, H. S. Hoe, A. J. Gray, S. S. Minami, K. Hamada, T. Niikura, F. Hua, H. Tsukagoshi-Nagai, Y. Horikoshi-Sakuraba, M. Mughal, G. W. Rebeck, F. M. LaFerla, M. P. Mattson, N. Iwata, T. C. Saido, W. L. Klein, K. E. Duff, P. S. Aisen and Y. Matsuoka (2008). "Females exhibit more extensive amyloid, but not tau, pathology in an Alzheimer transgenic model." Brain Res **1216**: 92-103.

Hirst, C. E., A. T. Major and C. A. Smith (2018). "Sex determination and gonadal sex differentiation in the chicken model." Int J Dev Biol **62**(1-2-3): 153-166.

Hoffman, J. M., K. E. Creevy and D. E. Promislow (2013). "Reproductive capability is associated with lifespan and cause of death in companion dogs." PLoS One **8**(4): e61082.

Hohman, T. J., L. Dumitrescu, L. L. Barnes, M. Thambisetty, G. Beecham, B. Kunkle, K. A. Gifford, W. S. Bush, L. B. Chibnik, S. Mukherjee, P. L. De Jager, W. Kukull, P. K. Crane, S. M. Resnick, C. D. Keene, T. J. Montine, G. D. Schellenberg, J. L. Haines, H. Zetterberg, K. Blennow, E. B. Larson, S. C. Johnson, M. Albert, D. A. Bennett, J. A. Schneider, A. L. Jefferson, C. Alzheimer's Disease Genetics and I. the Alzheimer's Disease Neuroimaging (2018). "Sex-Specific Association of Apolipoprotein E With Cerebrospinal Fluid Levels of Tau." JAMA Neurol **75**(8): 989-998.

Horvath, S., M. Gurven, M. E. Levine, B. C. Trumble, H. Kaplan, H. Allayee, B. R. Ritz, B. Chen, A. T. Lu, T. M. Rickabaugh, B. D. Jamieson, D. Sun, S. Li, W. Chen, L. Quintana-Murci, M. Fagny, M. S. Kobor, P. S. Tsao, A. P. Reiner, K. L. Edlefsen, D. Absher and T. L. Assimes (2016). "An epigenetic clock analysis of race/ethnicity, sex, and coronary heart disease." Genome Biol **17**(1): 171.

Itoh, Y., L. C. Golden, N. Itoh, M. A. Matsukawa, E. Ren, V. Tse, A. P. Arnold and R. R. Voskuhl (2019). "The X-linked histone demethylase Kdm6a in CD4+ T lymphocytes modulates autoimmunity." J Clin Invest **130**.

Itoh, Y., R. Mackie, K. Kampf, S. Domadia, J. D. Brown, R. O'Neill and A. P. Arnold (2015). "Four Core Genotypes mouse model: Localization of the Sry transgene and bioassay for testicular hormone levels." BMC Research Notes **8**.

Jack, C. R., Jr., D. A. Bennett, K. Blennow, M. C. Carrillo, H. H. Feldman, G. B. Frisoni, H. Hampel, W. J. Jagust, K. A. Johnson, D. S. Knopman, R. C. Petersen, P. Scheltens, R. A. Sperling and B. Dubois (2016). "A/T/N: An unbiased descriptive classification scheme for Alzheimer disease biomarkers." Neurology **87**(5): 539-547.

Jack, C. R., Jr., T. M. Therneau, S. D. Weigand, H. J. Wiste, D. S. Knopman, P. Vemuri, V. J. Lowe, M. M. Mielke, R. O. Roberts, M. M. Machulda, J. Graff-Radford, D. T. Jones, C. G. Schwarz, J. L. Gunter, M. L. Senjem, W. A. Rocca and R. C. Petersen (2019). "Prevalence of Biologically vs Clinically Defined Alzheimer Spectrum Entities Using the National Institute on Aging-Alzheimer's Association Research Framework." JAMA Neurol.

Jack, C. R., Jr., T. M. Therneau, H. J. Wiste, S. D. Weigand, D. S. Knopman, V. J. Lowe, M. M. Mielke, P. Vemuri, R. O. Roberts, M. M. Machulda, M. L. Senjem, J. L. Gunter, W. A. Rocca and R. C. Petersen (2016). "Transition rates between amyloid and neurodegeneration biomarker states and to dementia: a population-based, longitudinal cohort study." Lancet Neurol **15**(1): 56-64.

Jack, C. R., Jr., H. J. Wiste, S. D. Weigand, D. S. Knopman, P. Vemuri, M. M. Mielke, V. Lowe, M. L. Senjem, J. L. Gunter, M. M. Machulda, B. E. Gregg, V. S. Pankratz, W. A. Rocca and R. C. Petersen (2015). "Age, Sex, and APOE epsilon4 Effects on Memory, Brain Structure, and beta-Amyloid Across the Adult Life Span." JAMA neurology.

Jack, C. R., Jr., H. J. Wiste, S. D. Weigand, T. M. Therneau, D. S. Knopman, V. Lowe, P. Vemuri, M. M. Mielke, R. O. Roberts, M. M. Machulda, M. L. Senjem, J. L. Gunter, W. A. Rocca and R. C. Petersen (2017). "Age-specific and sex-specific prevalence of cerebral beta-amyloidosis, tauopathy, and neurodegeneration in cognitively unimpaired individuals aged 50-95 years: a cross-sectional study." Lancet Neurol **16**(6): 435-444.

Jansen, W. J., R. Ossenkuppele, D. L. Knol, B. M. Tijms, P. Scheltens, F. R. Verhey, P. J. Visser, G. Amyloid Biomarker Study, P. Aalten, D. Aarsland, D. Alcolea, M. Alexander, I. S. Almdahl, S. E. Arnold, I. Baldeiras, H. Barthel, B. N. van Berckel, K. Bibeau, K. Blennow, D. J. Brooks, M. A. van Buchem, V. Camus, E. Cavedo, K. Chen, G. Chetelat, A. D. Cohen, A. Drzezga, S. Engelborghs, A. M. Fagan, T. Fladby, A. S. Fleisher, W. M. van der Flier, L. Ford, S. Forster, J. Fortea, N. Fosskett, K. S. Frederiksen, Y. Freund-Levi, G. B. Frisoni, L. Froelich, T. Gabryelewicz, K. D. Gill, O. Gkatzima, E. Gomez-Tortosa, M. F. Gordon, T. Grimmer, H. Hampel, L. Hausner, S. Hellwig, S. K. Herukka, H. Hildebrandt, L. Ishihara, A. Ivanoiu, W. J. Jagust, P. Johannsen, R. Kandimalla, E. Kapaki, A. Klimkowicz-Mrowiec, W. E. Klunk, S. Kohler, N. Koglin, J. Kornhuber, M. G. Kramberger, K. Van Laere, S. M. Landau, D. Y. Lee, M. de Leon, V. Lisetti, A. Lleo, K. Madsen, W. Maier, J. Marcusson, N. Mattsson, A. de Mendonca, O. Meulenbroek, P. T. Meyer, M. A. Mintun, V. Mok, J. L. Molinuevo, H. M. Mollergard, J. C. Morris, B. Mroczko, S. Van der Mussele, D. L. Na, A. Newberg, A. Nordberg, A. Nordlund, G. P. Novak, G. P. Paraskevas, L. Parnetti, G. Perera, O. Peters, J. Popp, S. Prabhakar, G. D. Rabinovici, I. H. Ramakers, L. Rami, C. Resende de Oliveira, J. O. Rinne, K. M. Rodrigue, E. Rodriguez-Rodriguez, C. M. Roe, U. Rot, C. C. Rowe, E. Ruther, O. Sabri, P. Sanchez-Juan, I. Santana, M. Sarazin, J. Schroder, C. Schutte, S. W. Seo, F. Soetewey, H. Soininen, L. Spuru, H. Struyfs, C. E. Teunissen, M. Tsolaki, R. Vandenberghe, M. M. Verbeek, V. L. Villemagne, S. J. Vos, L. J. van Waalwijk van Doorn, G. Waldemar, A. Wallin, A. K. Wallin, J. Wiltfang, D. A. Wolk, M. Zboch and H. Zetterberg (2015). "Prevalence of cerebral amyloid pathology in persons without dementia: a meta-analysis." JAMA **313**(19): 1924-1938.

Jensen, L. R., M. Amende, U. Gurok, B. Moser, V. Gimmel, A. Tzschach, A. R. Janecke, G. Tariverdian, J. Chelly, J. P. Fryns, H. Van Esch, T. Kleefstra, B. Hamel, C. Moraine, J. Gecz, G. Turner, R. Reinhardt, V. M. Kalscheuer, H. H. Ropers and S. Lenzner (2005). "Mutations in the JARID1C gene, which is involved in transcriptional regulation and chromatin remodeling, cause X-linked mental retardation." Am J Hum Genet **76**(2): 227-236.

Jorm, A. F. and D. Jolley (1998). "The incidence of dementia: a meta-analysis." Neurology **51**(3): 728-733.

Kihira, T., S. Yoshida, K. Okamoto, Y. Kazimoto, M. Ookawa, K. Hama, H. Miwa and T. Kondo (2008). "Survival rate of patients with amyotrophic lateral sclerosis in Wakayama Prefecture, Japan, 1966 to 2005." J Neurol Sci **268**(1-2): 95-101.

Kivipelto, M., E. L. Helkala, T. Hanninen, M. P. Laakso, M. Hallikainen, K. Alhainen, H. Soininen, J. Tuomilehto and A. Nissinen (2001). "Midlife vascular risk factors and late-life mild cognitive impairment: A population-based study." Neurology **56**(12): 1683-1689.

Klein, W. L. (2002). "Abeta toxicity in Alzheimer's disease: globular oligomers (ADDLs) as new vaccine and drug targets." Neurochem Int **41**(5): 345-352.

Kodama, L., E. Guzman, J. I. Etchegaray, Y. Li, F. A. Sayed, L. Zhou, Y. Zhou, L. Zhan, D. Le, J. C. Udeochu, C. D. Clelland, Z. Cheng, G. Yu, Q. Li, K. S. Kosik and L. Gan (2020). "Microglial microRNAs mediate sex-specific responses to tau pathology." Nat Neurosci **23**(2): 167-171.

Koivisto, K., K. J. Reinikainen, T. Hanninen, M. Vanhanen, E. L. Helkala, L. Mykkanen, M. Laakso, K. Pyorala and P. J. Riekkinen, Sr. (1995). "Prevalence of age-associated memory impairment in a randomly selected population from eastern Finland." Neurology **45**(4): 741-747.

Kokalj-Vokac, N., C. Saint-Ruf, D. Lefrancois, E. Viegas-Pequignot, N. Lemieux, B. Malfoy and B. Dutrillaux (1991). "A t(X;15)(q23;q25) with Xq reactivation in a lymphoblastoid cell line from Fanconi anemia." Cytogenet Cell Genet **57**(1): 11-15.

Lapane, K. L., G. Gambassi, F. Landi, A. Sgadari, V. Mor and R. Bernabei (2001). "Gender differences in predictors of mortality in nursing home residents with AD." Neurology **56**(5): 650-654.

Lederer, D., B. Grisart, M. C. Digilio, V. Benoit, M. Crespin, S. C. Ghariani, I. Maystadt, B. Dallapiccola and C. Verellen-Dumoulin (2012). "Deletion of KDM6A, a histone demethylase interacting with MLL2, in three patients with Kabuki syndrome." Am J Hum Genet **90**(1): 119-124.

Lee, M. G., R. Villa, P. Trojer, J. Norman, K. P. Yan, D. Reinberg, L. Di Croce and R. Shiekhattar (2007). "Demethylation of H3K27 regulates polycomb recruitment and H2A ubiquitination." Science **318**(5849): 447-450.

Lei, X. and J. Jiao (2018). "UTX Affects Neural Stem Cell Proliferation and Differentiation through PTEN Signaling." Stem Cell Reports **10**(4): 1193-1207.

Lerman, P. M. (1980). "Fitting Segmented Regression Models by Grid Search." Journal of the Royal Statistical Society. Series C (Applied Statistics) **29**(1): 77-84.

Li, X., L. Hou, L. Yin and S. Zhao (2020). "LncRNA XIST interacts with miR-454 to inhibit cells proliferation, epithelial mesenchymal transition and induces apoptosis in triple-negative breast cancer." J Biosci **45**.

Lin, B., J. Xu, F. Wang, J. Wang, H. Zhao and D. Feng (2020). "LncRNA XIST promotes myocardial infarction by regulating FOS through targeting miR-101a-3p." Aging (Albany NY) **12**(8): 7232-7247.

Lopez-Otin, C., M. A. Blasco, L. Partridge, M. Serrano and G. Kroemer (2013). "The hallmarks of aging." Cell **153**(6): 1194-1217.

Lovell-Badge, R. and E. Robertson (1990). "XY female mice resulting from a heritable mutation in the primary testis-determining gene, Tdy." Development **109**(3): 635-646.

Lucchesi, J. C. and M. I. Kuroda (2015). "Dosage compensation in Drosophila." Cold Spring Harb Perspect Biol **7**(5).

Mahadevaiah, S. K., T. Odorisio, D. J. Elliott, A. Rattigan, M. Szot, S. H. Laval, L. L. Washburn, J. R. McCarrey, B. M. Cattanch, R. Lovell-Badge and P. S. Burgoyne (1998). "Mouse homologues of the human AZF candidate gene RBM are expressed in spermatogonia and spermatids, and map to a Y chromosome deletion interval associated with a high incidence of sperm abnormalities." Human molecular genetics **7**(4): 715-727.

Marshall, E. A., G. L. Stewart, A. P. Sage, W. L. Lam and C. J. Brown (2019). "Beyond sequence homology: Cellular biology limits the potential of XIST to act as a miRNA sponge." PLoS One **14**(8): e0221371.

Maures, T. J., L. N. Booth, B. A. Benayoun, Y. Izrayelit, F. C. Schroeder and A. Brunet (2014). "Males shorten the life span of *C. elegans* hermaphrodites via secreted compounds." Science **343**(6170): 541-544.

McCarthy, M. M. and A. P. Arnold (2011). "Reframing sexual differentiation of the brain." Nature neuroscience **14**(6): 677-683.

McCarthy, M. M., C. S. Woolley and A. P. Arnold (2017). "Incorporating sex as a biological variable in neuroscience: what do we gain?" Nat Rev Neurosci **18**(12): 707-708.

McCullough, L. D., M. A. Mirza, Y. Xu, K. Bentivegna, E. B. Steffens, R. Ritzel and F. Liu (2016). "Stroke sensitivity in the aged: sex chromosome complement vs. gonadal hormones." Aging (Albany NY) **8**(7): 1432-1441.

McQueen, H. A., D. McBride, G. Miele, A. P. Bird and M. Clinton (2001). "Dosage compensation in birds." Curr Biol **11**(4): 253-257.

Meyer, B. J. (2000). "Sex in the wormcounting and compensating X-chromosome dose." Trends Genet **16**(6): 247-253.

Mielke, M. M., P. Vemuri and W. A. Rocca (2014). "Clinical epidemiology of Alzheimer's disease: assessing sex and gender differences." Clin Epidemiol **6**: 37-48.

Min, K. J., C. K. Lee and H. N. Park (2012). "The lifespan of Korean eunuchs." Curr Biol **22**(18): R792-793.

Miyake, N., E. Koshimizu, N. Okamoto, S. Mizuno, T. Ogata, T. Nagai, T. Kosho, H. Ohashi, M. Kato, G. Sasaki, H. Mabe, Y. Watanabe, M. Yoshino, T. Matsuishi, J. Takanashi, V. Shotelersuk, M. Tekin, N. Ochi, M. Kubota, N. Ito, K. Ihara, T. Hara, H. Tonoki, T. Ohta, K. Saito, M. Matsuo, M. Urano, T. Enokizono, A. Sato, H. Tanaka, A. Ogawa, T. Fujita, Y. Hiraki, S. Kitanaka, Y. Matsubara, T. Makita, M. Taguri, M. Nakashima, Y. Tsurusaki, H. Saito, K. Yoshiura, N.

Matsumoto and N. Niikawa (2013). "MLL2 and KDM6A mutations in patients with Kabuki syndrome." Am J Med Genet A **161A**(9): 2234-2243.

Miyake, N., S. Mizuno, N. Okamoto, H. Ohashi, M. Shiina, K. Ogata, Y. Tsurusaki, M. Nakashima, H. Saitsu, N. Niikawa and N. Matsumoto (2013). "KDM6A point mutations cause Kabuki syndrome." Hum Mutat **34**(1): 108-110.

Morley, J. E., F. Kaiser, W. J. Raum, H. M. Perry, 3rd, J. F. Flood, J. Jensen, A. J. Silver and E. Roberts (1997). "Potentially predictive and manipulable blood serum correlates of aging in the healthy human male: progressive decreases in bioavailable testosterone, dehydroepiandrosterone sulfate, and the ratio of insulin-like growth factor 1 to growth hormone." Proc Natl Acad Sci U S A **94**(14): 7537-7542.

Mucke, L., E. Masliah, G. Q. Yu, M. Mallory, E. M. Rockenstein, G. Tatsuno, K. Hu, D. Kholodenko, K. Johnson-Wood and L. McConlogue (2000). "High-level neuronal expression of abeta 1-42 in wild-type human amyloid protein precursor transgenic mice: synaptotoxicity without plaque formation." J Neurosci **20**(11): 4050-4058.

Nelson, J. F., L. S. Felicio, H. H. Osterburg and C. E. Finch (1992). "Differential contributions of ovarian and extraovarian factors to age-related reductions in plasma estradiol and progesterone during the estrous cycle of C57BL/6J mice." Endocrinology **130**(2): 805-810.

Nelson, J. F., K. R. Latham and C. E. Finch (1975). "Plasma testosterone levels in C57BL/6J male mice: effects of age and disease." Acta Endocrinol (Copenh) **80**(4): 744-752.

Ongen, H., A. Buil, A. A. Brown, E. T. Dermitzakis and O. Delaneau (2016). "Fast and efficient QTL mapper for thousands of molecular phenotypes." Bioinformatics **32**(10): 1479-1485.

Ossenkoppele, R., C. H. Lyoo, J. Jester-Broms, C. H. Sudre, H. Cho, Y. H. Ryu, J. Y. Choi, R. Smith, O. Strandberg, S. Palmqvist, J. Kramer, A. L. Boxer, M. L. Gorno-Tempini, B. L. Miller, R. La Joie, G. D. Rabinovici and O. Hansson (2020). "Assessment of Demographic, Genetic, and Imaging Variables Associated With Brain Resilience and Cognitive Resilience to Pathological Tau in Patients With Alzheimer Disease." JAMA Neurol.

Overmyer, K. A., S. Tyanova, A. S. Hebert, M. S. Westphall, J. Cox and J. J. Coon (2018). "Multiplexed proteome analysis with neutron-encoded stable isotope labeling in cells and mice." Nat Protoc **13**(1): 293-306.

Palop, J. J., B. Jones, L. Kekoni, J. Chin, G. Q. Yu, J. Raber, E. Masliah and L. Mucke (2003). "Neuronal depletion of calcium-dependent proteins in the dentate gyrus is tightly linked to Alzheimer's disease-related cognitive deficits." Proc Natl Acad Sci U S A **100**(16): 9572-9577.

Panning, B. (2004). "X inactivation in mouse ES cells: histone modifications and FISH." Methods Enzymol **376**: 419-428.

Payer, B. (2016). "Developmental regulation of X-chromosome inactivation." Semin Cell Dev Biol **56**: 88-99.

Pessoa, B. S., D. E. Slump, K. Ibrahimi, A. Grefhorst, R. van Veghel, I. M. Garrelds, A. J. Roks, S. A. Kushner, A. H. Danser and J. H. van Esch (2015). "Angiotensin II type 2 receptor- and acetylcholine-mediated relaxation: essential contribution of female sex hormones and chromosomes." Hypertension **66**(2): 396-402.

Petersen, R. C., P. S. Aisen, L. A. Beckett, M. C. Donohue, A. C. Gamst, D. J. Harvey, C. R. Jack, Jr., W. J. Jagust, L. M. Shaw, A. W. Toga, J. Q. Trojanowski and M. W. Weiner (2010). "Alzheimer's Disease Neuroimaging Initiative (ADNI): clinical characterization." Neurology **74**(3): 201-209.

Petersen, R. C., R. O. Roberts, D. S. Knopman, Y. E. Geda, R. H. Cha, V. S. Pankratz, B. F. Boeve, E. G. Tangalos, R. J. Ivnik and W. A. Rocca (2010). "Prevalence of mild cognitive impairment is higher in men. The Mayo Clinic Study of Aging." Neurology **75**(10): 889-897.

Pike, C. J. (2017). "Sex and the development of Alzheimer's disease." J Neurosci Res **95**(1-2): 671-680.

Pipoly, I., V. Bokony, M. Kirkpatrick, P. F. Donald, T. Szekely and A. Liker (2015). "The genetic sex-determination system predicts adult sex ratios in tetrapods." Nature **527**(7576): 91-94.

Rideout, E. J., M. S. Narsaiya and S. S. Grewal (2015). "The Sex Determination Gene transformer Regulates Male-Female Differences in Drosophila Body Size." PLoS Genet **11**(12): e1005683.

Roberson, E. D., B. Halabisky, J. W. Yoo, J. Yao, J. Chin, F. Yan, T. Wu, P. Hamto, N. Devidze, G. Q. Yu, J. J. Palop, J. L. Noebels and L. Mucke (2011). "Amyloid-beta/Fyn-induced synaptic, network, and cognitive impairments depend on tau levels in multiple mouse models of Alzheimer's disease." J Neurosci **31**(2): 700-711.

Roberts, R. O., Y. E. Geda, D. S. Knopman, R. H. Cha, V. S. Pankratz, B. F. Boeve, E. G. Tangalos, R. J. Ivnik, W. A. Rocca and R. C. Petersen (2012). "The incidence of MCI differs by subtype and is higher in men: the Mayo Clinic Study of Aging." Neurology **78**(5): 342-351.

Robinson, M. D. and A. Oshlack (2010). "A scaling normalization method for differential expression analysis of RNA-seq data." Genome Biol **11**(3): R25.

Rockenstein, E. M., L. McConlogue, H. Tan, M. Power, E. Masliah and L. Mucke (1995). "Levels and alternative splicing of amyloid beta protein precursor (APP) transcripts in brains of APP transgenic mice and humans with Alzheimer's disease." J Biol Chem **270**(47): 28257-28267.

Ropers, H. H. and B. C. Hamel (2005). "X-linked mental retardation." Nat Rev Genet **6**(1): 46-57.

Rotheneichner, P., P. Romanelli, L. Bieler, S. Pagitsch, P. Zaunmair, C. Kreutzer, R. Konig, J. Marschallinger, L. Aigner and S. Couillard-Despres (2017). "Tamoxifen Activation of Cre-Recombinase Has No Persisting Effects on Adult Neurogenesis or Learning and Anxiety." Front Neurosci **11**: 27.

Sampathkumar, N. K., J. I. Bravo, Y. Chen, P. S. Danthi, E. K. Donahue, R. W. Lai, R. Lu, L. T. Randall, N. Vinson and B. A. Benayoun (2019). "Widespread sex dimorphism in aging and age-related diseases." Hum Genet.

Saykin, A. J., L. Shen, T. M. Foroud, S. G. Potkin, S. Swaminathan, S. Kim, S. L. Risacher, K. Nho, M. J. Huentelman, D. W. Craig, P. M. Thompson, J. L. Stein, J. H. Moore, L. A. Farrer, R. C. Green, L. Bertram, C. R. Jack, Jr., M. W. Weiner and I. Alzheimer's Disease Neuroimaging

(2010). "Alzheimer's Disease Neuroimaging Initiative biomarkers as quantitative phenotypes: Genetics core aims, progress, and plans." Alzheimers Dement **6**(3): 265-273.

Saykin, A. J., L. Shen, X. Yao, S. Kim, K. Nho, S. L. Risacher, V. K. Ramanan, T. M. Foroud, K. M. Faber, N. Sarwar, L. M. Munsie, X. Hu, H. D. Soares, S. G. Potkin, P. M. Thompson, J. S. Kauwe, R. Kaddurah-Daouk, R. C. Green, A. W. Toga, M. W. Weiner and I. Alzheimer's Disease Neuroimaging (2015). "Genetic studies of quantitative MCI and AD phenotypes in ADNI: Progress, opportunities, and plans." Alzheimers Dement **11**(7): 792-814.

Schoeftner, S., R. Blanco, I. Lopez de Silanes, P. Munoz, G. Gomez-Lopez, J. M. Flores and M. A. Blasco (2009). "Telomere shortening relaxes X chromosome inactivation and forces global transcriptome alterations." Proc Natl Acad Sci U S A **106**(46): 19393-19398.

Sejvar, J. J., R. C. Holman, J. S. Bresee, K. D. Kochanek and L. B. Schonberger (2005). "Amyotrophic lateral sclerosis mortality in the United States, 1979-2001." Neuroepidemiology **25**(3): 144-152.

Sherry, S. T., M. H. Ward, M. Kholodov, J. Baker, L. Phan, E. M. Smigielski and K. Sirotkin (2001). "dbSNP: the NCBI database of genetic variation." Nucleic Acids Res **29**(1): 308-311.

Shpargel, K. B., T. Sengoku, S. Yokoyama and T. Magnuson (2012). "UTX and UTY demonstrate histone demethylase-independent function in mouse embryonic development." PLoS Genet **8**(9): e1002964.

Sidik, K. and J. N. Jonkman (2002). "A simple confidence interval for meta-analysis." Stat Med **21**(21): 3153-3159.

Skuse, D. H. (2000). "Imprinting, the X-chromosome, and the male brain: explaining sex differences in the liability to autism." Pediatr Res **47**(1): 9-16.

Skuse, D. H. (2005). "X-linked genes and mental functioning." Hum Mol Genet **14 Spec No 1**: R27-32.

Skuse, D. H., R. S. James, D. V. Bishop, B. Coppin, P. Dalton, G. Aamodt-Leeper, M. Bacarese-Hamilton, C. Creswell, R. McGurk and P. A. Jacobs (1997). "Evidence from Turner's syndrome of an imprinted X-linked locus affecting cognitive function." Nature **387**(6634): 705-708.

Smith, S. M., R. S. Kimyon and J. J. Watters (2014). "Cell-type-specific Jumonji histone demethylase gene expression in the healthy rat CNS: detection by a novel flow cytometry method." ASN Neuro **6**(3): 193-207.

Snijders Blok, L., E. Madsen, J. Juusola, C. Gilissen, D. Baralle, M. R. Reijnders, H. Venselaar, C. Helsmoortel, M. T. Cho, A. Hoischen, L. E. Vissers, T. S. Koemans, W. Wissink-Lindhout, E. E. Eichler, C. Romano, H. Van Esch, C. Stumpel, M. Vreeburg, E. Smeets, K. Oberndorff, B. W. van Bon, M. Shaw, J. Gecz, E. Haan, M. Bienek, C. Jensen, B. L. Loeys, A. Van Dijck, A. M. Innes, H. Racher, S. Vermeer, N. Di Donato, A. Rump, K. Tatton-Brown, M. J. Parker, A. Henderson, S. A. Lynch, A. Fryer, A. Ross, P. Vasudevan, U. Kini, R. Newbury-Ecob, K. Chandler, A. Male, D. D. D. Study, S. Dijkstra, J. Schieving, J. Giltay, K. L. van Gassen, J. Schuurs-Hoeijmakers, P. L. Tan, I. Peditakis, S. A. Haas, K. Retterer, P. Reed, K. G. Monaghan, E. Haverfield, M. Natowicz, A. Myers, M. C. Kruer, Q. Stein, K. A. Strauss, K. W. Brigatti, K. Keating, B. K. Burton, K. H. Kim, J. Charrow, J. Norman, A. Foster-Barber, A. D. Kline, A. Kimball, E. Zackai, M. Harr, J. Fox, J. McLaughlin, K. Lindstrom, K. M. Haude, K. van Roozendaal, H. Brunner, W. K. Chung, R. F. Kooy, R. Pfundt, V. Kalscheuer, S. G. Mehta, N. Katsanis and T. Kleefstra (2015). "Mutations in DDX3X Are a Common Cause of Unexplained Intellectual Disability with Gender-Specific Effects on Wnt Signaling." Am J Hum Genet **97**(2): 343-352.

Solfrizzi, V., F. Panza, A. M. Colacicco, A. D'Introno, C. Capurso, F. Torres, F. Grigoletto, S. Maggi, A. Del Parigi, E. M. Reiman, R. J. Caselli, E. Scafato, G. Farchi, A. Capurso and G. Italian Longitudinal Study on Aging Working (2004). "Vascular risk factors, incidence of MCI, and rates of progression to dementia." Neurology **63**(10): 1882-1891.

Souyris, M., C. Cenac, P. Azar, D. Daviaud, A. Canivet, S. Grunenwald, C. Pienkowski, J. Chaumeil, J. E. Mejia and J. C. Guery (2018). "TLR7 escapes X chromosome inactivation in immune cells." Sci Immunol **3**(19).

Stegle, O., L. Parts, R. Durbin and J. Winn (2010). "A Bayesian framework to account for complex non-genetic factors in gene expression levels greatly increases power in eQTL studies." PLoS Comput Biol **6**(5): e1000770.

Stern, Y., M. X. Tang, M. S. Albert, J. Brandt, D. M. Jacobs, K. Bell, K. Marder, M. Sano, D. Devanand, S. M. Albert, F. Bylsma and W. Y. Tsai (1997). "Predicting time to nursing home care and death in individuals with Alzheimer disease." JAMA **277**(10): 806-812.

Tahiliani, M., P. Mei, R. Fang, T. Leonor, M. Rutenberg, F. Shimizu, J. Li, A. Rao and Y. Shi (2007). "The histone H3K4 demethylase SMCX links REST target genes to X-linked mental retardation." Nature **447**(7144): 601-605.

Tang, G. B., T. W. Mi, M. L. Sun, Y. J. Xu, S. G. Yang, H. Z. Du, Saijilafu, Z. Q. Teng, J. Gao and C. M. Liu (2020). "Overexpression of serotonin receptor 5b expression rescues neuronal and behavioral deficits in a mouse model of Kabuki syndrome." IBRO Rep **9**: 138-146.

Tang, G. B., Y. Q. Zeng, P. P. Liu, T. W. Mi, S. F. Zhang, S. K. Dai, Q. Y. Tang, L. Yang, Y. J. Xu, H. L. Yan, H. Z. Du, Z. Q. Teng, F. Q. Zhou and C. M. Liu (2017). "The Histone H3K27 Demethylase UTX Regulates Synaptic Plasticity and Cognitive Behaviors in Mice." Front Mol Neurosci **10**: 267.

Team, R. C. (2019). "R: A Language and Environment for Statistical Computing." R Foundation for Statistical Computing, Vienna, Austria **3.6.1**.

Tukiainen, T., A. C. Villani, A. Yen, M. A. Rivas, J. L. Marshall, R. Satija, M. Aguirre, L. Gauthier, M. Fleharty, A. Kirby, B. B. Cummings, S. E. Castel, K. J. Karczewski, F. Aguet, A. Byrnes, G. T. Consortium, D. A. Laboratory, G. Coordinating Center -Analysis Working, G. Statistical Methods groups-Analysis Working, G. g. Enhancing, N. I. H. C. Fund, Nih/Nci, Nih/Nhgri, Nih/Nimh, Nih/Nida, N. Biospecimen Collection Source Site, R. Biospecimen Collection Source Site, V.

Biospecimen Core Resource, B. Brain Bank Repository-University of Miami Brain Endowment, M. Leidos Biomedical-Project, E. Study, I. Genome Browser Data, E. B. I. Visualization, I. Genome Browser Data, U. o. C. S. C. Visualization-Ucsc Genomics Institute, T. Lappalainen, A. Regev, K. G. Ardlie, N. Hacohen and D. G. MacArthur (2017). "Landscape of X chromosome inactivation across human tissues." Nature **550**(7675): 244-248.

Ueki, A., H. Shinjo, H. Shimode, T. Nakajima and Y. Morita (2001). "Factors associated with mortality in patients with early-onset Alzheimer's disease: a five-year longitudinal study." Int J Geriatr Psychiatry **16**(8): 810-815.

United Nations (2015). "World Population Ageing 2015." United Nations, Department of Economic and Social Affairs, Population Division(ST/ESA/SER.A/390): 1-164.

Van Laarhoven, P. M., L. R. Neitzel, A. M. Quintana, E. A. Geiger, E. H. Zackai, D. E. Clouthier, K. B. Artinger, J. E. Ming and T. H. Shaikh (2015). "Kabuki syndrome genes KMT2D and KDM6A: functional analyses demonstrate critical roles in craniofacial, heart and brain development." Hum Mol Genet **24**(15): 4443-4453.

Vawter, M. P., S. Evans, P. Choudary, H. Tomita, J. Meador-Woodruff, M. Molnar, J. Li, J. F. Lopez, R. Myers, D. Cox, S. J. Watson, H. Akil, E. G. Jones and W. E. Bunney (2004). "Gender-specific gene expression in post-mortem human brain: localization to sex chromosomes." Neuropsychopharmacology **29**(2): 373-384.

Veldhuis, J. D. (2008). "Aging and hormones of the hypothalamo-pituitary axis: gonadotropic axis in men and somatotrophic axes in men and women." Ageing Res Rev **7**(3): 189-208.

Viechtbauer, W. (2010). "Conducting meta-analyses in R with the metafor package." Journal of Statistical Software **36**(3): 1-48.

Villeponteau, B. (1997). "The heterochromatin loss model of aging." Exp Gerontol **32**(4-5): 383-394.

Wagner, C. K., J. Xu, J. L. Pfau, P. S. Quadros, G. J. De Vries and A. P. Arnold (2004). "Neonatal mice possessing an Sry transgene show a masculinized pattern of progesterone receptor

expression in the brain independent of sex chromosome status." Endocrinology **145**(3): 1046-1049.

Walport, L. J., R. J. Hopkinson, M. Vollmar, S. K. Madden, C. Gileadi, U. Oppermann, C. J. Schofield and C. Johansson (2014). "Human UTY(KDM6C) is a male-specific N-methyl lysyl demethylase." J Biol Chem **289**(26): 18302-18313.

Wang, C., J. E. Lee, Y. W. Cho, Y. Xiao, Q. Jin, C. Liu and K. Ge (2012). "UTX regulates mesoderm differentiation of embryonic stem cells independent of H3K27 demethylase activity." Proc Natl Acad Sci U S A **109**(38): 15324-15329.

Wang, J., H. Tanila, J. Puolivali, I. Kadish and T. van Groen (2003). "Gender differences in the amount and deposition of amyloidbeta in APPswe and PS1 double transgenic mice." Neurobiol Dis **14**(3): 318-327.

Wang, M., N. D. Beckmann, P. Roussos, E. Wang, X. Zhou, Q. Wang, C. Ming, R. Neff, W. Ma, J. F. Fullard, M. E. Hauberg, J. Bendl, M. A. Peters, B. Logsdon, P. Wang, M. Mahajan, L. M. Mangravite, E. B. Dammer, D. M. Duong, J. J. Lah, N. T. Seyfried, A. I. Levey, J. D. Buxbaum, M. Ehrlich, S. Gandy, P. Katsel, V. Haroutunian, E. Schadt and B. Zhang (2018). "The Mount Sinai cohort of large-scale genomic, transcriptomic and proteomic data in Alzheimer's disease." Sci Data **5**: 180185.

Wareham, K. A., M. F. Lyon, P. H. Glenister and E. D. Williams (1987). "Age related reactivation of an X-linked gene." Nature **327**(6124): 725-727.

Webster, J. A., J. R. Gibbs, J. Clarke, M. Ray, W. Zhang, P. Holmans, K. Rohrer, A. Zhao, L. Marlowe, M. Kaleem, D. S. McCorquodale, 3rd, C. Cuello, D. Leung, L. Bryden, P. Nath, V. L. Zismann, K. Joshipura, M. J. Huentelman, D. Hu-Lince, K. D. Coon, D. W. Craig, J. V. Pearson, N. A.-N. Group, C. B. Heward, E. M. Reiman, D. Stephan, J. Hardy and A. J. Myers (2009). "Genetic control of human brain transcript expression in Alzheimer disease." Am J Hum Genet **84**(4): 445-458.

Weiner, M. W., D. P. Veitch, P. S. Aisen, L. A. Beckett, N. J. Cairns, R. C. Green, D. Harvey, C. R. Jack, W. Jagust, E. Liu, J. C. Morris, R. C. Petersen, A. J. Saykin, M. E. Schmidt, L. Shaw, J. A. Siuciak, H. Soares, A. W. Toga, J. Q. Trojanowski and I. Alzheimer's Disease Neuroimaging (2012). "The Alzheimer's Disease Neuroimaging Initiative: a review of papers published since its inception." Alzheimers Dement **8**(1 Suppl): S1-68.

Welstead, G. G., M. P. Creighton, S. Bilodeau, A. W. Cheng, S. Markoulaki, R. A. Young and R. Jaenisch (2012). "X-linked H3K27me3 demethylase Utx is required for embryonic development in a sex-specific manner." Proc Natl Acad Sci U S A **109**(32): 13004-13009.

Wiedemuth, R., S. Thieme, K. Navratil, B. Dorschner and S. Brenner (2018). "UTX - moonlighting in the cytoplasm?" Int J Biochem Cell Biol **97**: 78-82.

Wimo, A. and M. Prince (2015). World Alzheimer Report 2015: The Global Economic Impact of Dementia.

Wright, F. A., P. F. Sullivan, A. I. Brooks, F. Zou, W. Sun, K. Xia, V. Madar, R. Jansen, W. Chung, Y. H. Zhou, A. Abdellaoui, S. Batista, C. Butler, G. Chen, T. H. Chen, D. D'Ambrosio, P. Gallins, M. J. Ha, J. J. Hottenga, S. Huang, M. Kattenberg, J. Kochar, C. M. Middeldorp, A. Qu, A. Shabalina, J. Tischfield, L. Todd, J. Y. Tzeng, G. van Grootheest, J. M. Vink, Q. Wang, W. Wang, W. Wang, G. Willemsen, J. H. Smit, E. J. de Geus, Z. Yin, B. W. Penninx and D. I. Boomsma (2014). "Heritability and genomics of gene expression in peripheral blood." Nat Genet **46**(5): 430-437.

Xu, J., X. Deng, R. Watkins and C. M. Distech (2008). "Sex-specific differences in expression of histone demethylases Utx and Uty in mouse brain and neurons." J Neurosci **28**(17): 4521-4527.

Yamauchi, Y., J. M. Riel, Z. Stoytcheva and M. A. Ward (2014). "Two Y genes can replace the entire Y chromosome for assisted reproduction in the mouse." Science **343**(6166): 69-72.

Yang, F., T. Babak, J. Shendure and C. M. Distech (2010). "Global survey of escape from X inactivation by RNA-sequencing in mouse." Genome Res **20**(5): 614-622.

Yang, P., H. Tan, Y. Xia, Q. Yu, X. Wei, R. Guo, Y. Peng, C. Chen, H. Li, L. Mei, Y. Huang, D. Liang and L. Wu (2016). "De novo exonic deletion of KDM6A in a Chinese girl with Kabuki syndrome: A case report and brief literature review." Am J Med Genet A **170**(6): 1613-1621.

Yildirim, E., J. E. Kirby, D. E. Brown, F. E. Mercier, R. I. Sadreyev, D. T. Scadden and J. T. Lee (2013). "Xist RNA is a potent suppressor of hematologic cancer in mice." Cell **152**(4): 727-742.

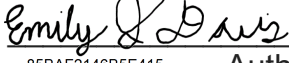
Zarulli, V., J. A. Barthold Jones, A. Oksuzyan, R. Lindahl-Jacobsen, K. Christensen and J. W. Vaupel (2018). "Women live longer than men even during severe famines and epidemics." Proc Natl Acad Sci U S A **115**(4): E832-E840.

Zechner, U., M. Wilda, H. Kehrer-Sawatzki, W. Vogel, R. Fundele and H. Hameister (2001). "A high density of X-linked genes for general cognitive ability: a run-away process shaping human evolution?" Trends Genet **17**(12): 697-701.

Publishing Agreement

It is the policy of the University to encourage open access and broad distribution of all theses, dissertations, and manuscripts. The Graduate Division will facilitate the distribution of UCSF theses, dissertations, and manuscripts to the UCSF Library for open access and distribution. UCSF will make such theses, dissertations, and manuscripts accessible to the public and will take reasonable steps to preserve these works in perpetuity.

I hereby grant the non-exclusive, perpetual right to The Regents of the University of California to reproduce, publicly display, distribute, preserve, and publish copies of my thesis, dissertation, or manuscript in any form or media, now existing or later derived, including access online for teaching, research, and public service purposes.

DocuSigned by:

85BAF2146B5E415... Author Signature

12/7/2020
Date